THE UNIVERSITY OF MICHIGAN
JUL 8 1963
PHOENIX LIBRARY

REACTOR MATERIALS

A Quarterly Technical Progress Review

Prepared for DIVISION OF TECHNICAL INFORMATION, USAEC, by
R. W. DAYTON, E. M. SIMONS, and ASSOCIATES, BATTELLE MEMORIAL INSTITUTE

May 1963

FEATURE ARTICLE:

Recent Developments with Coated-Particle Fuel Materials

● VOLUME 6

● NUMBER 2

TECHNICAL PROGRESS REVIEWS

To meet the needs of industry for concise summaries of current atomic developments, the Atomic Energy Commission is publishing this series, Technical Progress Reviews. Issued quarterly, each of the reviews digests and evaluates the latest findings in a specific area of nuclear technology and science.

The four journals published in this series are:

Nuclear Safety, Wm. B. Cottrell, W. H. Jordan, and associates, Oak Ridge National Laboratory

Power Reactor Technology, W. H. Zinn and J. R. Dietrich, General Nuclear Engineering Corporation

Reactor Materials, R. W. Dayton, E. M. Simons, and associates, Battelle Memorial Institute

Reactor Fuel Processing, Stephen Lawroski and associates, Chemical Engineering Division, Argonne National Laboratory

Each journal may be purchased ($2.00 per year for subscription and individual issues $0.55) from the Superintendent of Documents, U. S. Government Printing Office, Washington 25, D. C. See back cover for remittance instructions and foreign postage requirements.

The views expressed in this publication do not necessarily represent those of the United States Atomic Energy Commission, its divisions or offices, or of any Commission advisory committee or contractor.

Availability of Reports Cited in This Review

Unclassified AEC reports are available for inspection at AEC depository libraries and are sold by the Office of Technical Services, Department of Commerce, Washington 25, D. C. Some of the reports cited are not available owing to their preliminary nature; however, the information contained in them will eventually be made available in formal progress or topical reports.

Unclassified reports issued by other Government agencies or private organizations should be requested from the originator.

Unclassified British and Canadian reports may be inspected at AEC depository libraries. British reports are sold by the British Information Service, 45 Rockefeller Plaza, New York, N. Y.; Canadian reports (AECL series) are sold by the Scientific Document Distribution Office, Atomic Energy of Canada, Ltd., Chalk River, Ontario, Canada.

Classified U. S. and foreign reports identified in this journal as Classified may be purchased by properly cleared Access Permit Holders from the Division of Technical Information Extension, U. S. Atomic Energy Commission, P. O. Box 1001, Oak Ridge, Tenn. Such reports may be inspected at classified AEC depository libraries.

REACTOR MATERIALS

A REVIEW OF RECENT DEVELOPMENTS

Prepared for DIVISION OF TECHNICAL INFORMATION, USAEC,
by R. W. DAYTON, E. M. SIMONS, and ASSOCIATES,
BATTELLE MEMORIAL INSTITUTE

● MAY 1963

● VOLUME 6

● NUMBER 2

Foreword

Reactor Materials is one of a series of quarterly technical progress reviews broadly covering the field of nuclear science and technology. Under the auspices of the USAEC Division of Technical Information, *Reactor Materials* is prepared by Battelle personnel from worldwide literature. It covers properties, behavior, and fabrication processes of materials applicable to nuclear reactor components and associated equipment.

The reader will recognize that the scope of this Review is too broad to permit detailed coverage of every topic. Rather, the authors and editors attempt to combine the highlights of significant new developments into an information summary of current research for both management and the technical specialist. As a rule, enough of the results are presented to define the research and summarize the findings. For readers desiring more information on any particular topic, a complete set of references is provided at the end of each section.

Each quarter, a number of bibliographies, monographs, and books appear on subjects within the scope of *Reactor Materials*. Although the main purpose of this Review is to call attention to findings that are new and significant, such publications are noted in the text because they often represent excellent compilations of available information on important materials topics.

Owing to page limitations, the sections on Cladding and Structural Materials and on Special Fabrication Techniques do not appear in this issue. Important developments during the past quarter will be included in the next issue (Vol. 6, No. 3).

R. W. DAYTON
E. M. SIMONS
R. W. ENDEBROCK
Battelle Memorial Institute

DEPOSITED BY THE
UNITED STATES OF AMERICA

Contents

FEATURE ARTICLE

Recent Developments with Coated-Particle Fuel Materials 1

by Joseph H. Oxley, Battelle Memorial Institute

Foreword

I FUEL AND FERTILE MATERIALS . . . 15
Uranium Metal and Alloys 15
Plutonium 21
Thorium 25
Dispersion Fuels 25
Coated-Particle Fuel Materials 27
Refractory Fuel and Fertile Materials . . . 39
Basic Studies of Irradiation Effects on Fuel Materials 44
References 45

II MODERATOR MATERIALS 50
Graphite 50
Beryllium Metal and Alloys 52
Beryllium Oxide 59
Beryllides 60
Solid Hydrides 62
References 63

III NUCLEAR POISONS 67
Metallic Poison Materials 67
Dispersion Control Materials 67
References 69

Issued quarterly by the U. S. Atomic Energy Commission. Use of funds for printing this publication approved by the Director of the Bureau of the Budget on November 1, 1960.

FEATURE ARTICLE

Recent Developments with Coated-Particle Fuel Materials

By Joseph H. Oxley*

[*Editor's Note: Dr. Cunningham's Feature Article on nuclear applications of powder techniques, in the last issue of* Reactor Materials, *characterized coated-particle technology as "one of the potentially most useful developments" of our time, with "virtually unlimited" possible applications. The Feature Article below corroborates this observation with an abbreviated but rather thorough review of the history and state of the art of coated-particle developments.*

To most of us, coated particles represent a new and "exciting" (to use the author's word) horizon for fuel materials. However, as Dr. Oxley points out, particle coating is as old as hailstones, and nuclear fuel particles were being coated at Argonne National Laboratory as long as 14 years ago.

A pioneer in coated-particle-fuels development, Dr. Oxley is quick to call attention to the complexity of the problems stemming from the overwhelming number of variables to be considered. In spite of this, as you will note from the discussion that follows, the extensive research in progress in this important field is producing its share of positive results.]

Introduction

One of the most exciting types of fuel materials which have been intensively studied during the last few years consists of particulate fissionable material, with each tiny particle encapsulated in a coating. The coating can serve any or all of the following functions:

1. Retain fission products, thereby reducing the shielding and maintenance costs associated with noncore components
2. Protect the fuel from embrittling attack by the coolant or matrix materials
3. Minimize diffusion and decomposition of the fuel itself at high temperatures during irradiation
4. Protect the matrix of a dispersion fuel from fission-recoil damage
5. Permit fabrication of dispersions at lower cost and with better fuel distribution than those achievable with uncoated particles
6. Prevent hydrolysis by moisture in the air during fabrication of fuels containing thorium or plutonium carbides
7. Minimize safety hazards associated with plutonium fuels

Although the use of coated particles is not a panacea for all material problems in reactor technology, it frequently does provide another degree of freedom in solving these problems. A large number of core, matrix, and coolant combinations are possible for use over an extended temperature range by application of coatings to the fuel particles, as well as, of course, to the matrix or element itself. However, this additional degree of freedom has its price, and the price appears to be a seemingly

*Assistant Chief, Chemical Vapor Deposition Division, Battelle Memorial Institute.

endless assortment of variables to be considered. In considering coated-particle technology, three basic facts should be recognized:

1. There are many methods of coating particles.

2. There are many different coating materials.

3. The properties of a coating are functions of the coating method and the coating material.

Most of the current studies on preparation of coated-particle fuels involve chemical vapor-deposition processes. Many of the reactions used to vapor deposit these coatings chemically are described in the monograph *Vapor Plating*.[1] A wide variety of materials can be chemically vapor deposited, including metals, metalloids, oxides, carbides, nitrides, silicides, borides, and sulfides, either as single components or as solid solutions or multiphase deposits. However, other coating techniques are also possible and have been used for many years. Coated particles have been prepared by electrolytic, electrostatic, precipitation from solution, polymerization from solution, vacuum deposition, pelletizing, replacement reaction, spraying, solution evaporation, and coextrusion techniques. Since the chemical vapor-deposited coatings have been most extensively studied in the nuclear field, this discussion will be directed primarily toward these materials.

The properties of even a single pure vapor-deposited material can be varied over a wide range. In the case of oxide deposition, coatings deposited at low temperatures contain considerable porosity, whereas higher temperature coatings approach theoretical density. The density of pyrolytic carbon coatings is a complicated function of temperature, rate of deposition, and probably apparatus design. The density of metallic coatings can also be varied.

The orientation of the coatings can likewise be varied. Under some conditions it has been reported that the *c* axis of alumina coatings on UO_2 particles is nearly perpendicular to the surface, whereas other deposition conditions produce alumina coatings with the *c* axis aligned more nearly parallel to the surface. The crystallite size of most coatings is smallest at low deposition temperatures and increases with increasing temperatures. Finally, the nature of the substrate itself can affect the properties of the deposit, and the choice of reactants has also been found frequently to affect the coating structure. On the basis of this multitude of variables, it is understandable that crushing disappointments as well as pleasant surprises were found by early investigators in this field.

Background

At the present time it is fairly clear that no one person actually was responsible for a unique suggestion* concerning the manufacture and full utility of coated-particle nuclear fuels. Three of the reasons are as follows: (1) particles were being coated before the advent of nuclear energy, (2) when some of the advantages of coatings on nuclear fuel particles were recognized, techniques to prepare many of the coatings of interest were not known to those in the field, and (3) those investigators using and developing suitable coating processes in the more recent past for other applications were unaware of the problems in the nuclear materials field.

The techniques to prepare and consolidate coated particles are as old as history itself. Hailstones, a natural form of vapor-deposited coated particles, have been produced for the past 10^9 years. Roscoe[3] discussed vapor deposition of vanadium in 1869, and Mond[4] was using vapor deposition industrially in the last part of the nineteenth century to produce carbonyl nickel. The particle shown in Fig. 1 is an example of what is probably the first type of

*In attempting to go back and give this background information on the development of a "unique" concept, some comments of Pardee[2] on uniqueness appear pertinent. A modified expression for his "uniqueness coefficient" is

$$pU = \sum_{i=0}^{\infty} N_i e^{-q_i t_i}$$

where pU, equal to $-\log U$, is the uniqueness coefficient, U is the uniqueness, and N is the number of investigators who report on the concept with a time lag t. The "priority coefficient," q_i, is not a constant but a complex function of the date of written record, relative incompleteness of the written statement, classification status of the record, and the number of cocktail parties jointly attended by members of the various laboratories. One of the principal advantages of the logarithmic scale is that it is less likely to wound the price of the party concerned. A pU of 2 is much easier to bear than the flat statement that a contribution claimed by three people simultaneously is only 1/100 as unique as if it were truly unique.

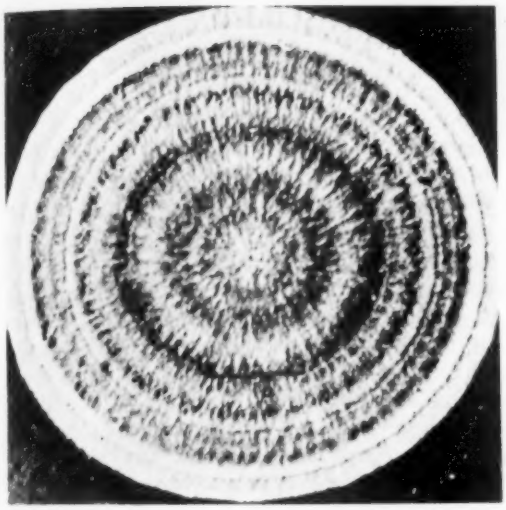

Fig. 1 The etched section of a particle of ME carbonyl iron powder, obtained by replica technique with the electron microscope.[5]

coated particle produced commercially; it was obtained by the pyrolysis of iron carbonyl.[5] Electrolytic-deposition techniques have been used on a commercial basis[6] since the 1860's, and electroless coatings were first patented by Liebig[7] in 1861. Pelletization techniques for iron-ore concentrates were invented by Andersson[8] in Sweden in 1912, and vacuum-evaporated coating technology is at least as old.

One of the earliest references to a coated particle per se was in 1928, when Gross and Zimmerley published the results of some studies on grinding which they had carried out for the U. S. Bureau of Mines.[9] In order to determine the surface areas of quartz powders used in grinding studies, they coated the quartz powder with thin uniform films of silver by the use of a modified mirroring solution. C. M. Heath, C. L. Faust, B. W. Gonser, and O. E. Harder of Battelle prepared tin-coated copper particles by hydrogen reduction of tin chlorides in January 1936 in attempting to develop new brazing compounds or improved metallurgical bodies. Patents to fabricate coated particles into massive bodies were awarded in 1936 for metal-coated particles[10,11] and in 1941 for oxide-coated particles.[12] The preparation of pigments by vapor-phase oxidation of halides, cracking of hydrocarbons to produce carbon black, and fluid coking are developments which have taken place in the thirties, forties, and fifties and which have led to process developments for coated particles in general.

One of the most significant steps leading to the advancement of coated-particle technology was an article written by Cline and Wulff[13] at the Massachusetts Institute of Technology (MIT) in 1951 and presented orally in April of that year. They reported on their studies to coat powders with thin metallic films using fluidized-bed vapor-deposition techniques and to use these materials to fabricate improved structural bodies. This article touched off a wave of investigations, particularly at Battelle and Du Pont. Intensive studies on fluidized-bed vapor-deposition processes for the production of metals and coating of powders were carried out by W. A. Jenkins, H. W. Jacobson, H. W. Ling, L. Bertrand, and C. M. Olsen at Du Pont, and by F. M. Stephens, W. A. Coffer, F. A. Sliemers, Jr., I. E. Campbell, C. F. Powell, J. M. Blocher, Jr., and J. H. Oxley at Battelle.

More recent work on coated particles involves solution techniques, and it is suspected that many new developments will be forthcoming from this area. Du Pont's T. D. nickel process, National Cash Register's polymerization process, Sherritt Gordon's nickel- and cobalt-coating process, Southwest Research's pulsed-extrusion process, and the sol techniques developed by W. R. Grace & Co., and Du Pont will continue to provide interesting material combinations.

The first work in the United States involving a coated fuel particle was evidently carried out at Argonne National Laboratory (ANL) in the summer[14] of 1949. Uranium spheres were coated on an experimental basis with electroless nickel films to avoid subsequent recoil damage to the cladding in a fast reactor. The studies were carried out at the suggestion of H. Stanton by R. N. Noland, G. B. O'Keeffe, and D. E. Walker. A photomicrograph of one of their compacts is shown in Fig. 2. The next step in the development of coated fuels was based on an extension of work carried out at Knolls Atomic Power Laboratory (KAPL) and Battelle Memorial Institute (BMI) on electrolytically depositing copper on beryllium to protect the beryllium against a sodium environment. A. P. Beard of KAPL suggested that the preparation and properties of beryllium components might be enhanced if copper-coated beryllium powder were used, and Backensto, Hopson, and Lenel at

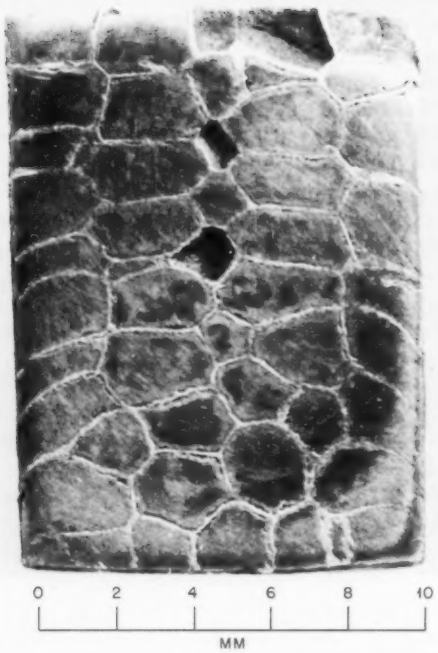

Fig. 2 Example of first fuel element fabricated from coated particles. Longitudinal section through specimen after 550 cycles. Several small remnant balls have dropped out.[14]

Rensselaer Polytechnic Institute (RPI) first reduced this to practice[15] in 1951. An interesting switch in emphasis was found in a patent filed in March 1951 by Flint in England.[16] He obtained a composition-of-matter patent on a fuel-coated particle in which the fissionable material was electrically deposited as a coating on a metal-coated BeO, or other nonfissionable oxide, core.

Subsequent work at KAPL by A. P. Beard, J. R. Peloka, and R. N. Honeyman in December 1955 was carried out using a milling technique to smear zirconium films on uranium particles from finely divided zirconium metal.[17] Photomicrographs of sections of their coated particles are shown in Fig. 3. Parallel studies on vapor deposition, spray coating, and electrolytic techniques were performed at KAPL and BMI on fuel slugs with moderate success, but no attempt was made to coat particles. General Electric began studies at its Nuclear Materials and Propulsion Operation (GE-NMPO) and General Engineering Laboratory (GE-GEL) in 1958 on the vapor deposition of oxide coatings on extended surfaces. In early 1959 ANL initiated a program on the fluidized-bed vapor deposition of uranium dioxide.[18] This program was suggested by S. Lawroski in 1958 as an extension of much earlier fluidized-bed studies on calcination of dissolved nitrate salts.

In April 1957 R. W. Dayton of BMI suggested the desirability of coating UO_2 particles with fission-product-retentive ceramic films, and H. C. Renken recommended the use of pelletizing techniques. This suggestion was reduced to practice in May 1958 by A. K. Smalley, R. C. Riley, and W. H. Duckworth. J. H. Oxley, working on fluidized-bed vapor-deposition processes for producing niobium and chromium, suggested the use of this technique to coat fuel particles for a fluidized-bed nuclear reactor in an informal letter proposal in August 1957. During the same month, Nuclear Materials & Equipment Corp. (NUMEC) submitted a proposal to the AEC entitled "The Preparation of Corrosion Resistant and Radiation Damage Resistant Uranium Metal." Vapor deposition of metal and oxide coatings on fuel particles was informally proposed by BMI to C. C. Browne of GE-ANP in September 1957 and again in January 1958 and also to L. R. Sitney of Los Alamos Scientific Laboratory (LASL) in January 1958. LASL sponsored the first study on vapor-deposited metallic coatings on fuel particles at Battelle in February 1958, and GE-ANP sponsored the first studies on vapor-deposited protective oxide coatings on fuel particles in February 1959. J. F. Hannah developed the tungsten-coating process, and N. D. Veigel developed the Al_2O_3 process. Between April and June 1958, J. L. Zambrow and I. Sheinhartz attempted to coat UO_2 particles with niobium films at Sylvania by hydrogen reduction of the pentachloride but were unsuccessful. Goslee[19] tried to coat UO_2 powder with zirconium at Martin Co. using the magnesium reduction of zirconium tetrachloride between August 1958 and April 1959.

Surprisingly, the concept of a carbon-coated particle in the United States apparently arose rather late in the history of coated-particle fuels. Carbon coating of fuel platelets was carried out for Bettis Atomic Power Division (BAPD) in February 1959 by E. H. Layer. The carbon coating of particles was discussed with L. D. Stoughton of Sanderson & Porter (S&P)

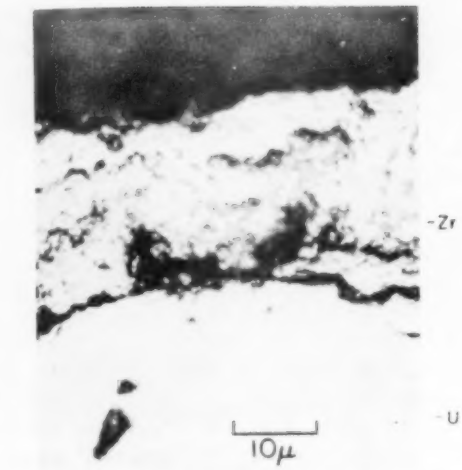

Bright field, as polished

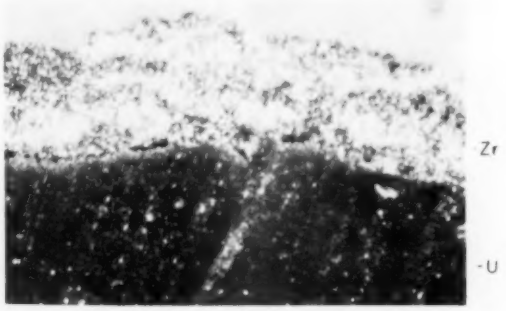

Polarized light, as polished

Fig. 3 Uranium particles coated with zirconium.[17]

and W. V. Goeddel and D. H. Gurinsky of General Atomic (GA) during 1959 and was reduced to practice at BMI by N. D. Veigel and J. M. Blocher, Jr., in October 1959 after they had completed their extensive program on metal and alloy coatings.[20] Carbide coatings on nuclear fuel particles had been discussed in some detail, particularly with W. W. Godsin, R. J. Pyle, and W. V. Goeddel of GA, during the previous year. Huddle[21] applied for a patent on a carbon-coated fuel particle in England in March 1959, and Minnesota Mining & Manufacturing Co. is believed to have started studies in this field about the same time.

Although a fairly extensive record of Battelle's activities in this field is available to the author, our knowledge of other research is obviously secondhand and may not be strictly accurate. In addition, we have almost no knowledge of early work in other countries or in industrial laboratories. Therefore this background information may not be complete, and, if serious omissions or errors have been made, the writer would be pleased to correct the record.

Materials Preparation

At least 16 companies and laboratories in the United States and 12 organizations in other countries are now known to be actively engaged in the preparation of coated-particle nuclear fuels. This list includes Allied Chemical Corp., General Dynamics Corp., Minnesota Mining & Manufacturing Co., Union Carbide Corporation, Nuclear Materials & Equipment Corp., Raytheon Co., Speer Carbon Co., United Nuclear Corp., W. R. Grace & Co., Diamond Alkali Company, Battelle Memorial Institute, The Martin-Marietta Corp., General Electric Company, Nippon Carbon Co., Ltd., Mitsubishi Metal Mining Co., United Kingdom Atomic Energy Authority, Royal Aircraft Establishment, Australiar Atomic Energy Commission, European Nuclear Energy Agency, Metallwerk Plansee, Geschäftsvenein der Osterreich Studiengesellschaft fuer Atomenergie, Nuklear-Chemie und -Metallurgie, G.m.b.H., Centre d'Étude de l'Énergie Nucléaire, Commissariat à l'Énergie Atomique, and the Polish Academy of Nuclear Sciences.

As evidenced by the above list, the amount of effort being expended in this area must be enormous, and already two American firms have decided to drop out of the field. It seems rather unlikely that all the remaining commercial organizations will be able to develop profitable operations, but it also seems rather unlikely that many potential fuel materials or applications will be neglected or missed. The only major application that has been announced is the Peach Bottom High-Temperature Gas-Cooled Reactor (HTGR) of General Atomic, which is scheduled for construction near Philadelphia in 1963. It will employ carbon-coated uranium-thorium dicarbide particles in a graphite-matrix element for operation at temperatures up to 1500°C.

Most of the information presented in the following sections was reviewed in detail at an

international symposium sponsored by AEC at BMI on Nov. 5 and 6, 1962. The papers presented at this meeting have been published as USAEC Report TID-7654, and the interested reader is referred to this report for the most complete review available today.[22]

Carbon Coatings

The most widely used carbon-coating process is based on vapor deposition of carbon in fluidized-bed equipment. However, the use of vibrating trays and rotating drums has also been reported, and most of the equipment used in various laboratories has been discussed in detail in Sec. I of this issue and previous issues of *Reactor Materials*. The feed materials for the vapor-deposition processes include methane, acetylene, propane, hexane, benzene, and natural gas. Coating temperatures between 950 and 2000°C have been reported, and temperatures of about 1400°C seem to be the most popular. In addition, Japanese investigators have recently revealed the preliminary results of a carbon-coating process based on carbonizing an organic coating obtained by polymerization techniques.

A suggested plant layout for coating particles on a commercial basis with carbon is shown in Fig. 4. The fuel is batch-charged from a feed hopper into a fluidized-bed reactor which is heated by the flow of electric current between electrodes immersed in the fluidized bed. This method of heating has been studied at Harwell and BMI. The principal fluidizing stream is dried natural gas which consists of about 95% methane and which is essentially free of nitrogen. Argon fluidization gas is also used during startup and shutdown to control the rate of deposition and to purge the system. The off-gases from the reactor are sent to a water scrubber to be cooled and to drop out elutriated radioactive dust. The cooled gases are then passed through a demister and a final filter before they are exhausted to the atmosphere. The scrubber water effluent is filtered and dumped.

The structure of a 1400°C pyrolytic coating varies from "columnar" to "laminar," depending on the deposition rate. These terms are applied because of the microscopic appearance of the material—the columnar type appears to consist of radially oriented grains (although the crystallite size is much smaller than the appearance would indicate), and the laminar coating appears to consist of concentric spherical shells. The type of coating obtained depends on the conditions of deposition. Coatings applied at deposition rates of less than 10 μ/hr at a temperature of 1400°C are columnar in appearance, as shown in Fig. 5, whereas those applied at higher rates have a laminar appearance, as

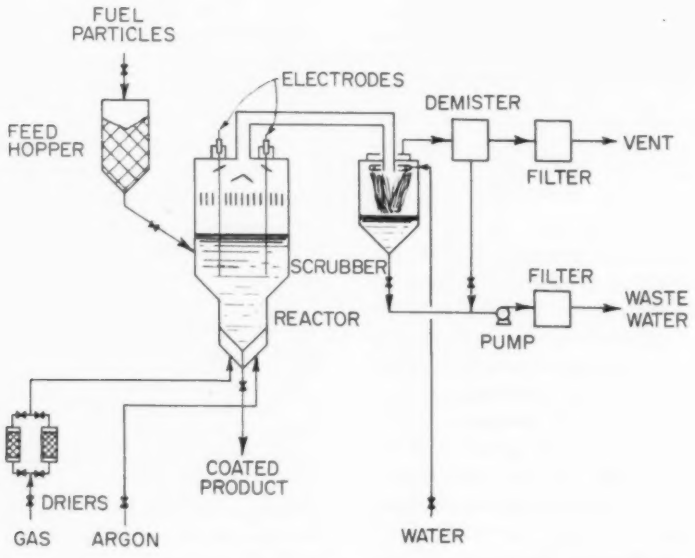

Fig. 4 Schematic diagram of plant for coating carbide powders with pyrolytic carbon in a fluidized bed.

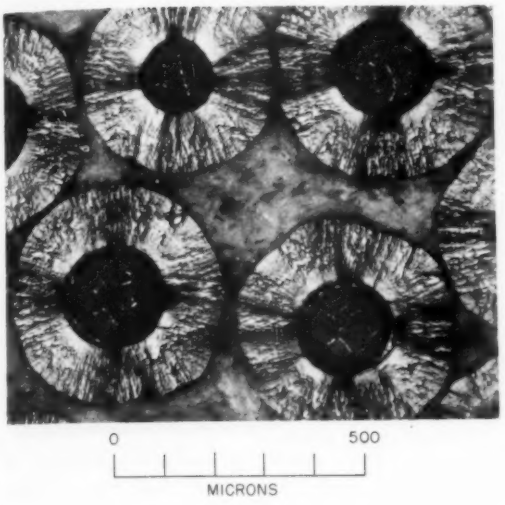

Fig. 5 Columnar carbon coating on uranium carbide fuel particles (courtesy of M. F. Browning)

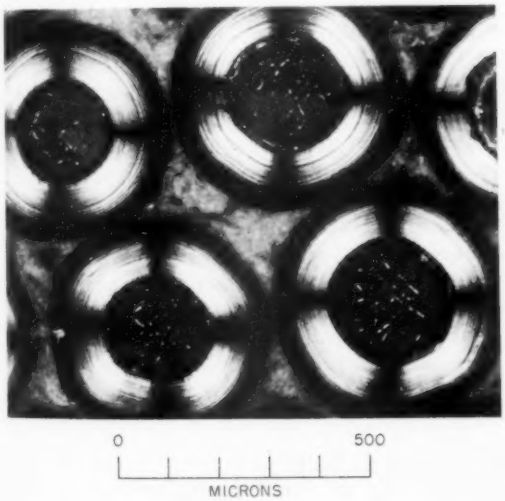

Fig. 6 Laminar carbon coating on uranium carbide fuel particles (courtesy of M. F. Browning).

shown in Fig. 6. The crystallite size of pyrolytic carbon (PyC) coatings also varies with temperature and rate. The c-axis crystallite size of a laminar coating deposited at 1400°C and below is about 25 A and increases to about 150 A at a coating temperature of 1800°C. Columnar coatings prepared at about 1400°C have a crystallite size of approximately 40 A. The structure of the deposited carbon is two dimensional, consisting of layers stacked in parallel groups with the c axis being radial, but the layer planes show a completely random orientation with respect to adjacent planes. A c-axis spacing of about 3.5 A has been reported. The apparent density of the coatings is also strongly affected by the deposition conditions. Figure 7 shows the effects of coating temperature and deposition rate on the coating density.

One of the most interesting carbon-coated uranium dicarbide materials is a sample prepared by Union Carbide for Oak Ridge National Laboratory (ORNL) and is shown in Fig. 8. It

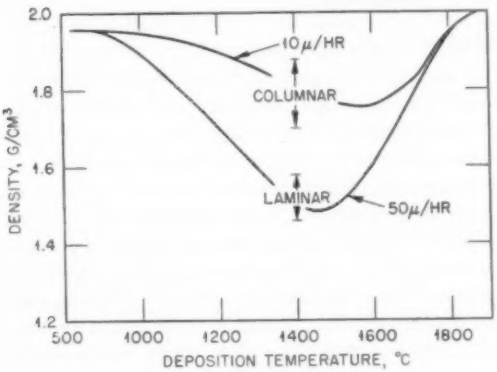

Fig. 7 Density of PyC coatings.[22]

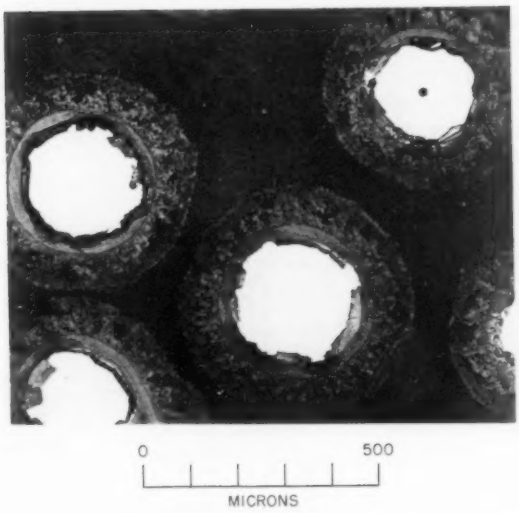

Fig. 8 Duplex carbon coating on uranium carbide fuel particles (courtesy of W. O. Harms).

consists of a 20-μ inner layer of laminar carbon, over-coated with an 80-μ layer of columnar carbon, and is generally referred to as a duplex coating. This material appears as though it was initially coated at a relatively low temperature (1400°C) and at a relatively high rate (50 μ/hr) and then over-coated at a relatively high temperature (1800°C) and moderate rate (25 μ/hr). This material has exhibited good fission-product retention at burnups of about 28 at.% uranium, and its performance will be discussed later in greater detail. Some of the newest types of carbon coatings being investigated have metal carbide additions and inner layers of porous carbon, metal carbides, and/or metal oxides.

Metallic Coatings

Although there is currently relatively little interest in metallic coatings, the major effort in the coated-particle fuel field started with these materials. The loss of interest is apparently the result of the desire to exploit higher temperature levels, where the various metal coatings are either not stable or have cross sections too high to be economically attractive for thermal reactors. A schematic flow diagram of the preferred process for coating particles with metallic films is shown in Fig. 9. Crude metal chloride feed would be purified by distillation and then pumped directly into a bed of fuel particles suspended at elevated temperatures by a fluidizing stream of hydrogen. The chloride feed vaporizes in the bed where it is subsequently reduced to metal, which deposits on the extended surface provided by the particles in the fluidized bed. Excess hydrogen from the reactor, containing by-product HCl gas, is then cooled and washed with water or alkaline solution to remove the HCl. The scrubbed hydrogen is then dried and recycled through a heat exchanger back into the reactor. Makeup reductant hydrogen is added periodically to maintain a balance of pressure, and makeup water is introduced in proportion to the rate of removal of HCl.

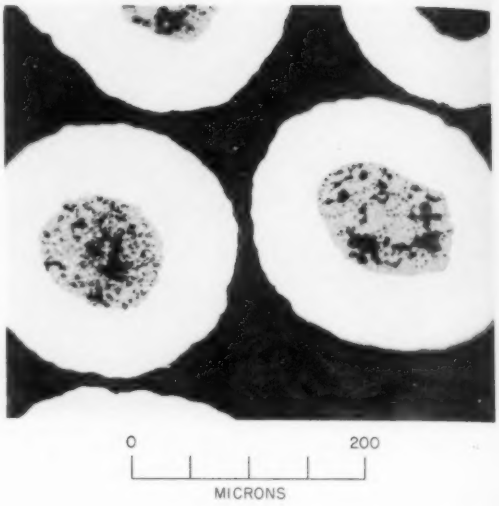

Fig. 10 Niobium-coated uranium dioxide fuel particles.[20]

Metals that have been prepared in such a process include niobium, tungsten, molybdenum, cobalt, chromium, iron, nickel, silicon, titanium, and tantalum, as well as the alloys Nichrome and niobium-vanadium. An example of the type of product that can be produced in such a process is shown in Fig. 10, which is a photo-

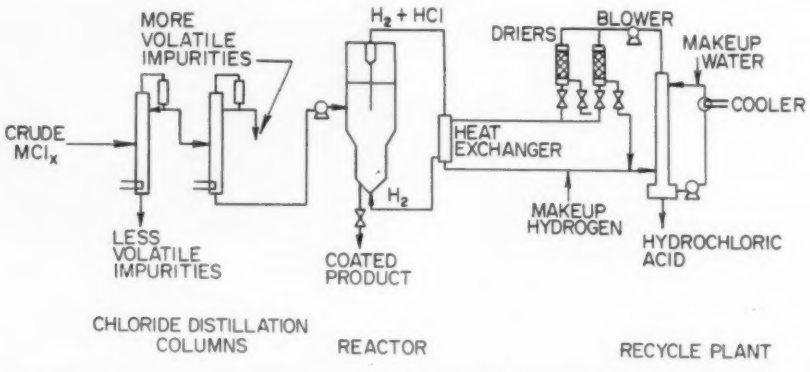

Fig. 9 Schematic diagram of plant for hydrogen reduction of a metal chloride in a fluidized bed.

micrograph of niobium-coated uranium dioxide particles. The coatings are generally of a very fine-grain structure, and their purity depends primarily on the purity of the chloride feed and the hydrogen reductant. Coating rates of up to 50 μ/hr have been achieved, although rates of 5 μ/hr are more typical in laboratory-scale equipment. Vibrating trays have also been used for preparing metal coatings, but no reference to rotating-drum reactors has been located. Procedures to deposit metallic coatings by electrolytic, electroless, and vacuum deposition have also been reported.

Oxide Coatings

The oxide-coating processes that have been reported involve the hydrolysis of volatile metal halides in fluidized-bed reactors. The water vapor can be injected directly into the reactor or synthesized indirectly by the reaction between hydrogen and carbon dioxide. A schematic plant layout for an oxide-coating facility is shown in Fig. 11. The major difference between this plant and the previously discussed units would be that the heat load in the reactor would be supplied by the combustion of natural gas, and the principal feed stream, a metal chloride, would be generated by reacting anhydrous hydrogen chloride with the metal. The other plant components are almost identical to those of a carbon-coating plant. Nitrogen should be a satisfactory purge gas for use with the oxide-coating chemistry.

The precise conditions necessary to produce dense, impermeable coatings in fluidized-bed deposition differ for the various oxides. In general, porous coatings are deposited at the lowest temperature, perhaps because under these conditions the oxide nucleates in the gas phase and subsequently attaches itself to the surface of the fuel particles, or possibly owing to the deposition of intermediate products such as the oxyhalides or hydrated oxides, which are subsequently converted to the oxide with corresponding density changes. At higher temperatures either the intermediates do not form, the nucleation tendency of the system is reduced as a result of a shift in the reaction equilibrium, or the material recrystallizes quickly so that dense material is obtained. At still higher temperatures rapid grain growth occurs, and the deposits are generally weaker and have an integrity inferior to that of coatings deposited at intermediate temperatures.

Alumina coatings deposited at temperatures from 500 to 700°C are porous and of low density, and X-ray diffraction examination indicates that they are amorphous. However, the coatings become crystalline on heating at

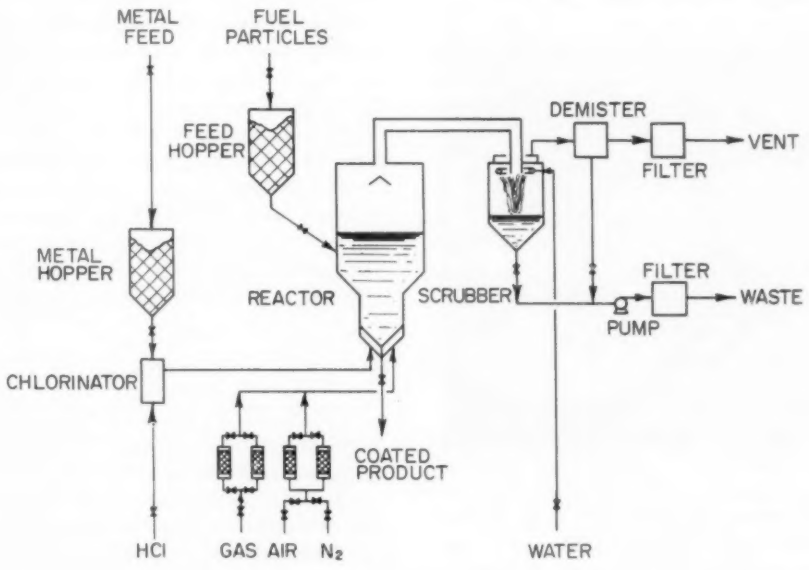

Fig. 11 Schematic diagram of plant for coating oxide particles with oxide films in a fluidized bed.

temperatures of about 1000°C and above. Alumina coatings of near theoretical density are deposited at 1000°C. These are impermeable and consist of small crystallites of alpha alumina with an average size of 0.3 μ, dispersed in what appears to be an amorphous matrix. Coatings deposited at higher temperatures become more crystalline. Those deposited at 1400°C are highly crystalline and have an average crystallite size of about 25 μ but exhibit a coating integrity inferior to that of 1000°C coatings. A photomicrograph of a coarse-grained Al_2O_3 coating prepared at a temperature of 1400°C is shown in Fig. 12. The hardness of the coatings prepared at 1000°C and above is equal to or higher than that of sapphire (2200 to 2500 KHN, 50-g load).

Beryllia coatings must apparently be deposited at higher temperatures than alumina coatings to obtain equivalent properties. Thus coatings deposited at temperatures between 800 and 1100°C are not obviously crystalline, and they are porous. However, at deposition temperatures of 1400°C, the coatings are impervious. Beryllia coatings prepared at 1400°C are of near theoretical density, are very crystalline, and have good integrity. A photomicrograph of a typical beryllia coating deposited at a temperature of 1400°C is shown in Fig. 13. The average crystallite size in the BeO coatings increases as a function of temperature.

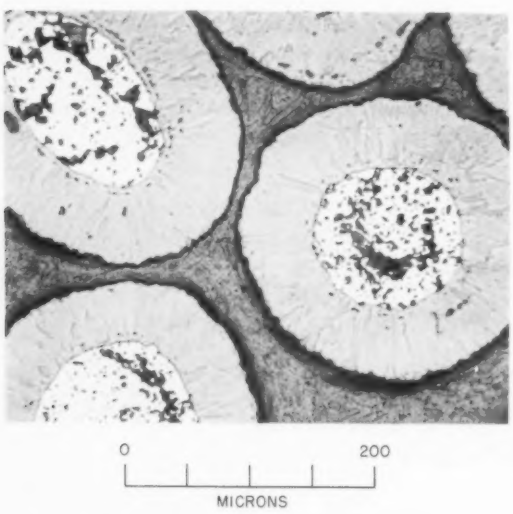

Fig. 12 Alumina-coated uranium dioxide fuel particles.[22]

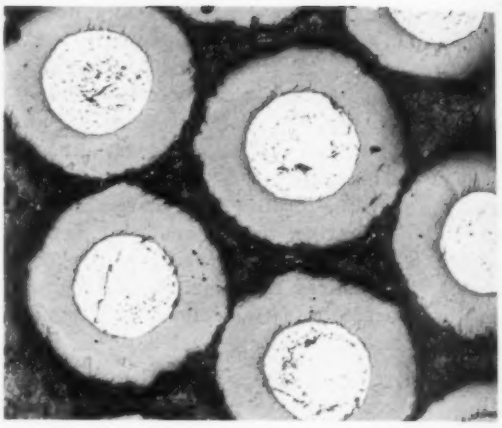

Fig. 13 Beryllia-coated uranium dioxide fuel particles.[22]

At temperatures below about 1100°C, the crystallites are of submicron size but increase to about 7 μ at temperatures of about 1400°C. The hardness of the 1400°C coating is essentially equal to that of single-crystal BeO (1200 to 1400 KHN, 50-g load).

Production of a number of combinations of oxide, metal, carbon, and carbide coatings on various types of fuel substrates, either with or without porous or void regions within the coating or core, is possible. The purpose of the void regions is to provide space for irradiation-induced expansion of fuel and possibly the coating, as well as space for accumulation of fission-product gases, or to serve as barriers to crack propagation. Inner layers of different types of materials can protect the outer coating from direct fission-recoil damage, trap fission products, and limit crack propagation.

Fabrication of Elements

Procedures to disperse coated particles in matrices or to fabricate elements directly were described in the February 1963 issue of *Reactor Materials* (Vol. 6, No. 1), in the feature article entitled "Recent Developments in Reactor Materials from Powders." The reader is referred to this review for a concise summary of the latest advances in this area.

Irradiation Behavior

The first investigation of the fission-product retentivity of coatings on fuel particles was carried out by BMI for Sanderson & Porter under the auspices of the AEC. The Sanderson & Porter experiment consisted of irradiating a $1^1/_2$-in.-diameter graphite sphere, fueled with 127-μ UO_2 particles coated with 42 μ vapor-deposited Al_2O_3, at temperatures between 730 and 510°C, to burnups of about 6 at.% uranium. The initial fractional fission-product release was in the range of 10^{-7} to 10^{-9} but increased with time to 10^{-2} to 10^{-5} after 150 days of irradiation, apparently as a result of temperature-dependent radiation damage. A summary of the irradiation results is shown in Fig. 14, where the fractional release of fission products is presented as a function of half-life of the fission product and the burnup level. A photomicrograph of a typical fuel particle before irradiation is shown[23] in Fig. 15; a photomicrograph of an undamaged fuel particle after irradiation is shown[24] in Fig. 16; and a photomicrograph of radiation-damaged particles is shown[24] in Fig. 17. It was found in subsequent postirradiation studies that the coating damage was a very strong function of radial position in the graphite sphere, the coating damage, expressed in terms of cracked coatings, being complete at the surface of the sphere and negligible at the center. The results are shown[23] graphically in Fig. 18. Later studies in a variable-temperature sweep capsule have provided strong evidence to suggest that the temperature gradient over the ball during irradiation led to this dependence of damage on radial position. Irradiation temperatures below about 500°C led to very rapid failure of Al_2O_3 coatings, whereas temperatures somewhat above about 500°C evidently permit radiation damage to anneal, and no significant coating failure is observed.

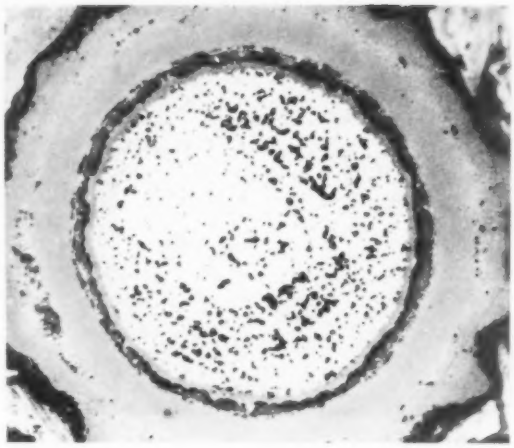

Fig. 15 Alumina-coated uranium dioxide prior to irradiation.[23]

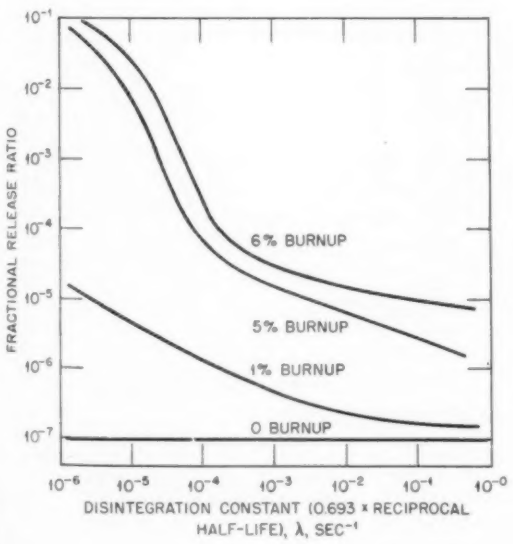

Fig. 14 In-pile fission-product-release behavior of alumina-coated dioxide particles during Sanderson & Porter experiment (courtesy of G. E. Raines).

A considerable accumulation of irradiation data are now available from ORNL, GA, and BMI. A summary of long-term sweep results is shown graphically in Fig. 19. All the ORNL data are based on 200-μ UC_2 particles having 100-μ PyC coatings without any support from a matrix. The vendors supplying the ORNL program have had difficulty putting the coated particles in matrices, and the data obtained at ORNL on matrix samples are not believed to be representative. The GA data were obtained at considerably higher temperatures than those used at ORNL or BMI, and, in addition, the particles were tested in a graphite matrix. The fuel consisted of 200-μ thorium-uranium dicarbide particles coated with 10 to 60 μ of PyC. The BMI studies were carried out at essentially the same temperature levels as those employed by ORNL, but all results are

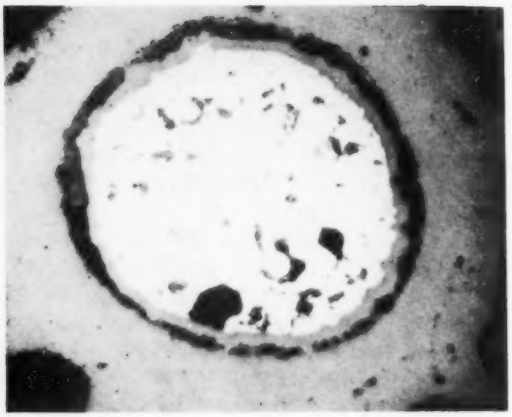

Fig. 16 Undamaged alumina-coated uranium dioxide particle after irradiation.[24] Magnification, 500×.

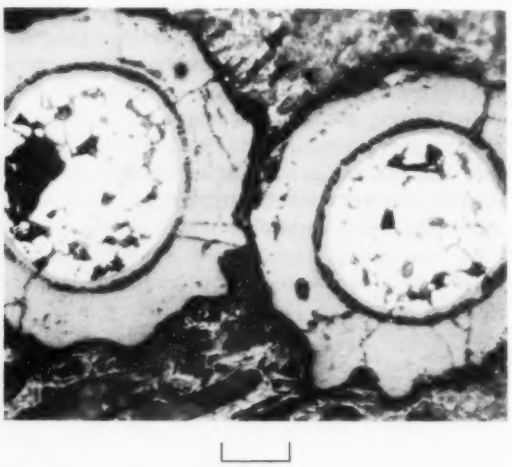

Fig. 17 Damaged alumina-coated uranium dioxide particles after irradiation.[24] Magnification, 250×.

for coated particles in graphite-matrix samples. At high temperatures (800 to 1100°C), the use of a graphite matrix is not believed to be a major variable, although at low temperatures it apparently does retain significant amounts of fission products. The fuel-particle diameters of 127 μ used in the BMI studies are smaller than the 200-μ material employed at GA and ORNL, and the data from BMI are only for uranium dioxide fuel. Although BMI has some limited sweep results on carbon-coated carbide fuel (<1% burnups), the results were similar to the ORNL data for simple laminar or columnar coatings.

Because of the wide variation in parameters being studied, it is difficult to reach firm conclusions. However, the following tentative conclusions are drawn from the data:

1. A 100-μ duplex coating consisting of an inner layer of laminar carbon and an outer layer of columnar carbon offers an order of magnitude improvement over simple laminar or columnar coatings at temperatures of 800 to 900°C.

2. Coatings of 40 to 60 μ of either BeO or Al_2O_3 offer 3 to 4 orders of magnitude improvement over PyC coatings on UO_2 at temperatures of 800 to 900°C.

3. PyC coatings exhibit about the same degree of fission-product retentivity on UO_2 as on UC_2 when the coating-thickness to core-diameter ratio is held constant at temperatures of about 800 to 900°C.

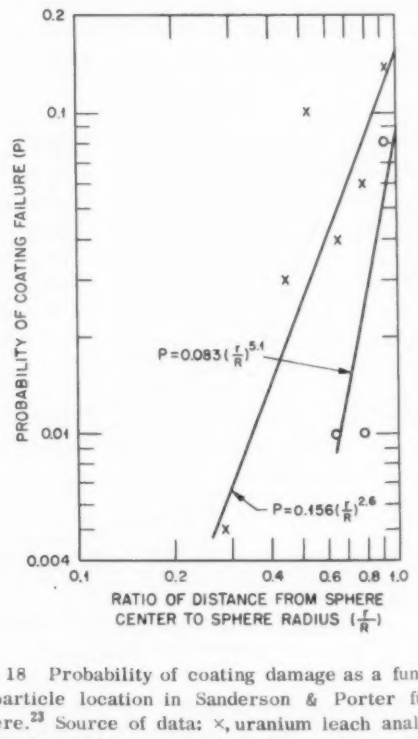

Fig. 18 Probability of coating damage as a function of particle location in Sanderson & Porter fueled sphere.[23] Source of data: ×, uranium leach analysis. ●, metallographic examination of separated particles.

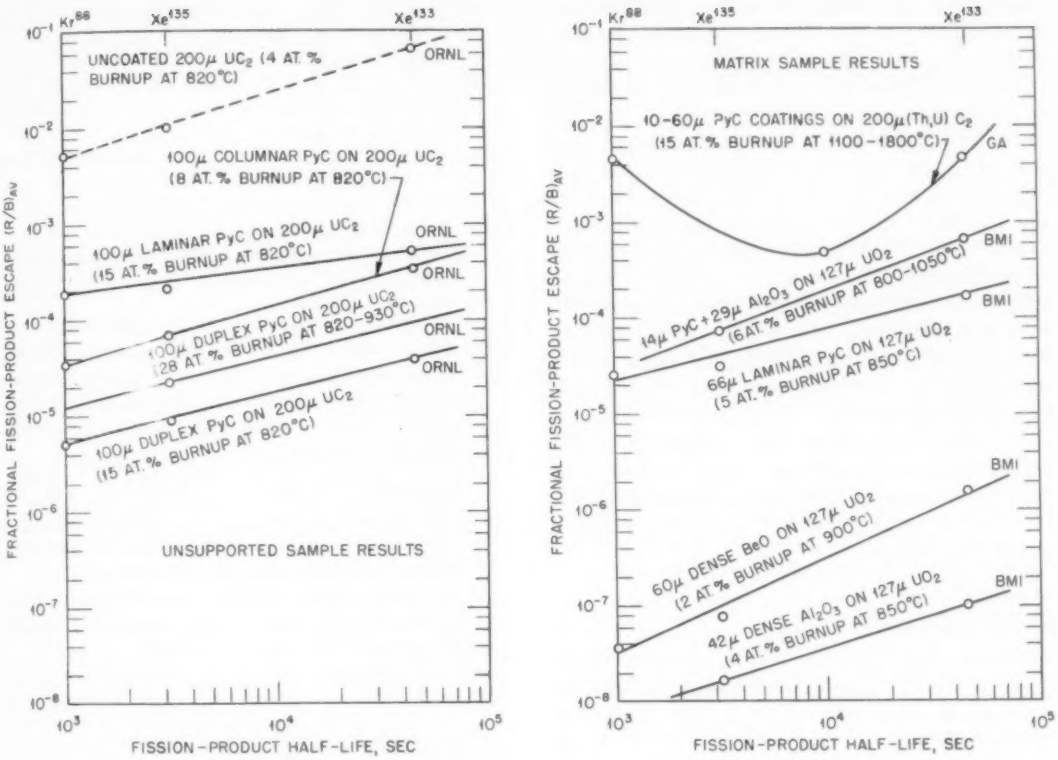
Kr88
Xe135
Xe133
UNCOATED 200μ UC2 (4 AT. % BURNUP AT 820°C)
ORNL
100μ COLUMNAR PyC ON 200μ UC2 (8 AT. % BURNUP AT 820°C)
100μ LAMINAR PyC ON 200μ UC2 (15 AT. % BURNUP AT 820°C)
100μ DUPLEX PyC ON 200μ UC2 (28 AT. % BURNUP AT 820-930°C)
100μ DUPLEX PyC ON 200μ UC2 (15 AT. % BURNUP AT 820°C)
UNSUPPORTED SAMPLE RESULTS
FRACTIONAL FISSION-PRODUCT ESCAPE (R/B)Av
FISSION-PRODUCT HALF-LIFE, SEC
MATRIX SAMPLE RESULTS
10-60μ PyC COATINGS ON 200μ(Th,U) C2 (15 AT. % BURNUP AT 1100-1800°C)
GA
14μ PyC + 29μ Al2O3 ON 127μ UO2 (6 AT. % BURNUP AT 800-1050°C)
BMI
66μ LAMINAR PyC ON 127μ UO2 (5 AT. % BURNUP AT 850°C)
60μ DENSE BeO ON 127μ UO2 (2 AT. % BURNUP AT 900°C)
42μ DENSE Al2O3 ON 127μ UO2 (4 AT. % BURNUP AT 850°C)

Fig. 19 Results of sweep experiments on coated-particle fuels.[22]

4. The behavior of a coating that consists of an inner layer of PyC under an Al_2O_3 coating is similar to that of a simple PyC coating at temperatures of 800 to 900°C.

ORNL has suggested that coating thickness may be one of the most significant factors in the performance of carbon coatings, and considerable work is in progress to test this hypothesis.

No information on the retention of fission products by metallic films has been found, but it is presumed that the metal coatings would offer relatively good retentivity on the basis of the resistance of many metals to irradiation damage.

It seems probable that, by the use of some of the many possible material or structural modifications, failure at ambient temperatures can be avoided. However, the other end of the temperature scale will probably present the final limitations on the use of coated-particle fuels. The knowledge in this temperature region is still extremely limited. GA has carried out experiments with carbon-coated particles at temperatures up to 2000°C, and, as expected, the coatings were not satisfactory for complete retention of fission products at these high-temperature levels. GA has also found evidence of severe migration of carbide fuel into a carbon coating under a temperature gradient of 3°C per particle at temperature levels of about 1800°C. Harwell, GA, and ORNL have reported on significant bulk diffusion of uranium in carbon coatings at temperatures above 1800°C, as well as the rapid mobility of barium, strontium, and other periodic Group II fission products at temperatures of about 1400°C.

Summary

On the basis of the potential of coated-particle fuels, the favorable irradiation performance of a number of the coatings, the availability of low-cost manufacturing tech-

niques, and the large amount of research and development effort being expended on these materials, the ultimate widespread use of coated particles seems assured. Reduction in coolant contamination by a factor greater than 10^6 over long periods of operation appears quite feasible, offering the possibility that shielding could be eliminated on all noncore components, thereby significantly reducing plant investment costs. The Peach Bottom reactor will be the first commercial unit to use a coated-particle fuel, and concepts similar to the Pebble Bed or the Dragon reactors will probably be next. During the next 10 to 20 years, a number of other reactor concepts for which coated-particle fuels are suitable will probably be brought to fruition. In addition, other applications for coated-particle fuels may also be developed, including their use in chemonuclear systems, for fuel-disposal purposes, and perhaps direct power conversion.

References

1. C. F. Powell, I. E. Campbell, and B. W. Gonser, *Vapor Plating*, John Wiley & Sons, Inc., New York, 1955.
2. A. B. Pardee, pU: A New Quantity in Biochemistry, *Am. Scientist*, 50: 130A (1962).
3. H. E. Roscoe, *Trans. Roy. Soc. (London)*, 159: 689 (1869).
4. L. Mond, Metallic Carbonyls, *Proc. Roy. Inst. Gt. Brit.*, 13: 668 (1892).
5. The Mond Nickel Company Limited, *Mond Carbonyl Iron Powders*, Raithby, Lawrence & Co., Ltd., Leicester.
6. I. Adams, U. S. Patent 93,157 (1869).
7. J. F. Liebig, U. S. Patent 33,721 (1861).
8. A. G. Andersson, Swedish Patent 35,124 (1912).
9. J. Gross and S. R. Zimmerley, Crushing and Grinding. I. Surface Measurements of Quartz Particles, *Am. Inst. Mining Met. Engrs., Tech. Publ. No. 46* (1928).
10. C. Hardy, U. S. Patent 2,027,532 (1936).
11. C. Hardy, U. S. Patent 2,033,240 (1936).
12. A. F. Bandur, U. S. Patent 2,241,441 (1941).
13. J. E. Cline and J. Wulff, Vapor Deposition of Metals on Ceramic Powders, *J. Electrochem. Soc.*, 98: 385 (1951).
14. Argonne National Laboratory, Metallurgy Division Quarterly Report, July–September 1949, USAEC Report ANL-4364, Sept. 30, 1949.
15. A. P. Backensto, Jr., N. F. Hopson, and F. V. Lenel, Powder Metallurgy of Beryllium, USAEC Report SO-3005, Rensselaer Polytechnic Institute, Dec. 31, 1951.
16. O. Flint, U. S. Patent 2,967,811 (1961).
17. C. A. Bruch, W. M. Cashin, and D. D. White, Metallurgy Report of the Technical Department for December 1955, January, February 1956, USAEC Report KAPL-1526(Del.), Knolls Atomic Power Laboratory, 1956.
18. I. E. Knudsen, N. M. Levitz, and S. Lawroski, Preliminary Report on Conversion of Uranium Hexafluoride to Uranium Dioxide in a One-Step Fluid-Bed Process, USAEC Report ANL-6023, Argonne National Laboratory, August 1959.
19. D. Goslee, Coated Particle Investigation, Final Report, USAEC Report MND-AC-1755-1, Martin Co., Nuclear Division, April 1959.
20. J. M. Blocher, Jr., N. D. Veigel, J. H. Oxley, V. M. Secrest, and E. E. Rose, Fluidized-Bed Coating of UO_2 Powder with Niobium and Other Elements, USAEC Report BMI-1440, Battelle Memorial Institute, May 25, 1960.
21. R. A. U. Huddle, British Patent 878,927 (1961).
22. Ceramic-Matrix Fuels Containing Coated Particles, Proceedings of a Symposium Held at Battelle Memorial Institute, November 5 and 6, 1962, USAEC Report TID-7654, March 1963.
23. R. J. Burian, R. L. Ritzman, J. E. Gates, and R. F. Dickerson, Evaluation of Irradiated Alumina-Coated UO_2 Particles Dispersed in Graphite Spheres, USAEC Report BMI-1572, Battelle Memorial Institute, Mar. 22, 1962.
24. G. E. Raines and W. H. Goldthwaite, In-Pile Fission-Gas-Release Behavior of Alumina-Coated UO_2 Particles Irradiated for High Burnup, USAEC Report BMI-1552, Battelle Memorial Institute, Nov. 6, 1961.

Section I

Reactor Materials

Fuel and Fertile Materials

Uranium Metal and Alloys

A two-volume set of books[1] entitled *Uranium Metallurgy* has just been published. Volume I, *Uranium Process Metallurgy*, includes sections devoted to uranium ore processing, reduction and purification of uranium, uranium fabrication, powder metallurgy of uranium, processing of fuel materials, and safety. Volume II is entitled *Uranium Corrosion and Alloys*. About one-sixth of this volume is devoted to uranium corrosion, and the remainder contains information on uranium alloys. These volumes are significant because they contain information that has become available since the issuance of the second edition of the *Reactor Handbook*. These volumes, however, are more than a compilation of data. They represent a comprehensive review of uranium metallurgy. The section on uranium alloys is the most complete story about the subject that can be found under one cover. (M. S. Farkas)

Unalloyed Uranium

Investigators at Argonne[2] have studied the anisotropy of self-diffusion in alpha uranium by tracer-sectioning techniques. Mosaic-structured single crystals of alpha uranium yielded the following diffusion coefficients at 625.5°C: $D_{[100]} = D_{[001]} = 1.95 \times 10^{-13}$ cm^2/sec, and $D_{[010]} = 10^{-14}$ cm^2/sec. The mosaic structure apparently has not affected the diffusion significantly.

In other self-diffusion experiments, the French[3] measured the activation energy for self-diffusion in alpha uranium and obtained a value of 40 kcal/gram atom.

The English[4] have measured the work function of uranium by the Kelvin contact-potential-difference method under high vacuum. A reproducible value of 3.203 ± 0.013 ev was found for the work function of the vacuum-deposited films. In the case of foil, the work function increased continuously and monotonically with the duration of electron bombardment and eventually reached a limiting value of 3.080 ± 0.005 ev after about a 33-hr bombardment. Reasons were advanced for believing that the surface of the foil was not clean but was a patchwork of uranium and uranium monoxide.

Russian scientists report[5] on the measurement of internal friction in uranium by use of a new method. The internal friction Q^{-1} in uranium was studied in the temperature range 20 to 500°C, and a maximum value of Q^{-1} was found at 250°C. The height of this maximum depends on the rate of temperature variation, a finding that corresponds to the observation made when carrying out measurements on zirconium regarding the existence of a "hydride" maximum. Additional experiments on the annealing of uranium in a hydrogen atmosphere confirm the hypothesis that the existence of a maximum is linked with the formation of uranium hydride, although it is not out of the question that the appearance of a maximum may also be due, in this case, to the influence of stresses within the sample. The role of stresses needs further investigation. When the material cools from 500°C to ambient temperature, the internal friction does not return to its initial level. The internal friction is subject to hysteresis which, generally speaking, is characteristic of phase transformations. It is suggested that the processes of formation and destruction of uranium hydrides during thermal cycling of uranium rods may be one of the causes of the variations in dimension which occur.

British investigators report[6] on the kinetics of the alpha-to-beta phase transformation of two grades of uranium. Dilatometric methods

were used to show that the transformation of uranium can proceed isothermally to completion only a few degrees above the alpha/beta equilibrium temperature, although the last stages are very sluggish. If the transformation is allowed to go to completion, the preferred orientation is largely destroyed at these low beta-phase temperatures. The mechanism of transformation is discussed.

The "Papers and Proceedings of the X-Ray Preferred Orientation Meeting Held at Hanford June 29 and 30, 1961" have been published[7] and report on the following uranium work: "The Atomic Position Parameter in Alpha Uranium at Room Temperature and Above," "Texture Gradients in Uranium Fuel Cores," "Preferred Orientation of Uranium," "Comparison of X-Ray Intensity Data-Peak Height Versus Peak Area," "Effects of Etching on Preferred Orientation Measurements," "Determination of Grain Size of Statistical Fluctuation in X-Ray Diffraction Intensity," "A Note on the Grain Structure and Orientation of 'Dynapak'-Extruded Uranium Tubes," and "Preferred Orientation Measurements with an Automated X-Ray Diffractometer." (M. S. Farkas)

Alpha-Phase Uranium Alloys

Experimenters at Ames Laboratory[8] have determined the uranium-rhenium phase diagram. Their results are shown in Fig. I-1. It was found that the maximum solubility of rhenium in alpha uranium is about 0.4 wt.% at 643°C, and that in beta uranium is 1.9 wt.% at 681°C. The solubility of rhenium in gamma uranium is 6 wt.% at 681°C and increases to about 7 wt.% at 975°C. The solubility of uranium in rhenium is 0.6 wt.% at room temperature, with little variation up to 2000°C.

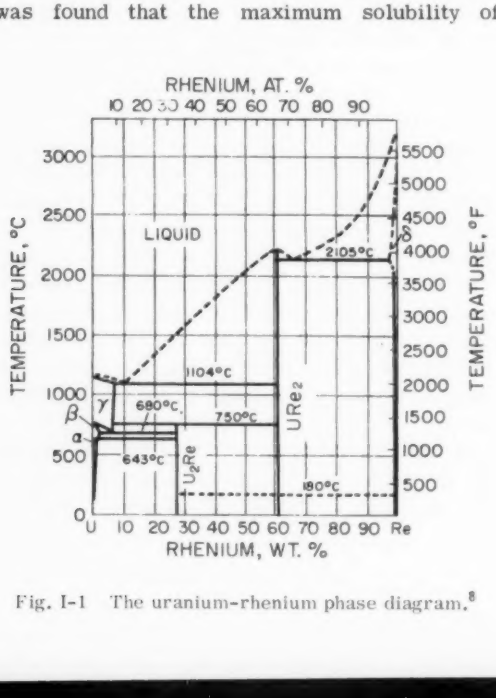

Fig. I-1 The uranium-rhenium phase diagram.[8]

The constitution of uranium-rich alloys of the uranium-silicon-aluminum system, extending to the quasibinary section U_3Si_2-UAl_2, was studied by the Germans.[9] They found four 4-phase transformations in the region examined: melt = alpha uranium + U_3Si_2 + UAl_2 (960°C), alpha uranium + U_3Si_2 = U_3Si + UAl_2 (890°C), alpha uranium = beta uranium + U_3Si + UAl_2 (730°C), and beta uranium = alpha uranium + U_3Si + UAl_2 (580°C). Although the uranium solid-solution fields extend only slightly into the ternary region, the intermetallic phases U_3Si, U_3Si_2, and UAl_2 show no extension at all in this direction.

The Russians[10] have reported on the phase relations existing in the systems uranium-molybdenum, uranium-niobium, uranium-zirconium-niobium, and uranium-molybdenum-chromium.

The kinetics of the isothermal decomposition of gamma-phase uranium – 2.5 wt.% molybdenum have been studied over the temperature range 670 to 340°C by Harwell investigators.[11] Dilatometry, metallography, hardness measurements, and X-ray diffraction were employed. Four different decomposition modes have been found; one of these, involving the formation of a fine granular structure, has not been reported before for alloys of similar composition.

Penetration-rate studies of stainless steel by molten uranium and uranium-fissium alloys have been reported.[12] The rate of penetration of type 304 stainless steel by molten uranium and uranium – 5 wt.% fissium alloy was investigated by a dip method in the range 1100 to 1350°C.

For the fissium alloy the rate increased rapidly from 0.6 mil/sec (1.5×10^{-3} cm/sec) at 1100°C to 12 mils/sec (3×10^{-2} cm/sec) at 1650°C. It then sharply reversed, decreasing to 2.5 mils/sec (6.3×10^{-3} cm/sec) at 1187°C, and then gradually increased to 5 mils/sec (1.3×10^{-2} cm/sec) at 1350°C.

Molten uranium was somewhat more aggressive than molten uranium – 5 wt.% fissium alloy. The rates to penetrate type 304 stainless steel were 15 mils/sec (3.8×10^{-2} cm/sec) at 1150°C,

4 mils/sec (1×10^{-2} cm/sec) at 1187°C, and 6.5 mils/sec (1.65×10^{-2} cm/sec) at 1350°C.

The unexpected reversal in penetration rate with temperature was attributed to the formation of an intermetallic compound which retards the reaction. It was found that the surface-film formation and phase transformation in the stainless steel were not the cause of this reversal.

The French[13] have shown that the addition of 10 at.% molybdenum, niobium, or zirconium retards the self-diffusion of uranium in the gamma phase.

Uranium specimens containing varying amounts of minor second-phase inclusions were irradiated at Harwell[14] to between 0.44 and 0.70 at.% burnup at a surface temperature of 550°C. Beta- or gamma-quenched specimens containing iron and aluminum additions (to refine the grain size) swelled significantly less than those which had low iron and aluminum contents or which had been slowly cooled from the gamma phase. The best result was obtained from a vacuum-cast specimen adjusted with 200 to 500 ppm iron and 500 to 1200 ppm aluminum, beta quenched, and alpha annealed. In a second experiment specimens of this type were irradiated to between 0.21 and 0.54% burnup at a mean surface temperature of 575°C, with superimposed thermal cycling of 0, ±5, or ±15°C. The volume increases were comparatively small and, together with the result from the earlier experiment, could be represented by the equation:

$$\Delta V = 14.8b^{3/2} + 2.4b - 1.1$$

where ΔV is the percentage volume increase, b is the percentage burnup, and $2.4b$ is the volume increase due to solid fission products.

Thermal cycling did not significantly affect the volume increases. Alpha grain-boundary cracking was found in all specimens, but the cracks were usually narrow (~ 1 μ). The grains contained large numbers of fine fission-gas bubbles of average diameter ~ 0.1 μ and maximum diameter 0.4 μ. In contrast the severely swollen unadjusted or unquenched specimens from the earlier experiment contained large ragged fissures at the grain boundaries and large numbers of nonspherical voids within the grains. These voids were typically about 25 by 2 μ, and they tended to have a common orientation, sometimes suggesting crystallographic directions.

The mechanism by which iron and aluminum affect swelling is not known. It is believed that in the adjusted and beta-quenched material the fission-gas bubbles are sufficiently large in number (i.e., sufficiently small in size) to be restrained from swelling chiefly by surface tension. The larger volume increases in the unadjusted or unquenched uranium indicate either that fewer bubbles were initially present or that bubble coalescence has occurred, so that the bubble size at which surface tension restraint becomes insignificant has been exceeded much earlier in the irradiation.

The French[15] report that uranium-iron alloys, dilute in iron, become badly distorted under irradiation to quite small burnups (0.1% of all uranium atoms). Micrographic examination revealed a very pronounced deformation of both the phases present, U_6Fe and alpha uranium. On X-ray diffraction patterns, the lines due to U_6Fe progressively disappeared under the influence of fission fragments. The disappearance was not associated with any change in lattice parameters. Each fission event produces an amorphous condition in a small volume, which was found to be approximately 1×10^{-17} cm^3.

Twelve 0.22-in.-diameter fuel specimens containing a longitudinal central vent and clad with 0.010 in. of type 304 stainless steel were irradiated by Argonne[16] to evaluate the effect of restraint and a central vent on fuel-element stability. The cladding of 10 of the specimens contained porous end plugs to vent any released fission gas and thus to minimize the buildup of gas pressure within the stainless-steel cladding. The specimens consisted of a 20% enriched uranium–2 wt.% zirconium alloy core surrounded by a natural uranium–2 wt.% zirconium alloy sleeve. This geometry was employed to produce a radial temperature gradient similar to that which will exist in the fuel of the Experimental Breeder Reactor No. 2 (EBR-II). The central vent was provided to enhance the release of fission gas and other volatile fission products from the fuel, thereby reducing the tendency for swelling. Eight of the specimens were irradiated to burnups of the enriched core of 6.9 to 12.8% of all atoms (1.2 to 2.2 at.% of the duplex assembly) at maximum fuel temperatures ranging from 280 to 760°C. The results are given in Tables I-1 and I-2. Most of the clad specimens exhibited negligible volume

Table I-1 SUMMARY OF IRRADIATION INFORMATION OBTAINED WITH RESTRAINED AND VENTED URANIUM–2 WT.% ZIRCONIUM ALLOY SPECIMENS[16]

Specimen	Pore size in end caps, μ	Core burnup, at.%	Max. fuel temp.,* °C	Cladding surface temp.,* °C	Length change, %	Diameter change, %	Volume increase,† %	% volume change/ at.% burnup	Comments
DF-2	65	11.8	630	320	0	0	0	0	Clad specimen, very good, fuel swollen to cladding; NaK in axial hole
DF-3	20	11.8	630	320	0	0	0	0	Clad specimen, very good, fuel swollen to cladding; NaK in axial hole
DF-4	20	12.8	760	380	‡	‡	‡	§	Unable to remove specimen from capsule
DF-5	5	11.8	630	320	‡	‡	‡	§	Unable to remove specimen from capsule
DF-6	5	12.6	710	360	0	0	0	0	Eutectic formation near top of specimen
DF-7	Solid	6.9	280	150	0	0	0	0	Fuel swollen to volume of cladding
DF-8	Unclad	11.8	630	Unclad	‡	‡	‡	§	Specimen broke into three pieces upon removal from capsule; NaK in axial hole of each piece
DF-9	Solid	9.5	430	230	0¶	0¶	0¶	0¶	Specimen off center in capsule and bent; welded to capsule at a point near bottom of specimen
DF-11	Unclad	6.9	280	Unclad	18	15	37	5.3	Specimen bent and surface irregular
DF-13	Top: 0.05-in. hole Bottom: 0.010-in. hole	9.8	430	230	0.6	0.4	1.2	0.1	Fuel swollen to volume of cladding

* The temperatures listed are those which existed at the beginning of the final 90% of the irradiation.
† Computed on the basis of measurements of lengths and diameters.
‡ Unable to remove specimen from irradiation capsule.
§ Specimen restrained by irradiation capsule after expanding to the capsule walls.
¶ Except for area where fuel was welded to the capsule wall.

Table I-2 SUMMARY OF MEGALLOGRAPHIC INFORMATION OBTAINED WITH RESTRAINED AND VENTED URANIUM–2 WT.% ZIRCONIUM FUEL ALLOY SPECIMENS[16]

Specimen	Metallographic observations
DF-2	Vent closed; core solid with small pores; zirconium foil broken in some areas and bonded with fuel alloy; slight zirconium alloying with stainless steel
DF-3	Vent closed; core has few large holes; zirconium foil broken in some areas, bonded to fuel alloy in some areas and to stainless steel in other areas
DF-4	Vent closed; large holes and voids due to melting in core and sleeve; no zirconium foil present, apparently dissolved by fuel alloy; stainless steel dissolved in some areas, allowing fuel to flow to the capsule wall
DF-5	Vent enlarged to 0.188 in. in diameter; some zirconium alloyed with fuel alloy; stainless steel difficult to find
DF-6	Vent partially closed; large holes and voids in core; zirconium foil broken in some areas, bonded to fuel alloy in others; slight stainless-steel–zirconium reaction
DF-6 burnout	Eutectic formation between fuel alloy and stainless steel; many radial cracks from zirconium foil to core, one crack through cladding at fused area
DF-7	Vent closed; large holes and voids in core and core-sleeve interface
DF-8	Vent closed; core solid with small voids; core and sleeve separated by a series of voids; residual NaK in these voids
DF-9	Vent closed; slight bonding of zirconium to fuel alloy; zirconium foil broken in some areas, with slight alloying with stainless steel
DF-11	Vent closed; core solid with small voids; large holes with residual NaK in fuel; fuel alloy severely eroded on outer surface
DF-13	Vent closed; core has very small voids; zirconium foil broken in very small areas and bonded to fuel alloy; slight zirconium–stainless-steel alloying

increases as a result of irradiation. Two specimens containing central vents but unclad were irradiated together with the clad specimens in an attempt to differentiate between the effects due to a central vent and the effects due to cladding. The central vent in itself did not appear to reduce the swelling characteristics of the alloy. A comparison of data from this experiment with data for previously irradiated uranium–2 wt.% zirconium (unvented and unrestrained) is shown[16] in Fig. I-2. Mechanical restraint appears to have extended the useful operating temperatures of the metallic fuel alloy by at least 200°C and also greatly extended the burnup levels to which the fuel could be irradiated. This approach is of greatest interest for fast reactors, which can more readily tolerate the amounts of cladding necessary to provide restraint and in which high burnups, high fuel temperatures, and high fissile and fertile atom densities are required.

(M. S. Farkas)

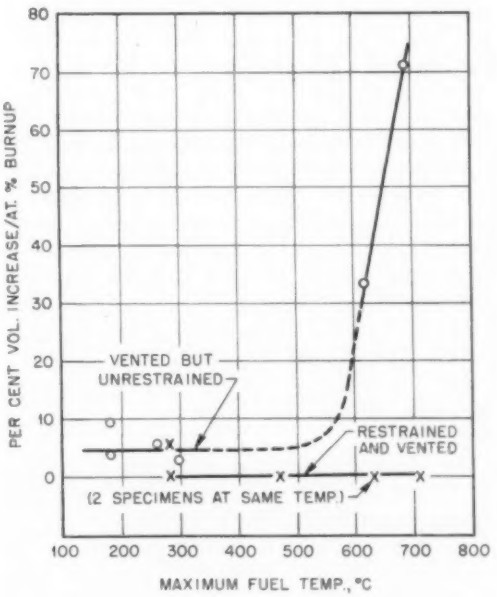

Fig. I-2 Effect of irradiation temperature on the rate of volume increase in the uranium–2 wt.% zirconium alloy.[16] ×, this experiment; ○, comparative data from USAEC Report ANL-5406.

Gamma-Phase Uranium Alloys

A compilation of technical papers in book form contains the results of gamma-phase alloy

studies by various Russian investigators.[10] Information concerning the systems of uranium with niobium, molybdenum, niobium-zirconium, molybdenum-zirconium, niobium-molybdenum, and niobium-molybdenum-zirconium is presented. Included are details concerning constitution and gamma-phase stability and transformation behavior for these systems.

Atomics International[17] has removed capsules containing uranium–10 wt.% molybdenum samples from the Materials Testing Reactor (MTR) for postirradiation examination. A gamma scan of the one capsule indicated less than a 0.5-in. length increase in the original 18.0-in. fuel column. A similar scan of the second capsule indicated approximately an 11% increase in overall fuel-column length. The samples in this latter capsule were irradiated at fission rates below 1×10^{13} fissions/(cm^3)(sec) and at time-averaged temperatures of less than 1000°F. Specimens near the high-burnup end of the capsule exhibited diametral growths of 30 to 40% at burnups of 13,000 to 14,000 Mwd/metric ton of uranium. Three specimens near the center of the capsule were destroyed by fire, and the three at the top were damaged by a NaK fire. These latter three specimens showed diameter increases ranging from 2 to 25%.

(A. A. Bauer)

Aluminum-Uranium Alloys

Chalk River[18] reports that additional data make it possible to modify slightly the solubility of uranium in aluminum at 646°C. The figure now reported is 0.06 ± 0.02 wt.%. Microstructures of a series of alloys which were solution treated at 620°C and of a series of alloys which were aged at 350°C after solution treatment revealed a grain-boundary precipitate in the aged alloys. These observations indicate a reduction of uranium solubility in aluminum at temperatures below 646°C. As an example the solubility is less than 0.04 wt.% uranium at 350°C.

The thermal conductivities of alloys containing 13 and 40 wt.% uranium remain unchanged between room temperature and 350°C.

The British have issued a patent[19] on the suppression of UAl_4 formation in alloys containing 80 to 90 wt.% aluminum and uranium in the atomic proportions of 90:10 and 96.5:3.5. The suppression is accomplished by adding enough of one of the Group IV elements to make up the balance. Silicon is preferred [in the past three years, this effect from silicon has been reported by U. S. laboratories such as Oak Ridge (U. S. Patent 2,950,188) and Battelle].

Fourteen aluminum–35 wt.% uranium alloy irradiation specimens clad with various types of aluminum and aluminum alloys have been removed from test and examined by Phillips Petroleum Co.[20] These specimens had indicated failure because of increased water activity after irradiation times varying from 2 to 22 cycles, with burnups from 11 to 82% of the U^{235} atoms. The irradiations were performed at a surface temperature of about 200°C. Various combinations of cladding and picture frames were represented by these specimens. The aluminum and alloys used include M-257, M-470, M-583, 1100, 5052, and 6061.

Postirradiation examination showed that one specimen failed because of insufficient bond strength, one was too thinly clad, and some failed because of voids in the core which enlarged, blistered, and cracked the cladding. It is interesting to note that three specimens indicated no failures. In these cases the high activity in the coolant can be attributed to diffusion of uranium through the cladding.[21]

After studying data obtained from the various aluminum-uranium alloy irradiations, Phillips Petroleum[20] reached the following conclusions:

1. Aluminum-uranium alloys containing up to 50 wt.% uranium clad with a number of aluminum alloys can be irradiated to long burnups in the MTR.

2. Irradiations can be performed at temperatures up to 350°F without changing structure.

3. The aluminum-uranium alloys show an increase in tensile strength and hardness after irradiation. The most severe change in a property is in elongation. These materials show 8 to 31% elongation before irradiation and 4.5% elongation after irradiation.

4. Cladding-to-core bonding is the cause of most problems. Some combinations, such as 6061 aluminum to itself, are not satisfactory.

Argonne reports[22] that aluminum–17.5 wt.% uranium alloy coupons clad with $\frac{1}{32}$-in.-thick aluminum on the two flat faces and with $\frac{1}{4}$-in.-thick aluminum on two edges have been irradiated and the test results evaluated. Specimens of this type, when subjected to burnups equal to or less than 1.6×10^{20} fissions/cm^3, have excellent resistance to swelling up to 550°C. However, if burnups are increased to

5.5×10^{20} fissions/cm^3, the specimens swell about 10 times more than the lower burnup specimens.

A CP-5 fuel element was removed from the reactor by Argonne[23] because of excessive activity. These elements are concentric tubes of aluminum–17.5 wt.% uranium–2 wt.% nickel alloy clad with X8001 aluminum. A postirradiation examination of this element showed that a blister was present on the inside diameter of the inner tube. Water had penetrated the blister and reacted with the fuel almost completely. Although no explanation for the occurrence of the defect has been reported, it is significant that the fuel was reacted by water. Previous data reported by Battelle[24] would indicate that the corrosion rate of either the aluminum–16, 30, or 45 wt.% uranium in 300°F water is, at the most, only about twice that of 2S aluminum. These data would not predict the reaction reported by Argonne.

Oak Ridge[25] completed postirradiation examination of aluminum-base fuel alloys containing 64 wt.% UAl_3 by performing X-ray diffraction studies. The studies showed no indication of the formation of UAl_4. However, the UAl_3 seemed to have undergone an ordered-disordered transformation as a result of irradiation. (R. F. Dickerson)

Mechanism of Corrosion of Uranium

National Lead Co. of Ohio[26] has been studying the mechanism of formation of the yellow $UO_3 \cdot 2H_2O$ which surrounds anodic sites during the atmospheric corrosion of uranium. Tests under applied potentials have produced $UO_3 \cdot 2H_2O$ accompanied by H_2O_2 on uranium cathodes. From these experiments it was concluded that the atmospheric corrosion of uranium is electrochemical in nature, and the formation of $UO_3 \cdot 2H_2O$ is explained as the oxidation of U^{4+} to U^{6+} by H_2O_2. (W. E. Berry)

Uranium-Steam Reaction

Argonne[27] has reported additional results of the reaction of solid uranium with steam by the volumetric method. Experiments have now been completed in which steam was reacted with pure uranium at temperatures up to 1500°C and uranium–1 wt.% aluminum alloy at temperatures up to 1400°C. Preliminary results indicate that aluminum has a negligible effect on the reaction. Results for pure uranium at 1400 and 1500°C do not appear to be consistent with results at lower temperatures. The parabolic rate constants are 50 to 100% higher than expected from previous results. For example, at 1400°C, the parabolic rate constant was 1360 (ml STP/cm^2)^2/min; previous data would have suggested a value of about 700 (ml STP/cm^2)^2/min. The wide variation in results was caused by the method used for sample support which allowed the uranium metal to sag and thereby caused excessive oxide cracking.

(A. W. Lemmon, Jr.)

Plutonium

Plutonium Metals and Alloys

Investigators at Harwell[28] report that, in the temperature range 320 to 480°C, the oxidation rate of plutonium in dry air passes through a minimum in the region of 416°C. This minimum is attributed to the formation of a protective oxide film. Alloys containing up to 30 at.% plutonium in iron, thorium, uranium, uranium-molybdenum, and zirconium have been oxidized in dry air at temperatures of 445 to 500°C. With the exception of a uranium–5 at.% plutonium alloy and possibly a uranium–25 at.% molybdenum–20 at.% plutonium alloy, the oxidation rates of these alloys are lower than that of pure uranium. Alloys containing up to 40 at.% plutonium in iron, uranium, uranium-molybdenum, and zirconium all exhibited lower oxidation rates than pure uranium when oxidized in dry carbon dioxide at temperatures between 500 and 800°C.

Hanford[29] has irradiated two Zircaloy-clad aluminum–2.1 wt.% plutonium–2.0 wt.% nickel alloy specimens that were fabricated by injection casting. A report[30] has been issued describing the fabrication and irradiation testing of aluminum–1.8 wt.% plutonium–1.35 wt.% nickel–1.10 wt.% silicon alloy fuel elements for the Plutonium Recycle Test Reactor (PRTR).

Chalk River[31] has irradiated Zircaloy-2–sheathed aluminum-plutonium alloys containing 5 to 20 wt.% plutonium for four months under water-cooled power-reactor conditions. Effects of irradiation and postirradiation annealing on volume are illustrated in Fig. I-3.

The plutonium-cerium phase diagram as determined by metallographic examination at Mound Laboratory[32] is shown in Fig. I-4.

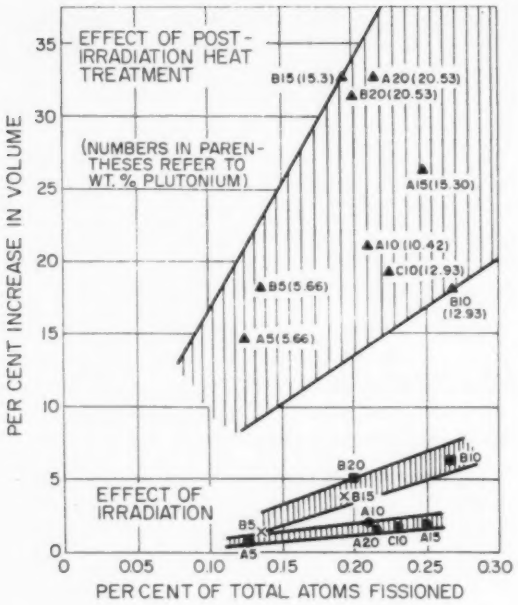

Fig. I-3 Effect of plutonium fissioning, irradiation temperature, and postirradiation heat-treatment at 640 to 650°C on the volumes of aluminum-plutonium alloys.[31] ●, specimens irradiated under restraint at 350 to 400°C; ×, specimens irradiated under no restraint; initial irradiation temperatures, 550 to 625°C; ■, specimens irradiated initially under no restraint at 600 to 625°C and later under restraint at ~400°C; ▲, specimens postirradiation annealed at 640 to 650°C after desheathing.

German investigators[33] have issued a compilation of data and phase diagrams for plutonium-containing binary and multicomponent systems. (V. M. Storhok)

Plutonium Compounds

In continuing experiments with plutonium-bearing glass, Mound[34] reports that density increases linearly from 2.48 g/cm^3 for pure glass to 2.93 g/cm^3 when 20 wt.% PuO_2 is incorporated. Investigation of the melting phenomenon of a glass containing 20 wt.% PuO_2 at 2000°C in argon showed that PuO_2 and SiO_2 vaporize.[35] This behavior may be attributed to a reaction between components of the glass. Excellent results have been obtained on spheroidization of PuO_2 in an argon plasma.[36] Mound has also found the addition of B_2O_3 to be beneficial in increasing the ability of a glass to dissolve[36] PuO_2. Nuclear Materials & Equipment Corp. (NUMEC) investigators[37] are continuing their extensive studies of the characterization and fabricability of $(Pu,U)O_2$ solid solutions. Attempts are being made to spheroidize particles of these solid solutions by plasma torch spraying.

Thermal-expansion data for PuO_2 obtained by Hanford by high-temperature diffractometer measurements[29] are shown in Table I-3. The sharp inflection noted at 1275°C is attributed to oxygen loss from the dioxide.

A new working phase diagram (see Fig. I-5) has been published for the plutonium-oxygen system.[38] The most significant anomalies of the system are explained, and an unusual two-phase solid immiscibility region at low temperatures between oxygen-to-plutonium ratios of 1.70 and 1.98 is postulated.[39] Hanford has reported[40] electromotive-force and electrical-resistivity measurements for PuO_2, Pu_2O_3, and PuO in connection with the development of this diagram. The same laboratory reports a melting point[41] for beta Pu_2O_3 of 2090 ± 30°C. Most recently,[42] pellets of varying ratios of PuO_2 and MgO pressed and sintered for 20 hr at 1600°C in helium show no solid solubility nor compound formation in the range 0 to 60 mole % MgO. Some evidence of the reduction of PuO_2 to alpha Pu_2O_3 was noted in PuO_2-rich specimens. Hanford[41,42] has also begun investigations of rate constants and kinetics for the reduction process involving PuO_2 and carbon to the various suboxides of plutonium.

Plutonium mononitride receives more interest constantly. The French[43] report that heating

Table I-3 THERMAL-EXPANSION DATA[29] ON PuO_2

Temp., °C	Lattice constant	1000 $\Delta a/a_0$
24	5.3960 ± 0.0002	
202	5.4033 ± 0.0007	1.35
280	5.4080 ± 0.0002	2.22
412	5.4148 ± 0.0007	3.48
500	5.4186 ± 0.0005	3.19
604	5.4227 ± 0.0004	4.95
701	5.430 ± 0.001	6.30
812	5.434 ± 0.001	7.13
900	5.439 ± 0.002	7.97
976	5.4462 ± 0.0024	9.30
1100	5.454 ± 0.003	10.75
1227	5.4632 ± 0.0010	12.45
1275	5.4656 ± 0.0008	12.90
1368	5.480 ± 0.002	15.57
1514	5.498 ± 0.003	18.90
1620	5.513 ± 0.010	21.68

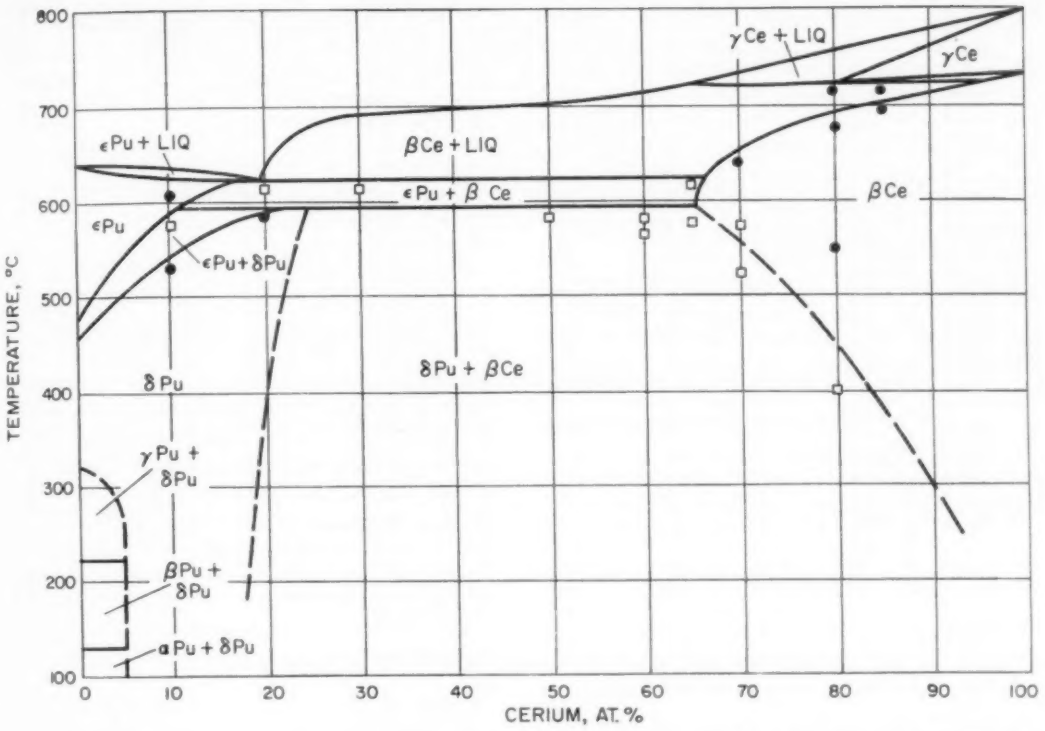

Fig. I-4 Metallographic examination of the plutonium-cerium system.[32] ●, single-phase alloy; □, two-phase alloy.

of sintered PuN for 30 min in vacuum at 1700°C causes approximately 50% weight loss, indicative of a high dissociation pressure. High-temperature X-ray diffraction techniques have been utilized to determine an average coefficient of linear thermal expansion[44] of 13.8×10^{-6}/°C from 26 to 800°C. Little success has been reported[29] in attempts to arc-melt alpha plutonium under nitrogen to form PuN. The most common synthesis technique is to hydride plutonium, followed by subsequent nitriding at 600 to 800°C. The best arc-melted material contains approximately 15 vol.% plutonium as a matrix around PuN dendrites. PuN has been found to react rapidly with boiling water to form PuO_2. Rapid dissolution is also reported in all organic acids at room temperature.[45]

Both British[105] and American[46] investigators have reported that lattice parameters of plutonium compounds can increase by as much as 0.2% per year as a result of alpha recoil damage effects.

Irradiation testing of plutonium fuels is beginning to accumulate data for future use. Hanford has charged 30 uniformly enriched UO_2-PuO_2 elements in PRTR and is irradiating and evaluating MgO–2.1 wt.% PuO_2 and ZrO_2–1.3 wt.% PuO_2 fuel rods clad in Zircaloy tubing.[29] Irradiation of PuC and (Pu,U)C solid solutions in the range 460 to 650°C showed superior fracture resistance as compared[43a] with PuC. However, density decreases and diameter increases could not be correlated with carbon content or fuel burnup. Arc-melted PuC showed fission-gas release of 0.24% of theoretical, whereas sintered (U,Pu)C released 12.0% of theoretical fission gas. This variation is attributed to density differences stemming from the different fabrication processes. UC–10 wt.% PuC was irradiated to varying burnups. With a surface temperature of 600°C and a center temperature of 700°C, 0.140-in.-diameter pellets of this material released 0.027% of the fission gas after 19,000 Mwd/ton burnup and 0.0012% after 23,000 Mwd/ton exposure. No explanation was given for the lower gas release at the higher burnup.

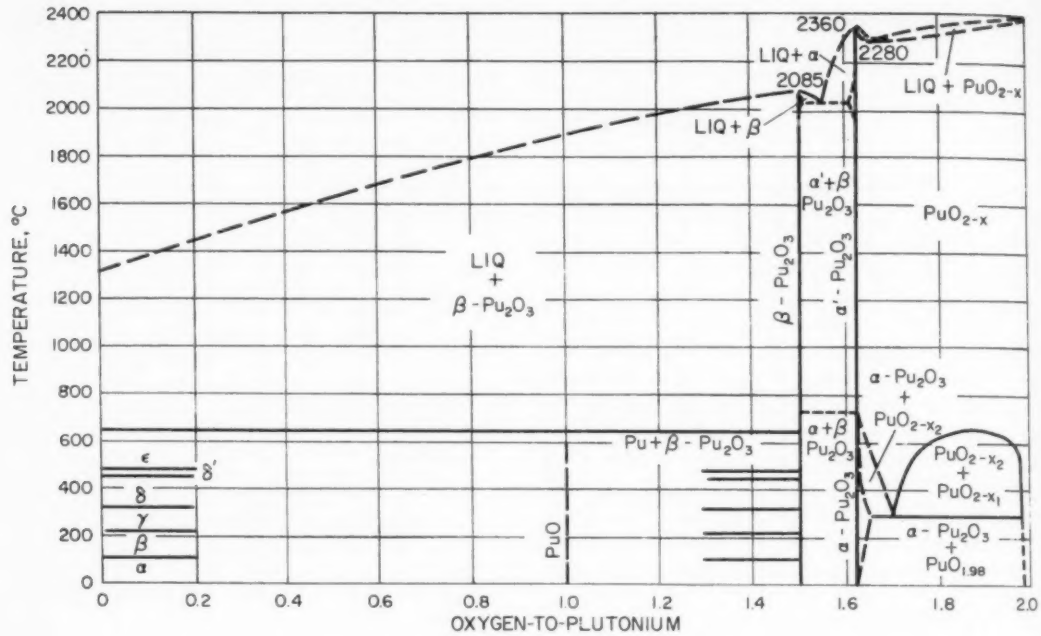

Fig. I-5 Proposed phase diagram for the plutonium-oxygen system.[29]

Hanford[47] has reported irradiation of UO_2–2.40 wt.% PuO_2 mechanical and physical mixtures to a maximum burnup of 2500 Mwd/ton. Postirradiation examination showed all cores to be cracked. On the other hand, General Electric[48] has irradiated UO_2-PuO_2 fuel pins (uranium:plutonium = 4:1) to burnups of 5000 to 99,000 Mwd/ton and at heat fluxes ranging from 0.5×10^6 to 1.6×10^6 Btu/(hr)(sq ft). No rupture of cladding was noted, and no gross longitudinal fuel movement occurred, but central voids were formed. Fission-gas release was approximately 42% of theoretical, or slightly higher than would be expected for UO_2 under the same conditions.

The thermal expansion of $PuC_{0.85}$ (45.8 at.% carbon) as a function of temperature is shown in Fig. I-6. These results, along with similar data for plutonium-carbon alloys containing 41.1, 43.2, 44.9, and 45.4 at.% carbon, were utilized by Los Alamos[49] in an attempt to interpret the phase diagram.

A recently printed Los Alamos report[50] contains estimates of the thermodynamic properties of PuC, Pu_2C_3, and the zeta phase. The thermal conductivities of various PuC-containing materials relative to that of UC are shown[43a] in Table I-4. The presence of Pu_2C_3

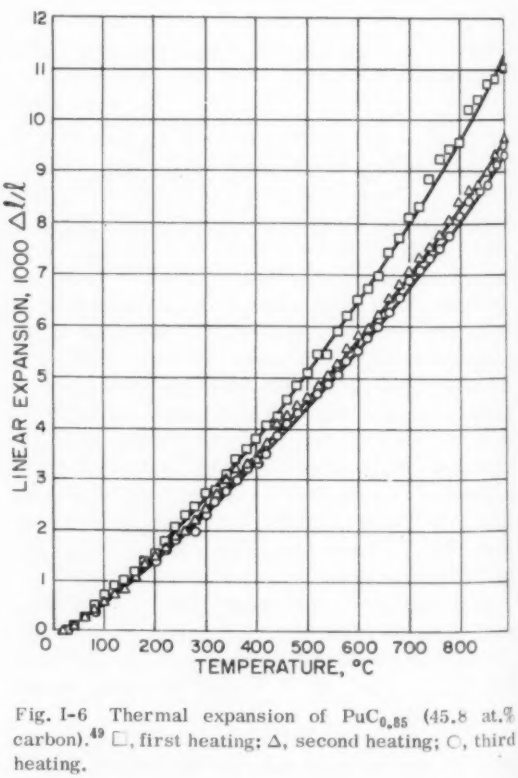

Fig. I-6 Thermal expansion of $PuC_{0.85}$ (45.8 at.% carbon).[49] □, first heating; Δ, second heating; ○, third heating.

Table I-4 THERMAL CONDUCTIVITY[43a] RELATIVE TO UC

Composition	Relative thermal conductivity
UC	1.0
UC–10 wt.% PuC	0.7
UC–15 wt.% PuC	0.5
PuC	0.2

lowers thermal conductivity, especially if present as a continuous grain-boundary phase.

Several laboratories[51–54] are investigating the fabrication of dense bodies of PuC and (U,Pu)C. Carbon reduction of PuO_2 almost invariably results in the presence of Pu_2C_3 in the end product. However, mixtures of UO_2, PuO_2, and carbon will react to produce a single-phase solid solution of plutonium and uranium monocarbides. Carburized tantalum appears to be the most suitable container material for these compounds.[51] PuC has been hot-pressed in graphite to 98% of theoretical density at 800°C, whereas Pu_2C_3 requires approximately 200°C higher temperatures to press to an equivalent density.

Various physical measurements of interest for plutonium carbides have been made. Los Alamos[53] reports that the vapor pressure over PuC_2 between 2000 and 2400°K can be represented by the equation

$$\log P(\text{atm}) = -17{,}920/T + 2.779$$

which gives $\Delta H^\circ_{298} = 95.1$ kcal/mole as the heat of vaporization. From 350 to 30°C, a measured heat capacity of 10.7 ± 0.6 cal/(gram mole)(°C) has been reported.[40] This compares with a calculated C_p value of 13.34.

PuO_2 and SiO_2 powders in the ratio 40:60 at.% have been reacted in an attempt to form Pu_2Si_3, but X-ray diffraction showed $PuSi_2$ to be the resultant product. Lattice parameters were: $a_0 = 3.97$ A and $c_0 = 13.59$ A, yielding a c/a ratio[55] of 3.42. The compound melts at 1795 ± 25°C in argon on a tungsten ribbon. Chemical analysis showed 78.4 wt.% plutonium as compared with a stoichiometric value of 81 wt.%. (W. M. Pardue)

Thorium

In attempts at purifying thorium by electron-beam melting, Ames[8] found that substantial decreases in oxygen, hydrogen, and, in most cases, iron were obtained. Hardness also decreased. No consistent change in carbon or nitrogen was noted.

In an investigation[8] of the variation in hardness of thorium with degree of cold work, the hardness increased rapidly up to about 10% reduction, increased very slowly thereafter up to about 80% reduction, and increased a bit more rapidly beyond 80% reduction.

The thorium-molybdenum system is reported[8] to be a eutectic type, with a eutectoid reaction associated with the thorium alpha-to-beta transformation. The eutectic occurs at 1380 ± 10°C and 7.0 ± 0.5 wt.% molybdenum, whereas the eutectoid is at 1358 ± 5°C and less than 0.1 wt.% molybdenum. No solubility of thorium in molybdenum was detected at 1325°C.

Vapor pressure of magnesium over thorium-rich magnesium alloys consisting of thorium and $ThMg_2$ may be represented[8] by the equation

$$\log P(\text{mm Hg}) = \frac{(9080 \pm 240)}{T(^\circ\text{K})} - (10.28 \pm 0.32)$$

The electrical resistivity[56] of a magnesium–39 wt.% thorium eutectic alloy is 69.5 μohm-cm at 589°C (melting point) and 64.8 μohm-cm at 900°C.

The Bureau of Mines[57] studied the effects of holmium, neodymium, and praseodymium on the mechanical properties of thorium. Holmium additions increased the tensile strength, yield strength, and elongation. The tensile strength of pure thorium is 31,500 psi at 320°C and 22,500 psi at 540°C. A thorium–50 wt.% holmium alloy showed a tensile strength of 44,000 psi at 320°C and 28,000 psi at 540°C. Elongation increased from 5% for thorium to 9% for thorium–50 wt.% holmium at 320°C and from 8 to 16% at 540°C. Neodymium additions reduced the tensile strength and yield strength of thorium. At 320°C a thorium–50 wt.% neodymium alloy showed a tensile strength of 23,400 psi and an elongation of 6%. Praseodymium showed effects similar to those of neodymium. (V. W. Storhok)

Dispersion Fuels

Oak Ridge reports[58] that the outer-annulus fuel plates containing dispersions of U_3O_8 in aluminum have been successfully fabricated for the High-Flux Isotope Reactor. Both fuel sections and filler pieces were prepared by hot-press forging. Core dimensions were obtained within desired tolerances, and no blisters

were evident after a 500°C anneal. It was also reported that favorable results were obtained from a feasibility study concerned with forming fuel plates by an electrohydraulic process. The technique appears most useful when used for restriking plates rejected for not meeting dimensional tolerances after the low-pressure forming.

Initial phases of postirradiation examination of 34 highly enriched UO_2–type 347 stainless-steel dispersions clad with type 347 stainless steel have been completed by Oak Ridge.[59] The specimens were prepared by Battelle and irradiated in the Engineering Test Reactor (ETR). The U^{235} depletion ranged from 52 to 82%, and the surface temperatures went as high as 1290°F. Initial examination shows that the lower-fuel-loaded (24 to 26 wt.% UO_2) dispersions can be operated to approximately 70% U^{235} depletion at surface temperatures near 600°F.

Phillips Petroleum personnel[60] have completed the analyses of different samples of irradiated fuel plates containing varying percentages of UO_2 dispersed in aluminum. Forty percent of the samples tested had zero elongation in a 1-in. gauge length. These samples were scattered throughout the ranges of compositions tested and levels of irradiation attained. The change in percent elongation, due to the fissioning, ranged from −58 to −100%, with a maximum elongation of 4.5% in 1 in. for any one fissioned specimen. For specimens retaining some degree of ductility, the following was indicated: (1) ductility decreases rapidly due to fission damage (Fig. I-7); (2) strength

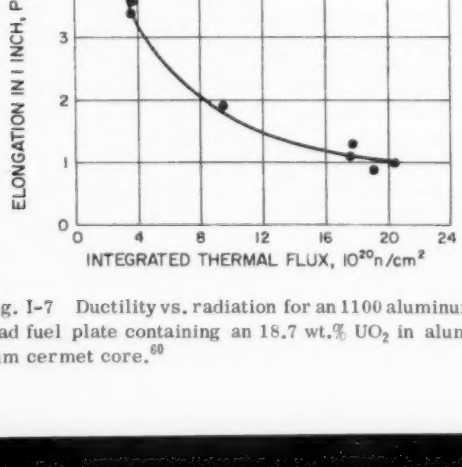

Fig. I-7 Ductility vs. radiation for an 1100 aluminum-clad fuel plate containing an 18.7 wt.% UO_2 in aluminum cermet core.[60]

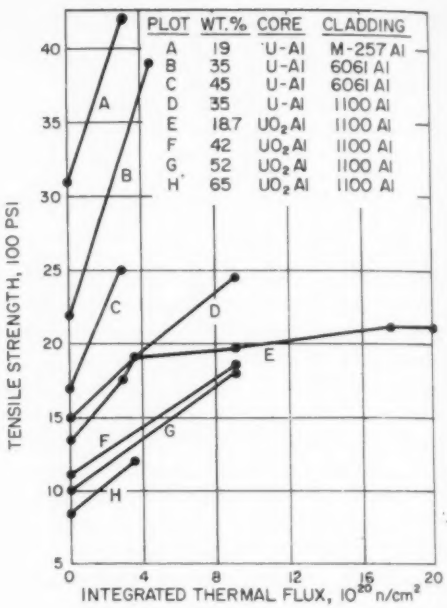

Fig. I-8 Strength vs. exposure for fuel plates of various compositions.[60]

decreases with an increase in fuel content (Fig. I-8); (3) for a given fuel content, alloys are substantially stronger than oxides; (4) in initial stages of irradiation, the amount of strength increase depends on the type of cladding material; and (5) increase in strength is proportional to the percent increase in hardness of the cladding material (Fig. I-9).

Additional work has been completed by Phillips Petroleum[60] toward identifying phases evident in the UO_2-aluminum cermets after being heat-treated to produce reaction between the UO_2 and aluminum, irradiated to various burnups at 200°F, and postirradiation annealed at 390°F. Metallographic examination (see Fig. I-10) revealed porous UO_2 particles surrounded by a layer of reaction products. Electron-probe analysis and X-ray diffraction examination identified the gray layers as UAl_4 or UAl_3 and the dark phases as UC or UN.

Hanford reports[46] that a series of tungsten-UO_2 cermets was fabricated by a high-rate densification at 1200°C and 277,000 psi on the Dynapak machine. Evenly blended mixes of −65 +200-mesh UO_2 and −325-mesh tungsten were densified to 96% of theoretical with a 66 vol.% loading of UO_2. This particular high-density cermet was machined and encapsulated

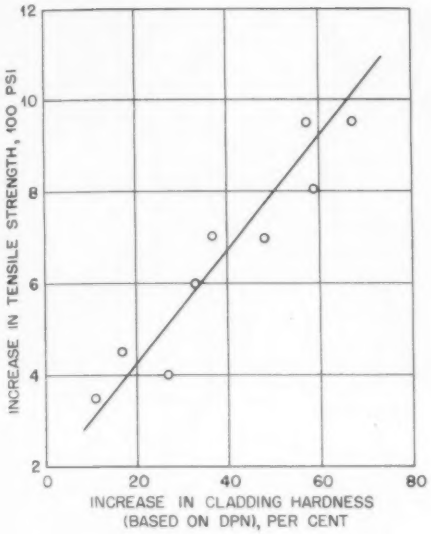

Fig. I-9 Increase in plate strength vs. percent increase in cladding hardness for plates clad with 1100 aluminum and having various core compositions.[60]

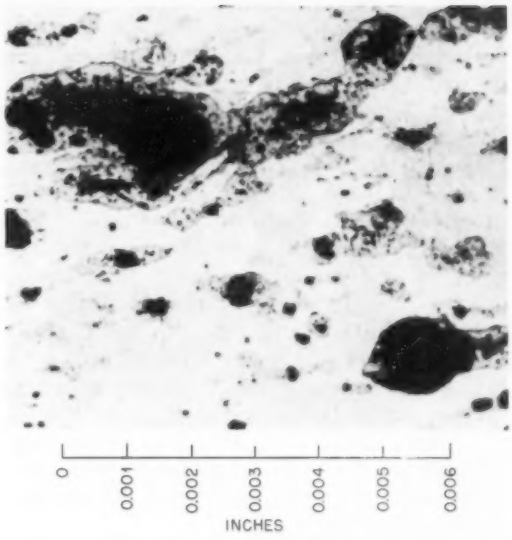

Fig. I-10 Microstructure of 24 wt.% UO_2 in aluminum cermet, irradiated to 45 at.% burnup (as polished).[60]

in 0.200-in.-ID by 0.25-in.-thick-wall tungsten cladding. The tungsten-clad specimen was irradiated for 1 hr under conditions chosen to give a surface temperature of 2300°C. Comparison of the microstructure of the irradiated sample with microstructures of other samples heated out-of-reactor verified[42] that a temperature greater than 2100°C was achieved. During the irradiation the tungsten matrix sintered to form a high-integrity barrier due to gross relocation of UO_2 and fission products. UO_2 sublimed from a thin surface layer of the cermet and deposited on the inner surface of the tungsten cladding. No evidence of reaction between the UO_2 and the tungsten matrix or cladding was observed.

The United Kingdom Atomic Energy Authority (UKAEA) has given cermet fuels [$(U,Pu)O_2$ in stainless steel] the highest priority of all fuel types being considered for future fast-reactor use.[43a] It is felt that sufficient oxide content [50 vol.% UO_2 (PuO_2)] can be incorporated in this fuel to make it attractive. The British believe that production fabrication is feasible. Irradiation experiments indicate promise of high burnup and high performance for this fuel.

The fuel-element development effort at Dounreay[43a] is presently concerned with cermets containing 50 vol.% $(U,Pu)O_2$ dispersed in a stainless-steel matrix. The thermal and mechanical properties of the cermets produced have been measured. Ductilities of 7% were achieved and considered adequate. The thermal expansion of the cermet has been reported identical to that of the stainless-steel matrix, whereas the thermal conductivity ranged from 0.029 to 0.04 cal/(cm)(sec)(°C) at 600°C. The tensile strengths for the 50 vol.% oxide cermets were 6.5 tsi at room temperature and 2.85 tsi at 800°C. The 40 vol.% oxide cermets have strengths of 8.5 tsi at room temperature and 3.6 tsi at 800°C.

Postirradiation annealing of irradiated stainless-steel–UO_2 dispersion fuels is being carried out at Harwell.[43a] Investigators found negligible density changes in an 18 wt.% UO_2 dispersion with 14 at.% burnup, heated at 700°C for 48 hr. Similarly, a 19 wt.% UO_2 dispersion with a 9.7 at.% burnup decreased in density only 3% after being heated at 1100°C for 48 hr.

(D. L. Keller)

Coated-Particle Fuel Materials

Preparation and Fabrication

Oxide-Base Fuels. An international symposium, sponsored by AEC, was held at Battelle

on Nov. 5 and 6, 1962, to review recent developments in the preparation and use of coated particles in ceramic fuels. The presentations on oxide-base fuel by the Australian Atomic Energy Commission (AAEC), Flight Propulsion Laboratory Department of General Electric, Nippon Carbon Co., Ltd., Mitsubishi Metal Mining Co., Ltd., Commissariat à l'Énergie Atomique (CEA), and Nuklear-Chemie und-Metallurgie G.m.b.H. were of special interest, since no previous disclosures of their studies had been made. The AAEC revealed that it had deposited Al_2O_3 coatings on UO_2 and $(U,Th)O_2$ particles using the vapor hydrolysis of $AlCl_3$ in fluidized-bed equipment.[61] Experiments were carried out at temperatures of up to 1050°C, and coating rates of 1 to 20 μ/hr were obtained. Coatings of 3 to 65 μ in thickness were prepared. Preliminary studies on beryllia coatings had also been initiated.[61a]

General Electric described a spiral-bed apparatus for coating oxide fuel particles less than 50 μ in diameter with oxidation-resistant ceramic materials.[62] A sketch of their apparatus is shown in Fig. I-11. In the spiral-bed apparatus, the reacting gases are brought to the reaction chamber along two separate paths. Along one path the gases enter tangentially through the wall of the reaction chamber, and the fuel particles are thus caused to spiral upward. The increase in hydraulic diameter with height causes a gradual decrease in velocity of the spiraling gases and thus permits the particles to drop from the gas stream alongside the tube projecting from the floor of the chamber. Therefore the particles pass repeatedly through the coating zone near the bottom of the chamber. The fluidizing efficiency of the bed appears to be quite high, and fuel particles as small as 37 μ in diameter have been fluidized for up to 8 hr at 1000°C without any evidence of agglomeration of particles or freezing of the bed. A photomicrograph of a sample of UO_2 coated with Al_2O_3 in this apparatus is shown in Fig. I-12.

A new approach to carbon coating of fuel particles was described by Nippon Carbon Co.[61b] The UO_2 particles are suspended by means of a suitable dispersing agent in a monomer of divinylbenzene, which is then polymerized as a coating on the particles. The coated material can then be heat-treated to 800°C to carbonize the polymeric coating to carbon. The coated material can also be heat-

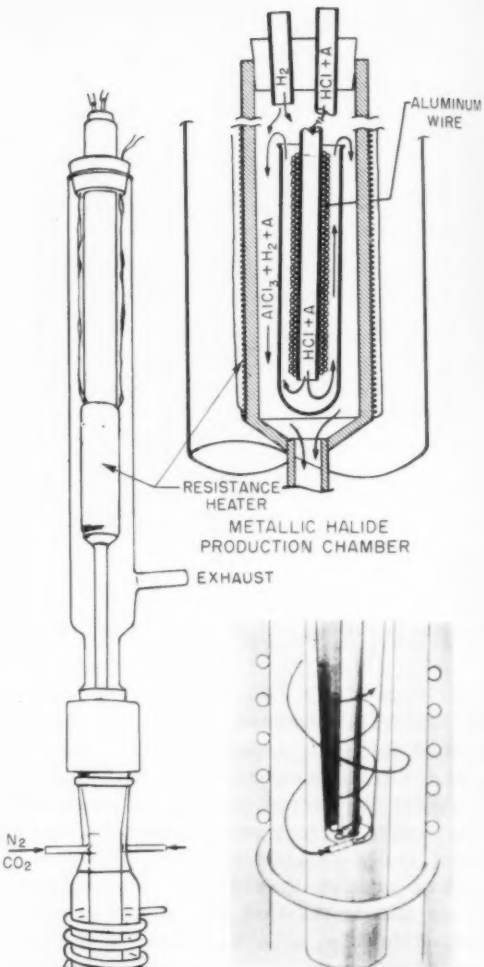

Fig. I-11 Spiral-bed vapor-reaction coating apparatus.[62]

treated at temperatures up to 2000°C, whereby the UO_2 is transformed into UC_2, and the carbon coating is reported to remain intact. Mitsubishi Metal Mining Co. reviewed progress on coating[61c] UO_2. They have employed the hydrogen

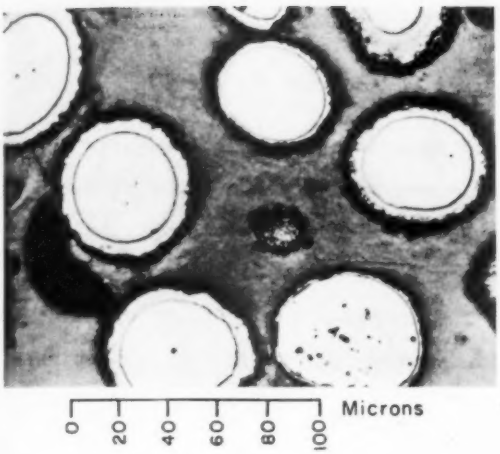

Fig. I-12 Urania-containing spheres coated with Al_2O_3 in the spiral-bed apparatus.[62]

reduction of $NbCl_5$ and WCl_6 to deposit niobium and tungsten coatings in fluidized-bed equipment. Nuklear-Chemie und-Metallurgie discussed attempts to improve the thermal conductivity of UO_2 compacts to be used in a fast-breeder reactor.[61d] Vapor deposition of molybdenum from molybdenum pentacarbonyl and pelletizing techniques using powdered molybdenum were investigated. Fairly extensive information on pyrolytic carbon (PyC) coating of UO_2 with C_2H_2 and CH_4 was presented by the CEA and Battelle-Geneva.[61e] The microstructure, crystallography, density, permeability, and resistance to heat-treatment of the coatings, as well as the kinetics of carbon deposition, were discussed in considerable detail. Photomicrographs of the coated particles after various heat-treatments are shown in Fig. I-13.

Codeposition of MgO in Al_2O_3 coatings has shown some promise as a grain-growth inhibitor during subsequent heat-treatments. The grain size in Al_2O_3 coatings containing 3 wt.% MgO increased only a few microns during heating for 15 hr at 1550°C, whereas coatings without MgO exhibited grain growth from an initial value of 5 μ to about 25 μ. Lesser amounts of MgO were not as satisfactory in retarding grain growth. A modified heat-treatment schedule for shrinking a porous UO_2 substrate away from an Al_2O_3 coating was also developed this period. A 13-hr hold at 1250°C appears to be necessary before heating the material up to 1500°C for final densification of the UO_2 core.

Carbide-Base Fuel. A number of organizations have also disclosed some details of their experience in coated carbide fuels for the first time. This group includes the UKAEA Establishments at Harwell and Springfields, the U. K. Royal Aircraft Establishment at Farnborough, Metallwerk Plansee, and the Raytheon Company. Harwell revealed[61f] that it has prepared both columnar and laminar types of carbon coatings on uranium and thorium dicarbide particles. The advantages of coating at higher temperatures and the provision of porosity in the substrate to avoid coating failure due to thermally induced stresses were pointed out. The rapid diffusion of alkali and alkaline-earth isotopes in PyC, as compared with the rare gases for instance, has been demonstrated, and further effort in the preparation of carbide coatings was recommended. The Springfields laboratory[61g] has started preliminary studies with silicon carbide coatings on uranium monocarbide particles.

Harwell also presented[61h] a good summary of their techniques used to incorporate carbon-coated carbide particles into graphite matrices. A two-stage mixing process is used. In the first stage the graphite grist and binder are mixed in the sigma-blade dough mixer. The coated particles are then added to the grist/binder mix in a second mixer in the presence of a small amount of solvent for the binder. This mixer has a single mechanical processing stirrer that rotates very slowly and has large clearances at the wall. Scraper blades, spring loaded against the sides of the mixer, eliminate dead volume and give some volume blending. The solvent is subsequently evaporated from the mix before forming at pressures of about 3500 psi or extruding at 130°C using a pressure of 4000 to 5000 psi. The green extrusions and pressings are packed lightly in coarse coke grist within metal or graphite pots and are baked slowly to 850°C. Volume loadings of 50% were achieved.

The Dragon program on coated-particle fuels[61i,63] was reviewed in detail. Propane, methane, and hexane have been used to prepare PyC coatings on fuel particles, and methyltrichlorosilane in hydrogen has been used to prepare silicon carbide coatings. A photomicrograph of carbon-coated uranium-thorium dicarbide particles, with an interlayer of silicon carbides, is shown in Fig. I-14. The purpose of the silicon carbide inner layer is to retard

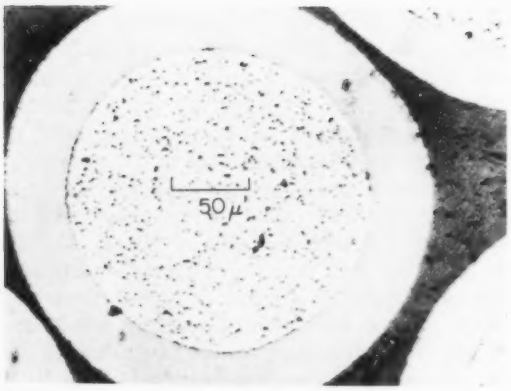

(*a*) 1500°C

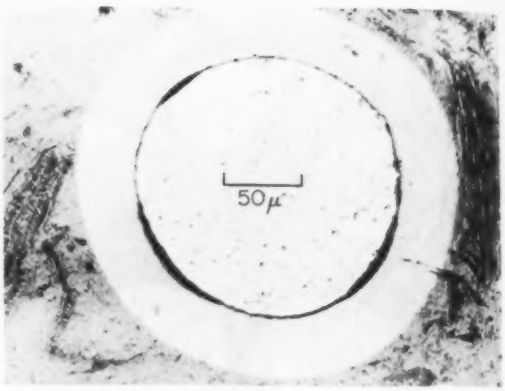

(*b*) 1700°C

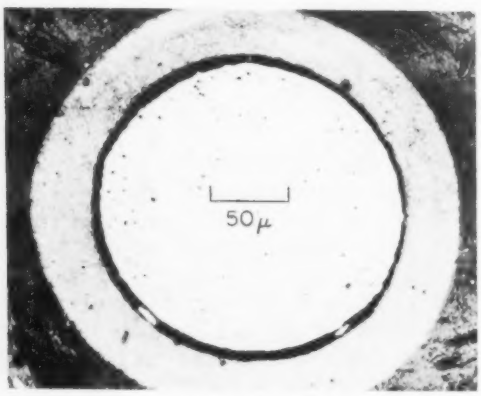

(*c*) 1800°C

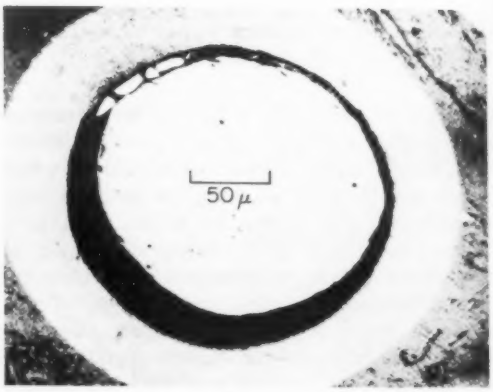

(*d*) 1900°C

Fig. I-13 Carbon-coated UO_2 particles after heat-treatments at various temperatures.[61e]

the diffusion of fission products (such as barium) at high temperatures. As has been reported elsewhere, the coating conditions were found to affect the structure and density of the deposits. On the basis of studies at Farnborough and at Winfrith, a minimum density was found at temperatures of about 1600°C, and lower deposition rates resulted in higher densities. Pyrolytic deposition of carbon from benzene was also employed to infiltrate the pores of graphite-matrix elements. A prototype coating unit has now been constructed on the basis of studies at Metallwerk Plansee, and a sketch of the unit is shown in Fig. I-15. The apparatus has a 1-kg-charge capacity.

The Metallwerk Plansee results[64] were recently published separately. A semiautomatic high-temperature fluidized-bed system was de-

Fig. I-14 Uranium-thorium dicarbide particle coated with PyC, silicon carbide, and PyC.[61f]

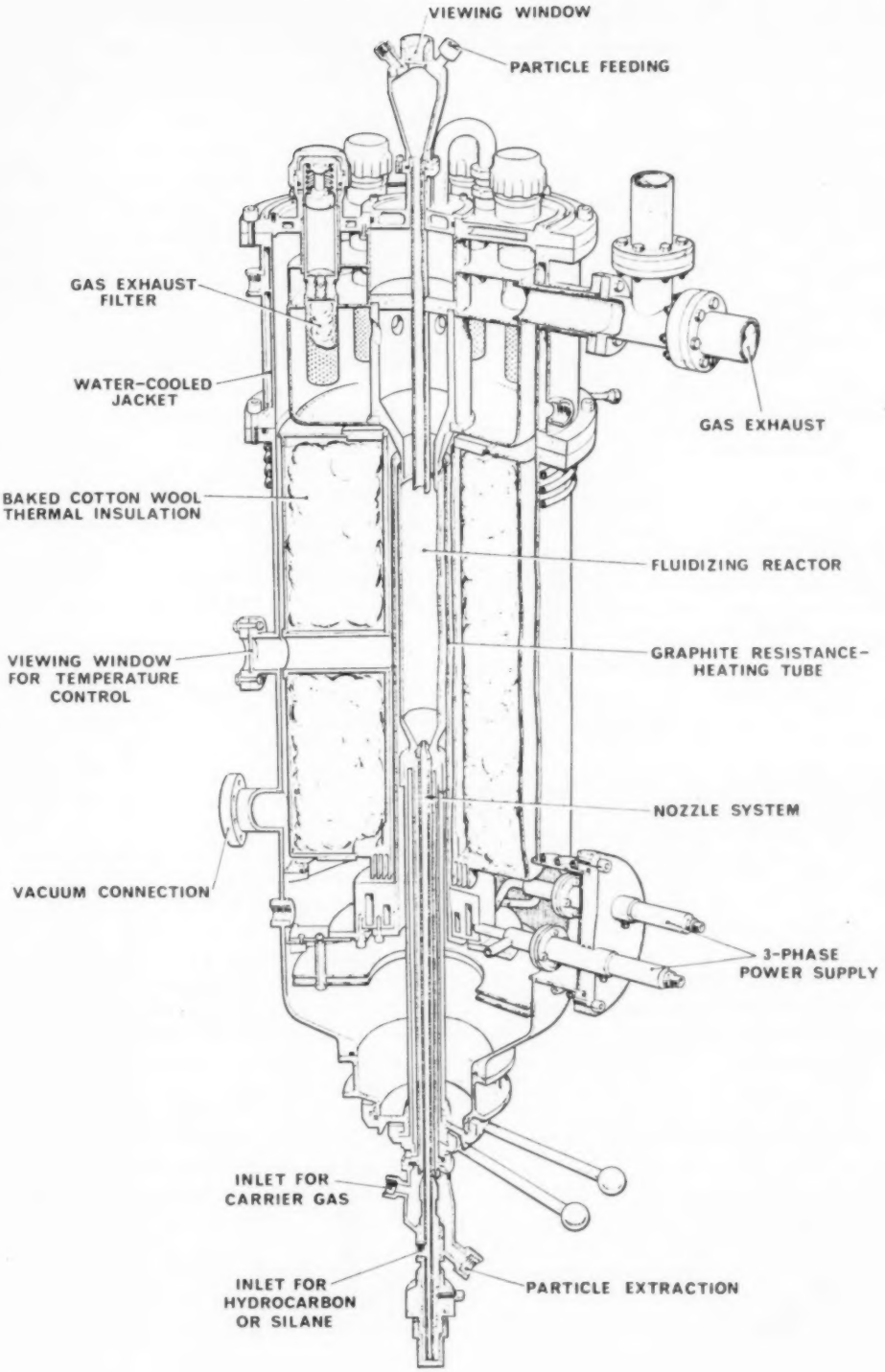

Fig. I-15 Prototype production-scale fluidized bed.[61i]

scribed, and it permits operation at temperatures up to 2200°C. A schematic diagram of the unit is shown in Fig. I-16. Rates of deposition of up to 200 μ/hr were obtained. Studies at Raytheon[61j] on PyC coating of carbide fuel particles have involved both rotating drums and fluidized-bed units. Both benzene and methane gas have been used as the feed for these units. A sketch of the rotating-drum device is shown in Fig. I-17, and the fluidized-bed unit is depicted in Fig. I-18. General Atomic also presented[65] a comprehensive review of its processes for preparing mixed-carbide fuel particles, coating with PyC, and preparing dispersions in graphite. In addition, information on the stability of the coated particles at temperatures between 1500 and 2000°C was summarized. Figure I-19 shows the effect of a temperature gradient at temperature levels of about 1850°C on early lots of coated carbide fuel. As was reported earlier by General Atomic, the carbide apparently goes into solid solution in the carbon on the high-temperature side of the particles, and carbon is precipitated on the low-temperature side. This effect was not observed at temperature levels of about 1500°C. General Atomic reports that its own materials resist such attack at temperatures of at least 1700°C and that coatings prepared from methane are superior to those prepared from acetylene.

Recent work with carbide fuels at Battelle[66–68] has been limited to the preparation of relatively

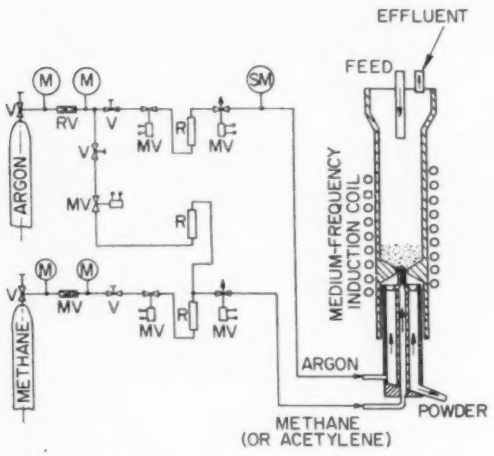

Fig. I-16 Schematic diagram of the Plansee apparatus for preparing PyC coatings in a fluidized bed.[64] V = valve, RV = pressure-reducing valve, M = manometer, MV = solenoid valve, R = rotameter, and SM = control valve.

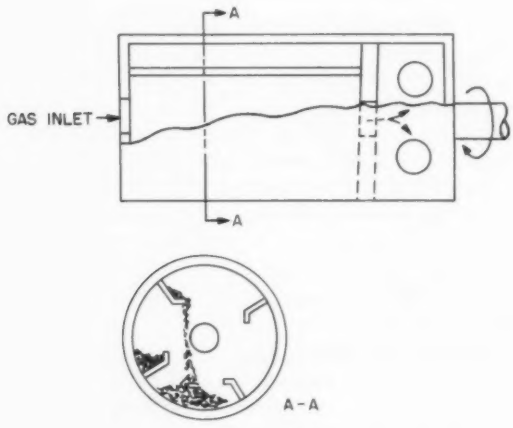

Fig. I-17 Sketch of Raytheon's rotary-cage apparatus for carbon coatings.[61j]

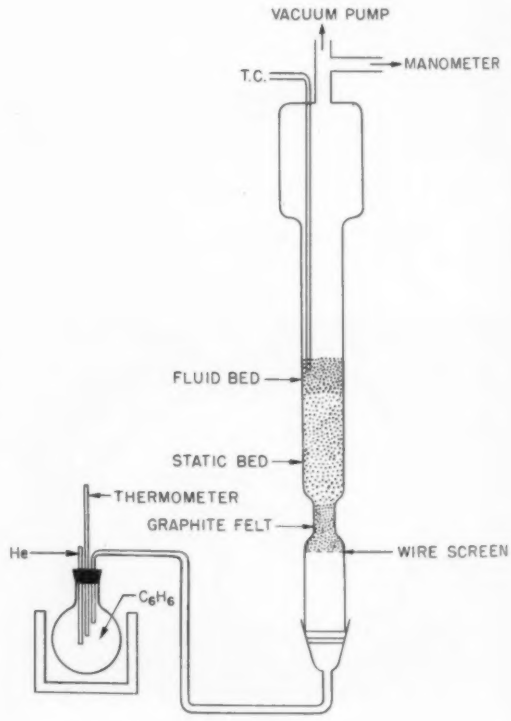

Fig. I-18 Sketch of Raytheon's fluidized-bed apparatus for carbon coatings.[61j]

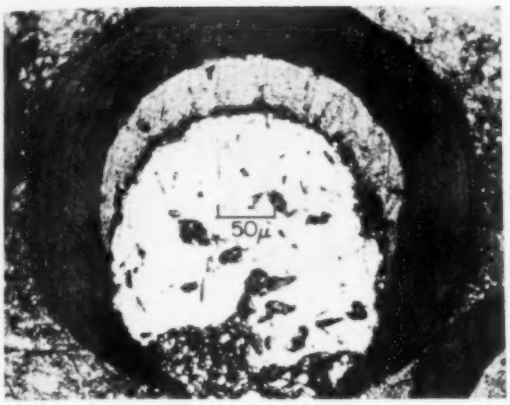

Fig. I-19 Carbon-coated thorium-uranium dicarbide particle showing severe migration of substrate after heat-treatment[65] at 1850°C.

thick coatings (about 100 μ) on uranium dicarbide particles and the addition of zirconium to the coatings in attempting to increase their resistance to radiation damage. (J. H. Oxley)

Irradiation and Evaluation

Oxide-Base Fuel. The only work in progress on the fission-product retention of coated UO_2 fuels is being done at Battelle.[66–68] The diameter of the fuel particles is about 127 μ, and three high-temperature sweep experiments are currently under way. UO_2 particles with 42-μ Al_2O_3 coatings, being irradiated at 850°C, have reached about 4 at.% burnup with an R/B (ratio of rate of release to rate of generation) for Xe^{133} of 10^{-7}. Another sweep capsule operating at 850°C, containing UO_2 particles coated with 60 μ of BeO, has accumulated a burnup of about 1 at.%, and has exhibited an R/B for Xe^{133} of about 10^{-6}. The third high-temperature sweep experiment was started late in November and contains additional UO_2 with 42-μ Al_2O_3 coatings in the sweep section of the capsule. The initial fission-gas-release ratio for Xe^{133} estimated from adsorption samples is on the order of 10^{-9} at an irradiation temperature of 1100°C.

The capsule design used for these higher temperature levels[61k] is shown in Fig. I-20. One sample is held in the sweep section, and six other samples are located in static compartments. The electric heater is a tantalum wire wound in a helical groove on an alumina tube. The heater is supported on a thin-walled tantalum tube that also acts as the primary seal for the sweep gas. The graphite sweep-specimen holder is surrounded by an alumina tube that acts as a barrier to prevent the flow of sweep gas over the tantalum support tube and the niobium static-specimen cores. Tantalum-sheathed tungsten: tungsten-rhenium thermocouples are positioned between the tantalum tube and the alumina barrier tube.

Irradiated Al_2O_3-coated particles with cracked coatings[61m] are shown in Fig. I-21. The appearance of these particles was generally the same before and after leaching. The light and dark areas on the intact particles are adjacent pieces of the cracked coatings. The sharp lines between the light and dark portions of the coatings are the location of cracks. The impression of an elevated ridge in the coating at the location of a crack is an optical illusion. A third phase has been found at the interface between the UO_2 and the Al_2O_3 coating in all cracked Al_2O_3-coated particles but never in undamaged particles. Approximately 30 to 40 vol.% of the UO_2 has been converted to this third-phase material. Examples of undamaged and damaged Al_2O_3-coated UO_2 particles after irradiation are shown in Figs. I-22 and I-23.

Carbide-Base Fuel. Oak Ridge has reported[69] considerable additional information on the irradiation behavior of carbon-coated carbide-fuel particles. Evidence for the treatment of irradiation temperature as an important variable for carbon coatings was shown in the experiments carried out in the B9 facility of the Oak Ridge Research Reactor (ORR). At 15 at.% burnup at temperatures of 820°C, the Xe^{133} R/B for NCC-AD (duplex coating) particles was 1×10^{-5}. Raising the irradiation temperature to 925°C and increasing the burnup to 28 at.% resulted in a higher Xe^{133} R/B value of 4×10^{-5}. Lowering the capsule temperature to between 320 and 525°C and increasing the burnup still further to 30 at.% lowered the Xe^{133} R/B to 2×10^{-5}. A new sample of the same lot irradiated at a constant temperature of 425°C yielded an R/B value for Xe^{133} of about 2×10^{-5} after 8 at.% burnup.[58] Since there was no increase in fission-gas release with burnup for this second sample, it was suggested that it contained more defective particles initially.

Two sweep capsules, currently being irradiated in the ORR poolside facility, contain Minnesota Mining & Manufacturing Co. (MMM) and National Carbon Company (NCC) carbon-coated carbide particles in graphite bushings.[69]

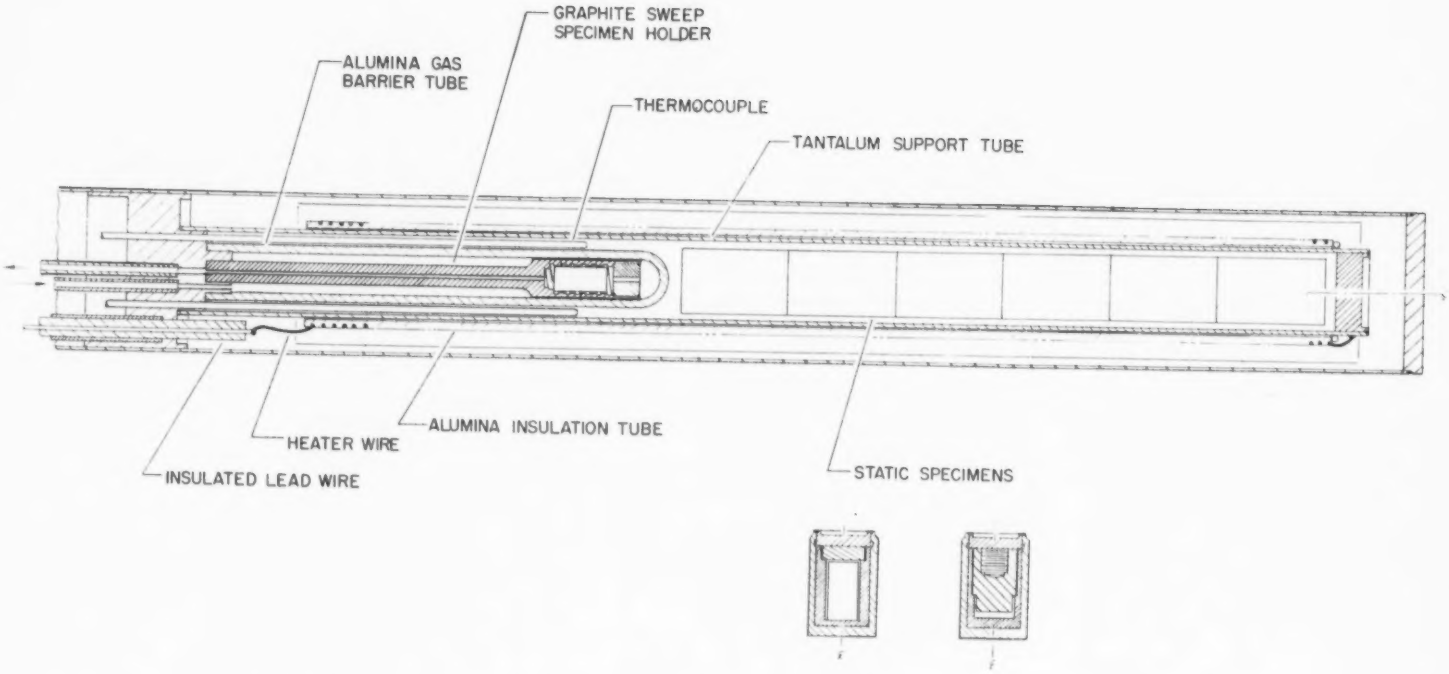

Fig. I-20 Capsule design for 2200 to 2400°F coated-fuel-particle irradiations.[61k]

The I
700°C
10^{-2} a
are b
burnu
The
for ir
is sho
in a m
porous
in the
peratu
sample
Fig. I-

Fig. I-21
UO_2 par

Fig. I-2
Al_2O_3-co

The MMM material is being irradiated at 700°C and has shown an Xe^{133} R/B of about 10^{-2} after 8 at.% burnup. The NCC particles are being irradiated at 880°C, and at 8 at.% burnup the R/B for Xe^{133} is approximately 10^{-3}.

The sweep-capsule design used at Oak Ridge for irradiating unsupported coated particles[70] is shown in Fig. I-24. The particles are mounted in a monolayer between concentric cylinders of porous graphite with thermocouple wells drilled in the graphite to measure the surface temperature of the particle coatings. For matrix samples a design similar to that shown in Fig. I-25 is employed. The fueled bushings are supported in an AGOT graphite sleeve, and the bushings surround an AGOT graphite central thermocouple well. The central temperature is measured with tantalum-sheathed tungsten: rhenium and platinum–10% rhodium: platinum thermocouples. The graphite sleeve contains

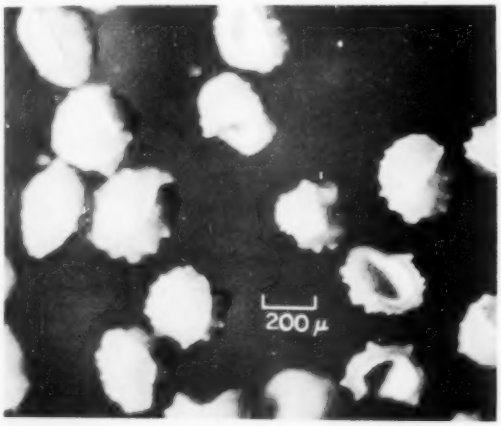

Fig. I-21 Stereophotograph of irradiated Al_2O_3-coated UO_2 particles with failed coatings.[61m]

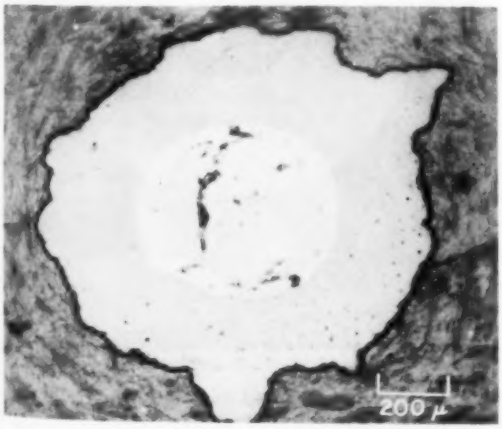

Fig. I-22 Photomicrograph of typical irradiated Al_2O_3-coated UO_2 particle with intact coating.[61m]

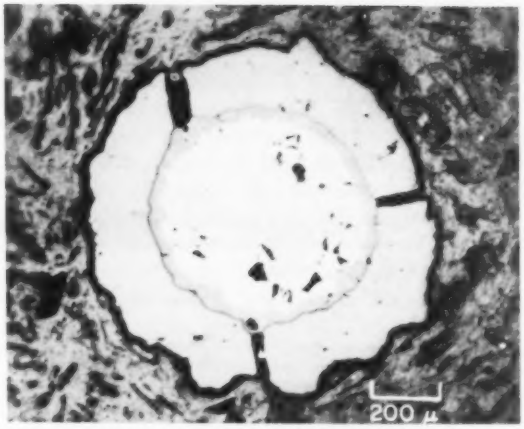

Fig. I-23 Photomicrograph of typical irradiated Al_2O_3-coated UO_2 particle with failed coating.[61m]

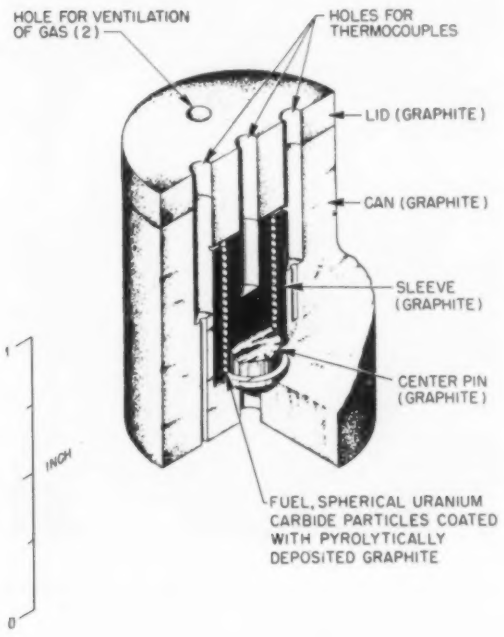

Fig. I-24 Coated-particle capsule type 2 for irradiation in ORR-C-1 Facility.[70]

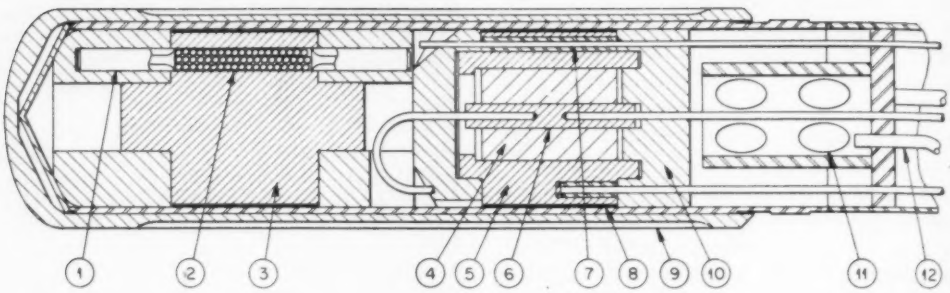

1. Capsule containing loose fuel particles
2. Pyrolytic-carbon-coated uranium carbide or uranium-thorium carbide particles
3. Graphite support for capsule; contains sheathed Chromel vs Alumel thermocouples
4. Graphite matrix fuel cylinder containing pyrolytic-carbon-coated uranium-thorium carbide particles
5. Graphite support sleeve for fuel cylinder; contains sheathed Chromel vs Alumel thermocouples
6. Graphite well containing sheathed tungsten vs rhenium and platinum–10% rhodium vs platinum thermocouples
7. Helium purge gas supply tube
8. Thermal barrier gap (filled with helium)
9. Containment vessel wall
10. Thermal insulator supports of porous carbon or graphite
11. Specimens for fission-product deposition experiments
12. Helium purge gas outlet tube

Fig. I-25 ORNL experimental assembly MTR-48-6 (Ref. 70).

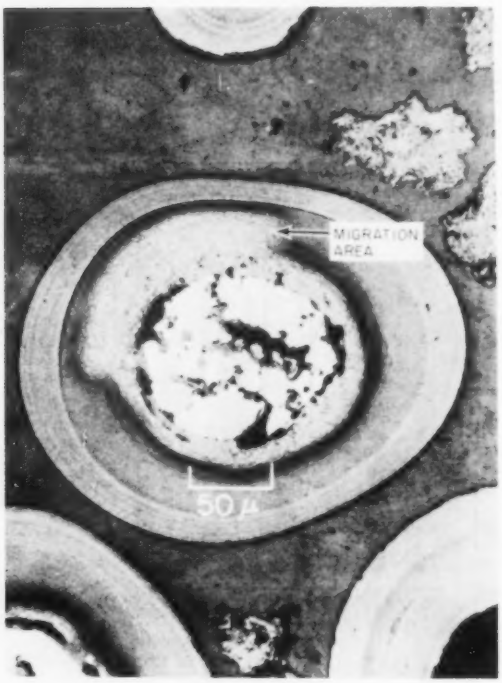

Fig. I-26 Typical unbroken particle from irradiated capsule B9-6 showing uranium carbide migration outward through part of the PyC coating.[70]

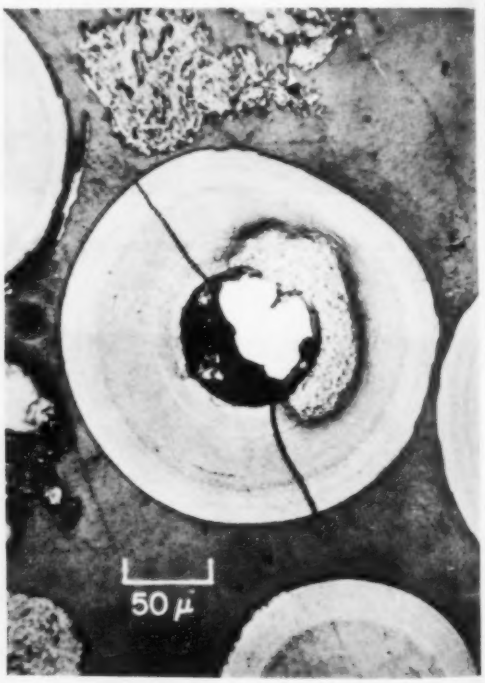

Fig. I-27 Typical broken PyC-coated particle from irradiation capsule B9-6 (Ref. 70).

the helium-purge-gas supply tube and flux-monitor wires in longitudinal holes. Loose particles can also be irradiated in a static section.

Damaged carbon-coated particles after irradiation[70] are shown in Figs. I-26 to I-28. It should be emphasized that these damaged particles do not necessarily represent the average appearance of the irradiated sample but were selected to demonstrate the type of damage that can occur. Undamaged coatings generally appear the same as unirradiated coatings, except at high burnups, where Oak Ridge indicates some limited migration occurs in all cases.[58]

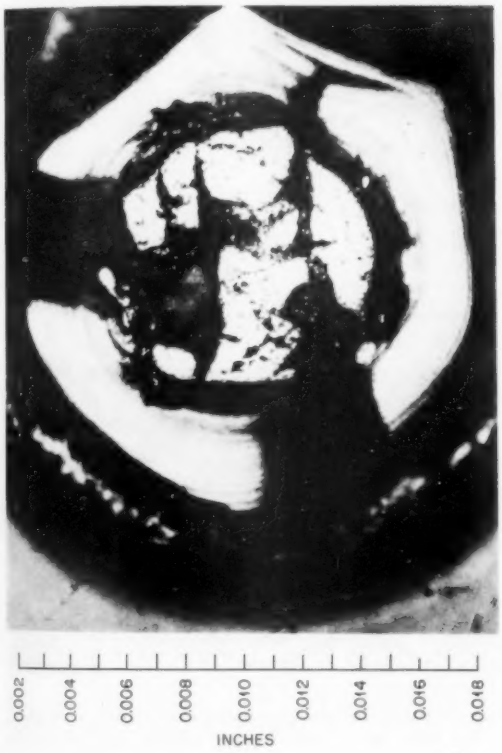

Fig. I-28 One of the particles that failed in Low-Intensity Test Reactor (LITR) capsule LCP-2 (Ref. 70).

The General Atomic irradiation results of the 309 series of experiments have been summarized.[61m] In these experiments, fuel compacts containing carbon-coated $(Th,U)C_2$ particles were irradiated in purge capsules placed in the water reflector adjacent to the core of the General Electric Test Reactor (GETR). The design of the capsule[65] is shown in Fig. I-29. The temperature of the capsule was determined by fission heating plus the composition of the purge gas, a helium-neon mixture in a control annulus located between the first specimen and the capsule coolant. The fuel compacts were annular (1 in. in outside diameter, 0.5 in. in inside diameter, and 1.75 in. long), and they contained 18 to 24 wt.% fuel (Th : U = 2.2 : 1) in a graphite matrix. The fuel particles were approximately 200 μ in diameter and were coated at 1400°C. The variation in the type of coatings used in the various capsules is shown in Table I-5.

The irradiation behavior of these capsules, together with the data for a full-diameter quarter-length High-Temperature Gas-Cooled Reactor (HTGR) fuel element, is shown in Fig. I-30, where the Xe^{133} R/B ratio is used as a measure of performance. Although the temperature of the various capsules varied over a considerable range during the experiments, an attempt has been made to normalize all the data to a temperature of 1400°C. It was suggested[61m] that krypton and xenon (or their precursors) are significantly released only from particles with broken or defective coatings and that such release is similar to release from uncoated fuel. It was pointed out that the R/B's show a pronounced increase with time in the reactor. This effect was tentatively explained on the basis that a time-dependent permeation of the coating takes place. In addition, it was believed that radiation and thermal cycling might either develop microcracks in the coatings, and then increase the effective permeation coefficient, or cause large cracks or breaks in the coating to develop, and completely release the fission

Table I-5 FUEL PARTICLES FOR IN-PILE PURGE-CAPSULE RUNS IN GA-309 IRRADIATION SERIES[61m]

Capsule	Coating	Mass of U^{235}, g
GA-309-4	25-μ pyrocarbon (BMI) from C_2H_2	2.64
GA-309-5	25-μ pyrocarbon (BMI) from C_2H_2	1.81
GA-309-6	25-μ pyrocarbon (BMI) from C_2H_2	2.29
GA-309-7	10- to 15-μ carbon from C_2H_2	2.62
GA-309-8	50- to 60-μ carbon from CH_4	1.80
GA-309-9	50- to 60-μ carbon from C_2H_2	2.27

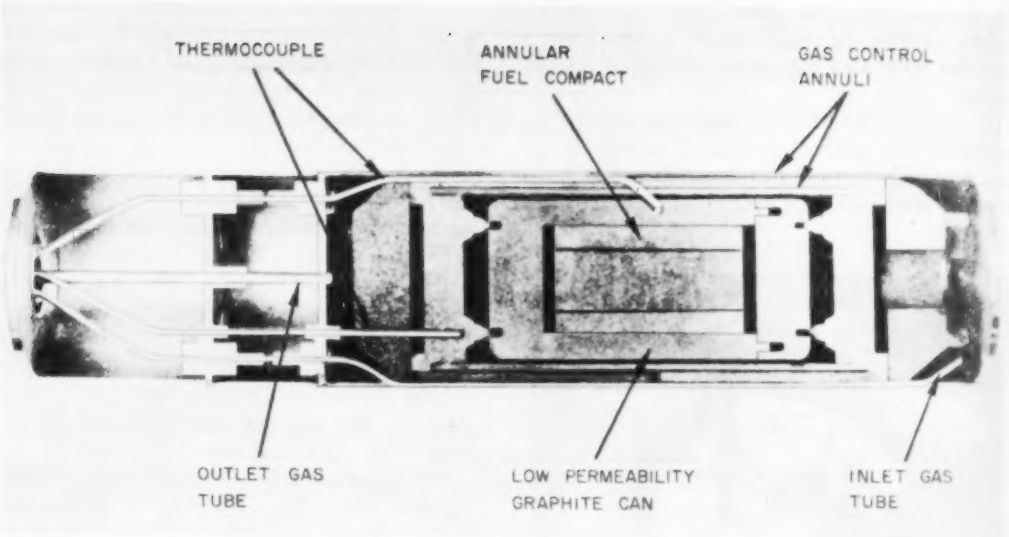

Fig. I-29 GA-309 series irradiation capsule.[65]

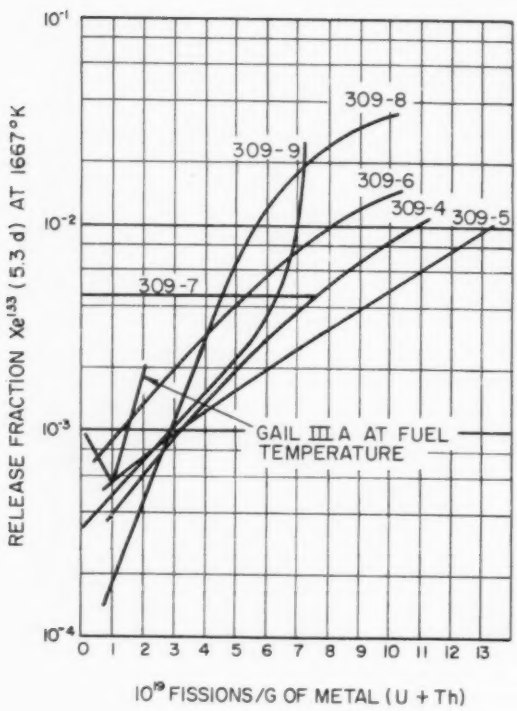

Fig. I-30 In-pile steady-state release of Xe^{133} for GA-309 experiments.[61n]

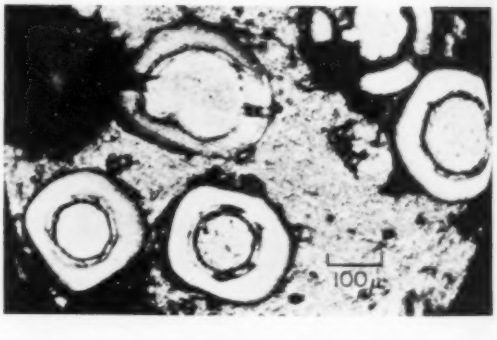

Fig. I-31 Photomicrograph of a group of fuel particles with intact and broken carbon coatings from capsule GA-309-9 (Ref. 65).

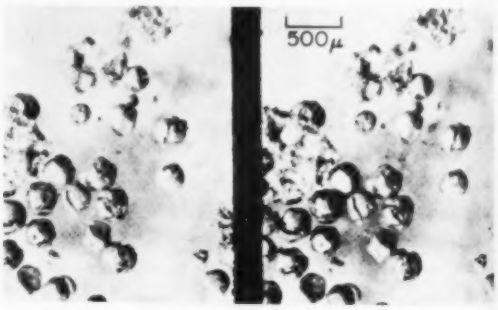

Fig. I-32 Stereophotograph of fuel particles with broken carbon coatings removed from end of capsule GA-309-9 (Ref. 65).

products diffusing from the particles. The appearance of typical coatings after irradiation is shown in Figs. I-31 and I-32.

Several new experiments with relatively thick carbon coatings on carbide particles are being initiated at Battelle,[68] but no significant data are presently available. However, results of postirradiation studies of previously irradiated carbon-coated carbide particles are available.[61m] Particles of UC_2 with failed laminar carbon coatings are shown in Fig. I-33. The coatings on these particles appear to be peeling off in layers, exposing lower layers of PyC. The coatings on these particles were deposited in two layers, the first being 17 μ in thickness and the second being about 38 μ in thickness.

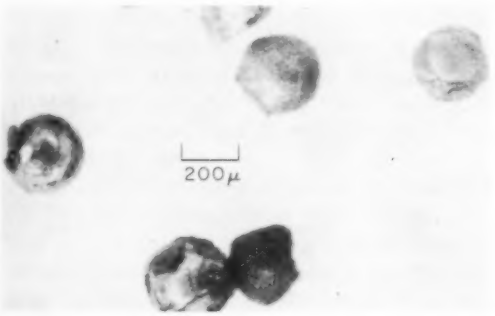

Fig. I-33 Stereophotograph of irradiated laminar carbon-coated UC_2 particles.[61m]

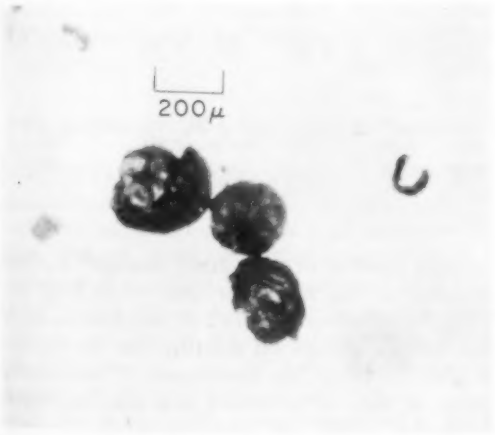

Fig. I-34 Stereophotograph of irradiated columnar carbon-coated UC_2 particles.[61m]

From a comparison of the relative thickness of the peeling layers, it appeared that the peeling layers were thinner than a coating layer. Particles with failed columnar coatings are shown in Fig. I-34. The coatings appeared to fail in a manner such that whole segments or sections of the coating pull away from the core.

(J. H. Oxley)

Refractory Fuel and Fertile Materials

High-Temperature Fuels Data

On behalf of the Oak Ridge Gas-Cooled Reactor Program, Battelle has issued a compilation of "Properties of Fuels for High-Temperature Reactor Concepts."[71] This report presents available data on properties and behavior of all fuels considered promising for operation at surface temperatures of 650°C or higher.

Data sheets for each fuel are standardized in form, giving physical, mechanical, thermal, and electrical properties, as well as corrosion and irradiation behavior. Fuels covered are the alloys, compounds, cermets, and dispersions listed in Table I-6. This table, taken directly from the report, provides a quick comparison among the various fuels on the basis of four important properties.

Properties and Behavior of Uranium Oxide Fuels

Information from Bettis pertaining to the development of new pressurized-water-reactor fuels covers irradiation studies of Zircaloy-clad UO_2 plates[72] and ZrO_2-UO_2 fuels.[73] This information is quite extensive and should be of considerable value to anyone currently concerned with reactor-fuel applications of these materials.

A constitution diagram for the UO_2-BaO system has been reported by the Russians.[74] The binary UO_2-BaO system forms $BaUO_3$ with a pseudocubic perovskite structure. The $BaUO_3$ and UO_2 form eutectic mixtures. BaO was found to be insoluble in the UO_2 solid solution, and the presence of Ba_3UO_6 was observed in the

Table I-6 FUEL COMPARISON TABLE[71]

Fuel material	Contained uranium or plutonium		Melting point		Thermal conductivity, cal/(sec)(cm)(°C)			Fission-to-absorption cross-section ratio
	Wt.%	G/cm³	°C	°F	At 20°C	At 600°C	At 1200°C	
Alloys								
Nb–10 wt.% U	10 U	0.955 U	2400	4350		0.0936		0.12
Nb–20 wt.% U	20 U	1.82 U	2300	4175		0.0774		0.22
Compounds								
PuC	95.6 to 96.1 Pu	13.0 to 13.1 Pu	1650	3000				
PuO_2	88.2 U	10.1 Pu	2280	4130				
$(Th_9U)B_4$	10 U					0.891		
$(Th_9U)C$	10 U					0.0375		
$(Th_9U)C_2$	10 U					0.0566		
UC	95.2 U	12.9 U	2400	4350	0.08	0.055	0.055	0.55
UN	94.4 U	13.5 U	2630	4770	0.032	0.046	0.058	0.44
UO_2	88.2 U	9.67 U	2760	5000	0.11	~0.035	0.022	0.55
U_3Si_2	86.2 U	11.3 U	1665	3030	0.035			0.53
Ceramic Dispersions								
20 wt.% UO_2–80 wt.% Al_2O_3	17.6 U		~2030	~3700				0.33
30 wt.% UO_2–70 wt.% Al_2O_3	26.5 U		~2030	~3700				0.45
10 wt.% UO_2–90 wt.% BeO	8.8 U	0.26 U	~2450	~4440	0.25			0.48
80 wt.% UO_2–20 wt.% Be	70.6 U							0.53
95 wt.% UO_2–5 wt.% MgO	83.8 U							0.54
2.57 wt.% UO_2–7.3 wt.% ThO_2–90 wt.% BeO	2.24 U							0.13
25 wt.% UO_2–35.5 wt.% ThO_2–39.1 wt.% BeO	22.1 U							0.22
UO_2-graphite	19 U	0.38 U			0.052 to 0.073			0.54
UO_2-graphite	45 U	1.21 U			0.035 to 0.051			0.58
UC_2-graphite	10 U	0.19 U			~0.13			0.51
UC_2-graphite	20 U	0.40 U			~0.14			0.53
Metallic Dispersions								
20 wt.% UO_2–stainless steel	17.6 U	1.43 U	1400 to 1460	2550 to 2650	0.017	0.037	0.067	0.064
40 wt.% UO_2–stainless steel	35.3 U	3.06 U	1400 to 1460	2550 to 2650	0.022	0.028	0.034	0.13
50 wt.% UO_2–stainless steel	44.1 U	3.95 U	1400 to 1460	2550 to 2650	0.022	0.027	0.032	0.18
Cermets								
Mo–80 vol.% UC	76.16 U	9.44 U	2625	4760	0.039	0.036	0.071	0.47
Mo–80 vol.% UN	75.55 U	9.79 U	2625	4760	~0.05	0.055		0.39
Mo–80 vol.% UO_2	70.48 U	7.32 U	2625	4760	~0.05	0.045		0.44

BaO-UO_3 system. Workers at the Bureau of Standards[75] have studied the stabilizing effects of various oxide additives on UO_2.

Surface-tension measurements were performed on liquid UO_2 at Hanford[41] by a pendant-drop technique. Analysis of three pendant-drop profiles by two independent methods gave values between 340 and 760 dynes/cm with a mean of 490 dynes/cm. The temperature of the liquid UO_2 was assumed to be constant at 2800°C, the melting point of UO_2. In other studies[46] the heat of fusion of UO_2 was determined to be 3300 cal/mole. This value is based on measurements of the volume change on melting and the surface tension of UO_2. The dependence of the melting point of UO_2 on pressure was also estimated from the same data. Increasing the pressure from 1 to 100 atm would be expected to result in an 8°C increase in the melting point. The coefficient of linear expansion of liquid UO_2

was measured as 37×10^{-6}/°C over the temperature range from 2800 to 3100°C.

The liquidus for the UO_2-ThO_2 system was determined at Hanford.[41] The salient features of these studies are complete miscibility of the two components and a eutectic of 2760°C at 2 wt.% ThO_2. Material used in these studies showed evidence of loss of uranium to the vapor phase, which reflects the higher vapor pressure of UO_2 relative to that of ThO_2.

Alexander[76] has investigated the vapor pressure of UO_3 over nonstoichiometric oxides ranging in composition from UO_2 to U_3O_8 at temperatures from 1410 to 1965°K, using the transpiration method. Free energies of formation were calculated for UO_3 and the other compositions which were studied. From literature data the free energy for $UO_{2.67}$ was found to be $\Delta F = -281{,}960 + 49.71T(°K)$ cal/mole over the range 1405 to 2000°K. From this result and the vapor-pressure data, the free energy of formation for gaseous UO_3 was determined to follow the relation $\Delta F = -202{,}080 + 20.79T(°K)$ cal/mole, whereas UO_2 followed $\Delta F = -257{,}530 + 41.47T(°K)$ cal/mole.

Owens-Corning[77] reports research on nuclear fuel-bearing glasses. About 400 glass compositions containing oxides of uranium, thorium, and plutonium, or combinations of these oxides were studied. Glasses containing 50 wt.% U_3O_8 and up to 65 wt.% ThO_2 with UO_2 were successfully produced in fiberized form. Special high-temperature glasses that melt at temperatures in excess of 1600°F have been developed. Irradiation tests on Vycor-UO_2 fuel elements at Knolls[78] indicate that silica-uranium systems appear promising for high-temperature fuel applications. (R. H. Barnes)

Fabrication of UO_2-Containing Ceramics

Investigators at United Nuclear[79] are pursuing a program aimed at characterizing 12 UO_2 powders of varying degrees of sinterability. One of the tests involves measurement of infrared transmission of compacts containing small amounts of the powders. In this work, 1.5-mg samples of UO_2 were mixed with 300 mg of KBr powder, and the mixtures were compacted to form wafers. The infrared transmission of the wafers was measured at wavelengths between 2 and 15 μ with a Perkin-Elmer model 21 infrared spectrophotometer. The transmission of infrared energy through the wafers was calculated as a percent of the transmission through air and plotted against wavelength.

Examination of the transmission curves showed apparent differences between the transmission of the oxide types at wavelengths of 4 and 6.5 μ. Using the transmission at 12 μ as a standard, the transmission ratios 12 μ : 4 μ and 12 μ : 6.5 μ were calculated. These ratios were compared with the observed sinterability of the UO_2 powders under standard conditions and are shown below.

Transmission ratio		Degree of sinterability
12 μ : 4 μ	12 μ : 6.5 μ	
0.08	0.03	High
0.20	0.11	Moderate
0.32	0.17	Low

The physical basis for these excellent correlations is not explained. However, infrared transmission measurement does seem to offer another means of distinguishing between active and inactive UO_2 powders.

Battelle[80] has been working on the synthesis of UO_2 single crystals for property measurement. A means of producing crystals containing less than 100 ppm of metallic impurities and measuring ¼ by ¼ by ½ in. was sought. Several reaction techniques were investigated, including these:

$$UF_4(g) + 2H_2O(g) \rightarrow UO_2(c) + 4HF(g) \quad (1)$$

$$UO_2Cl_2 \rightarrow UO_2(c) + Cl_2(g) \quad (2)$$

$$UO_2 \text{ in KF solution} \rightarrow UO_2(c) + KF(s) \quad (3)$$

$$UO_3(g) \rightarrow UO_{2+x}(c) + \frac{1-x}{2} O(g) \quad (4)$$

Millimeter-size crystals were produced by reactions 1 and 3 and submillimeter-size crystals by reaction 4. Reaction 2 did not proceed as indicated but produced substantial-size U_3O_8 crystals.

Direct methods such as vaporization-condensation and fusion were also investigated. Millimeter-size crystals were given by vaporization-condensation in a period of a few hours at 2500°C. Verneuil type boules, made by plasma-jet melting, were strained, cracked, and impure.

The authors concluded that low-temperature methods are useful for producing strain-free millimeter-size UO_2 crystals. Crystals formed by high-temperature techniques invariably contained porosity and free uranium. It appeared that disproportionation is a thermodynamic property of UO_2 at temperatures exceeding 2000°C.

A volume of the collected papers of the December 1961 meeting at Oak Ridge on the characterization of uranium dioxide has recently been published.[81] Twenty-nine papers are included, and many sites are represented. The papers deal with various aspects of UO_2 powder and sintered-body characterization. Numerous processing methods are described, and effects of processing variables and purity on sinterability of powders and irradiation performance of sintered bodies are discussed.

(A. K. Smalley)

Properties of Carbides, Nitrides Sulfides, and Phosphides

Baldock et al.[82] have identified a ternary compound in the uranium-carbon-iron system having the composition $UFeC_2$. The compound is tetragonal, with cell dimensions of $a = 4.965$ A and $c = 7.450$ A. It has a theoretical density of 11.5 g/cm^3 and a hardness of 450 kg/mm^2. The compound apparently forms by a peritectic reaction at about 1750°C and forms a eutectic with iron.

Rhenium and tungsten–26 wt.% rhenium alloy layers are ineffective in stopping the diffusion of carbon from UC_2 to molybdenum and tungsten at 1800°C. However, a layer of ZrC is an effective barrier to such diffusion. After 50 hr at 1800°C, the depth of penetration of uranium into ZrC from UC was 45 μ. After 30 hr at 2000°C, the penetration was 1300 μ, according to Weinberg et al.[83]

A survey of the reactions of UC, UC_2, and UN with various metals at temperatures of 1000°C and below has been made by Katz.[84] Studies were made with aluminum, chromium, iron, molybdenum, nickel, niobium, thorium, titanium, vanadium, zirconium, and stainless steel. Iron did not react with UC_2 or UN in 500 hr at 1000°C. Niobium reacted slowly with all three fuels at 1000°C, and a depleted zone of UC was formed between UC_2 and niobium. Stainless steel did not react with UN in 500 hr at 1000°C. More rapid reactions were noted with the other combinations.

Peakall and Antill have published data[85] supporting the thesis that the rates of reaction of 1 atm of CO_2, oxygen, nitrogen, or CO with uranium monocarbide are less than or similar to the rates of reaction of these gases with uranium metal at temperatures from 350 to 1000°C. A possible exception is noted for CO_2 in the temperature range from 500 to 700°C. Data for uranium were obtained from the literature. Data for UC were obtained on material having a density of only 11.7 to 12.7 g/cm^3.

Atomics International reports[17] that at 2000°F both hypo- and hyperstoichiometric UC react with stainless steel to form a liquid eutectic. Liquid calcium does not react with stoichiometric UC after 330 hr at 1600°F. The uranium–5.2 wt.% carbon alloy is slightly decarburized by calcium at 1600°F. In 430 hr at 1600°F, lead showed no attack on UC and hyperstoichiometric UC; however, lead dissolves the uranium in the grain boundaries of hypostoichiometric UC. No reaction was observed between magnesium and uranium-carbon alloys in 330 hr at 1600°F.

A review[86] of the mechanical and physical properties, the compatibility, and the irradiation resistance of uranium carbides has been published by Dickerson and Chubb.

Data obtained by Chang of Atomics International[17] show that at 1500°C and at a strain rate of 4×10^{-4}/min the flow stress for hypostoichiometric UC is 1900 to 2300 psi, the flow stress for stoichiometric UC is 2100 to 2900 psi, and the flow stress for hyperstoichiometric UC is 5100 to 9800 psi. Additional data are given for temperatures up to 2000°C. It is suggested that deformation at these temperatures in UC occurs in the (1 1 0) direction on the (1 1 1) plane.

Irradiations of ½-in.-diameter slugs of UC have been performed at Atomics International.[17] These were sodium or NaK bonded to type 304 stainless-steel or nickel cladding materials. Average surface temperatures were about 1200°F or lower. Burnups ranged from 6000 to 20,500 Mwd/metric ton of uranium, diameter changes ranged from about 0.5 to 5%, and gas releases ranged from 0.06 to 7.1% of theoretical, except for larger values obtained on one sample which formed a eutectic melt with its cladding material. The stainless-steel clad-

dings of hyperstoichiometric UC samples were embrittled and contained up to 1.4% carbon after these irradiations.

Benesovsky and Rudy report[87] that, at 1700°C, UC_2 dissolves about 30 mole % ThC_2 and ThC_2 dissolves about 30 mole % UC_2. A ternary diagram drawn by them shows tentative tie lines from uranium metal and thorium metal converging on the (U,Th)C solid-solution region at about 40 at.% thorium, 12 at.% uranium, and 48 at.% carbon. Tentative tie lines from UC_2–30 mole % ThC_2 alloy and ThC_2–30 mole % UC_2 alloy converge on the (U,Th)C solid-solution region at about 78 mole % UC–22 mole % ThC.

Marchal and Trouve[88] have studied the rate of formation of ThC_2 between ThC and graphite. The thickness of the reaction layer is described by the equation: $x = 8 \times 10^{-4} \exp(-39{,}000/RT)$. The linear-thermal-expansion coefficient of ThC_2 from 0 to 1000°C is 8.5×10^{-6}/°C. The thermal conductivities of ThC and ThC_2 are shown in Table I-7.

Table I-7 THERMAL CONDUCTIVITIES OF THORIUM CARBIDES[88]

Temp., °C	Thermal conductivity, cal/(cm)(sec)(°C)	
	ThC	ThC_2
200	0.020	0.056
300	0.019	0.050
400	0.019	0.049

Table I-8 COMPATIBILITY OF URANIUM MONOSULFIDE WITH VARIOUS MATERIALS[22,91–93]

Material in contact with US	Test conditions		Results
	Time, hr	Temp., °C	
Chromium	1	1500	No reaction
Molybdenum	2	1930	No reaction
Molybdenum	1	2200	No reaction
Niobium	336	800	No reaction
Niobium	1	2000	No reaction
Niobium	1	2200	No reaction
Stainless steel	336	800	No reaction
Tantalum	2	1930	Possible slight reaction
Tantalum	1	2200	No reaction
Tungsten	1	2200	No reaction
Vanadium	336	800	No reaction
Zirconium	336	800	0.7-mil reaction zone
Water	8	100	No reaction
NaK	336	800	No reaction
Hydrogen		800	No reaction
Air		250	Adherent oxide formed
Air		460	Ignites

Keller has obtained additional data on the properties[89,90] of UN. The hardness is 500 DPH at 25°C and 50 DPH at 1400°C; the specific heat of UN is 0.045 cal/(g)(°C) at 0°C and 0.063 cal/(g)(°C) at 1150°C; the thermal conductivity of UN is 0.03 cal/(sec)(cm)(°C) at 25°C and 0.06 cal/(sec)(cm)(°C) at 1000°C. The solubility of hydrogen in fully dense UN is less than 1 ppm. At pressures over 2 atm, UN melts congruently at 2885 ± 30°C.

Reports from Argonne[22,91,92] and General Electric[93] have provided a considerable body of data relating to the compatibility of US with other materials, as shown in Table I-8. Other properties of US, ThS, and UP are shown in Table I-9. US and ThS form a complete series of solid solutions at 1700°C. (W. Chubb)

Table I-9 PROPERTIES[22,91] OF US, ThS, AND UP

Property	US	ThS	UP
Crystal structure	Fcc, NaCl	Fcc, NaCl	Fcc, NaCl
Lattice parameter, A	5.49	5.68	5.57
Theoretical density, g/cm³	10.8	9.6	10.3
Resistivity, μohm-cm	158	22	
Hardness, DPH	160–280	220–250	
Expansion coefficient, 10^{-6}/°C	11.8	10.2	
Rupture modulus, psi	20,000	30,000	

Fabrication of Refractory Fuels Other Than Uranium Oxides

Densification rate vs. temperature curves for ThO_2 powder compacts have previously shown both a maximum and a minimum (inflection). Oak Ridge investigators[58] have established that the minimum is caused by impurity ions. The curve for the purest ThO_2 available did not exhibit this minimum. In addition, the minimum could be shifted by the addition of small amounts of impurities. The impurity-ion influence was shown to vary with temperature.

Alloys of UC with other metal carbides are being investigated for high-temperature fuel and thermionic applications. Dense, homogeneous material for testing is required, and a fabrication process that fulfills these requirements, allows good compositional control, and does not introduce impurities that could affect the high-temperature properties has not yet been developed. (E. O. Speidel)

Basic Studies of Irradiation Effects on Fuel Materials

Metallic Fuels

Megaw and Bridges[94] measured the release of I^{131} from uranium during complete oxidation in air and in CO_2 at 800°C. In air the release occurs during oxidation to U_3O_8; 53% of the I^{131} is released, with no further release on continued heat-treatment. In CO_2 the uranium oxidizes to $UO_{2.27}$ with no iodine release; the oxygen content then slowly decreases to $UO_{2.01}$, with a gradual release of 70% of the I^{131}. No explanation of this behavior is given. In a study at Hahn-Meitner,[95] the release of rare gas from uranium and from uranium monocarbide during postirradiation heating is discussed. A critical review is also given of rare-gas diffusion from UO_2. Much of the earlier data available in the literature is confused by oxidation occurring during the experiment. Nevertheless the current results on specimens that are being oxidized are often indistinguishable from pure diffusion. The specimens are carefully examined both before and after the experiment. At Atomics International,[17] diffusion coefficients and activation energies have been measured for the diffusion of Xe^{133} in uranium. These are functions of both purity of the material and burnup. Increasing burnup leads to lower fractional releases.

Agranovich and Miklin[96] present calculations of the swelling behavior of a uranium specimen that initially contained 10^{13} pores/cm^3. Irradiation at a flux necessary to form 3×10^{12} fission fragments/(cm^3)(sec) results in a time to initial swelling of 1.2 years at 327°C and 60 days at 727°C. In Japanese work[97] the behavior of vacancies and gas atoms in uranium has been calculated as a function of the number of trapping sites. Critical temperatures for homogeneous nucleation of bubbles and for vacancy recombination can be shown to depend on the concentration of traps.

The swelling of a number of gamma-uranium alloys has been reported by Greenwood.[98] No irradiation-induced cracks were observed. The average bubble size varied from small fractions of a micron to a few hundred microns, depending on the amount of swelling observed in the particular alloy. In every case surface tension was the chief restraining force for bubble growth. Uranium–14 wt.% molybdenum and uranium–54 wt.% niobium proved particularly resistant to swelling.

Blackburn[99] has obtained solutions for the mean strains and stresses in a clad uranium fuel element. The equations are deduced by assuming that the swelling of the uranium is due to equally spaced spherical bubbles, that gas atoms obey the perfect-gas law and enter the nearest bubble as soon as the gas is produced, and that the presence of the bubbles does not affect the mechanical properties of the uranium. The cladding is a more effective restraint as the bubble size increases, even though the swelling is greater for larger bubbles than for smaller bubbles under an equal restraint.

In Russian work[5] the internal-friction peak observed in uranium at 220 to 300°C has been identified with the presence of hydrogen. It is suggested that growth during thermal cycling might be due in part to defects produced by the repeated formation and decomposition of the hydride in this temperature range. Bloch[15] reports that the compound U_6Fe is rendered amorphous, as measured by X-ray methods, by irradiations short enough so that the microstructure is unaffected. There is no change of lattice parameter — only a progressive decrease in intensity. This leads to rejection of a mechanism involving point defects. Instead, the thermal effects in a fission spike are postulated to decrease the final grain in size to the point where the diffraction pattern disappears. Atomics International[17] has continued to measure the kinetics of the γ-γ' transformation in uranium-molybdenum alloys. The formation of metastable alpha phase was confirmed and time-temperature-transformation (TTT) curves were obtained.

(F. R. Winslow)

Radiation Effects in Ceramic Fuels

Lindner et al.[100] report activation energies and preexponential factors for the diffusion of uranium, krypton, xenon, and radon in UO_2 and U_3O_8; xenon and radon in ThO_2; and xenon in UC. The UO_2 samples are high-density sintered tablets, but no indication is given of the purity of the starting materials. For uranium in UO_2, D_0 = 1.0 cm^2/sec, and Q = 108 kcal/mole. The other results are given in Table I-10. Auskern and Osawa[101] report the value for the diffusion

Table I-10 DIFFUSIVITIES OF RARE GASES IN REFRACTORY FUELS[100]

(Q = Activation Energy, Kcal/Mole)

	Kr^{85}		Xe^{133}		Rn^{222}	
	$-\log D_0$	Q	$-\log D_0$	Q	$-\log D_0$	Q
$UO_{2.00}$	7.7	46.9	7.6	48.9	5.9	59
$UO_{2.12}$	6.0	48.1	6.2	48.0		
U_3O_8	16.2	17.3	9.6	19.7	11.0	26.1
UC			6.9	42.5		
ThO_2				30	6.6	51

for xenon in uranium carbide powder. The diffusion can be represented by the equation

$$D = 2.1 \times 10^{-5} \exp(-85{,}100/RT) \quad cm^2/sec$$

for the temperature range 1000 to 1400°C. These values are about an order of magnitude smaller than those for xenon in UO_2.

Harwell[102] presents the results of both in-pile and out-of-pile measurements of the release of fission gases from UO_2-BeO and UO_2-ThO_2-BeO specimens. Most of the fission-product movement is in BeO. The release due to diffusion is small over the temperature range 200 to 1000°C. Calculations based on the assumption of a diffusion coefficient varying exponentially with time do not reproduce the release kinetics. Chalk River[18] reports a small but significant effect of the initial specimen density on the xenon release from UO_2, even at high densities.

Hanford[103] reports the property changes in a UO_2 single crystal irradiated to 1.4×10^{20} fissions/cm^3 at a temperature below 400°C. Most properties are essentially unchanged. However, the hardness increases by 18 to 22%, depending on the orientation of the crystal. In a second experiment the thermal conductivity of a UO_2 single crystal during postirradiation heating decreases to a minimum at 700°C and increases markedly above this temperature. These are the first quantitative data in support of predictions of increased thermal conductivity in UO_2 at high temperatures. Harwell[104] has observed fission-fragment tracks in single-crystal UO_2 films after irradiating prethinned films. The UO_2 is probably not stoichiometric. These tracks are different in nature from those observed in vacuum-deposited UO_2 films in that they consist of vacancy-rich strained regions probably surrounded by interstitials. Diameters are approximately 100 A. Dislocation loops occur along the tracks. In fine-grained deposits, fission-fragment tracks occur at 100 A furrows, with some of the material evaporated and redeposited on the edges of the furrow. Interactions of grain boundaries with the energy carriers are suggested as a possible mechanism for formation of these tracks.

Rand et al.[105] report the occurrence of radiation self-damage in plutonium compounds. This has been checked by lattice-parameter measurements. The lattice of PuO_2 expands by only about 0.1% in one year, but the expansions of $PuC_{0.6}$ and $PuN_{0.9}$ are larger and are increasing almost linearly with time.

(F. R. Winslow)

References

1. W. D. Wilkinson, *Uranium Metallurgy: Vol. I, Uranium Process Metallurgy; Vol. II, Uranium Corrosion and Alloys*, Interscience Publishers, New York, 1962.
2. S. J. Rothman, J. J. Hines, J. Gray, Jr., and A. L. Harkness, Anisotropy of Self-Diffusion in Alpha Uranium, *J. Appl. Phys.*, 33: 2113-2116 (June 1962).
3. Y. Adda and A. Kirianenko, Study of Self-Diffusion in Alpha-Phase Uranium, *J. Nucl. Mater.*, 6: 130-134 (May–June 1962).
4. J. C. Rivière, The Work Function of Uranium, *Proc. Phys. Soc. (London)*, 80: 116-123 (July 1962).
5. V. E. Ivanov and B. C. Shapoval, Internal Friction in Uranium (in Russian), USAEC Translation AEC-tr-5372 (translated from IAEA Preprint SM-24/84 to be published in *Proceedings of the IAEA Symposium on Radiation Damage in Solids and Reactor Materials*, Held at Venice, Italy, May 7–11, 1962).
6. I. F. Barwood and B. R. Butcher, The Alpha to Beta Phase Transformation in Uranium, British Report AERE-R-4128, August 1962.
7. W. G. Jolley (Ed.), Papers and Proceedings of the X-Ray Preferred Orientation Meeting at Hanford, June 29 and 30, 1961, USAEC Report HW-74429, Hanford Atomic Products Operation, August 1962.
8. Ames Laboratory, Annual Summary Research Report in Chemistry, Engineering, Metallurgy and Physics, July 1, 1961–June 30, 1962, USAEC Report IS-500, September 1962.
9. G. Petzow and I. Kvernes, The Constitution of Uranium-Rich Uranium-Silicon-Aluminum Alloys (in German), *Z. Metallk.*, 53: 248-256 (April 1962).
10. Academy of Sciences of the USSR, Institute of Metallurgy, *Structures of Alloys of Certain Systems with Uranium and Thorium* (in Russian),

Gosatomizdat, Moscow, 1961; abstracted in *Ref. Zh. Met.*, (8): 22, 23 (1962).

a. O. S. Ivanov, T. A. Badayeva, A. T. Semenchenkov, and R. I. Kuznetsova, Investigating the Structure of the Uranium-Molybdenum System at 600 to 1200°C and the Properties of Its Alloys (Abstract 8I142).

b. O. S. Ivanov and G. I. Terekhov, The Phase Diagram and the Structure of Alloys of the Uranium-Columbium System (Abstract 8I143).

c. O. S. Ivanov and L. I. Gomozov, Phase Diagram of the Uranium-Zirconium-Columbium System (Abstract 8I149).

d. O. S. Ivanov and L. I. Gomozov, The Phase Diagram of Uranium-Zirconium-Columbium (Abstract 8I150).

e. T. A. Badayeva and R. I. Kuznetsova, Phase Diagram of the Uranium-Molybdenum-Chromium System (Abstract 8I151).

11. B. W. Howlett, A. J. Eycott, I. K. Kang, and D. R. F. West, The Kinetics of the Isothermal Decomposition of a Gamma-Phase Uranium–6 At.% Molybdenum Alloy, British Report AERE-R-4076, June 1962; to appear in *J. Nucl. Mater.*
12. C. M. Walter and L. R. Kelman, Penetration Rate Studies of Stainless Steel by Molten Uranium and Uranium-Fissium Alloy, *J. Nucl. Mater.*, 6(3): 281-290 (August 1962).
13. Y. Adda and A. Kirianenko, Reduction of Self-Diffusion Coefficients in Gamma-Phase Uranium by Additions of Molybdenum, Zirconium, or Niobium (in French), *J. Nucl. Mater.*, 6: 135-136 (May–June 1962).
14. R. G. Bellamy, The Swelling of Alpha Uranium Under Neutron Irradiation to 0.7% Burn-up, in *Institute of Metals Symposium on Uranium and Graphite, Monograph No. 27*, p.52, 1962.
15. J. Bloch, Effect of Neutron Irradiation on Uranium-Iron Alloys with Low Iron Content, Hanford Translation HW-TR-43 [translated from *J. Nucl. Mater.*, 6: 203-212 (July 1962)].
16. J. A. Horak, J. H. Kittel, and F. L. Yaggee, Irradiation Behavior of Restrained and Vented Uranium–2 Wt.% Zirconium Alloy, USAEC Report ANL-6431, Argonne National Laboratory, June 1962.
17. Atomics International, Annual Technical Progress Report, AEC Unclassified Programs, Fiscal Year 1962, USAEC Report NAA-SR-7400, Nov. 15, 1962.
18. Atomic Energy of Canada, Ltd., 1962. (Unpublished)
19. Uranium-Aluminum Alloy Containing One or More Additional Elements for the Purpose of Suppressing UAl_4 Formation, British Patent 893,189, Apr. 4, 1962.
20. G. W. Gibson and W. C. Francis, Annual Progress Report on Fuel-Element Development for Fiscal Year 1962, USAEC Report IDO-16799, Phillips Petroleum Co., Aug. 15, 1962.
21. R. J. Beaver, J. H. Erwin, and R. S. Mateer, An Evaluation of the Uranium Contamination on the Surfaces of Aluminum-Clad Uranium-Aluminum Alloy Research Reactor Fuel Plates, USAEC Report ORNL-3206, Oak Ridge National Laboratory, Mar. 19, 1962.
22. Argonne National Laboratory, Metallurgy Division Annual Report for 1961, USAEC Report ANL-6516.
23. Argonne National Laboratory, Reactor Development Program Progress Report, July 1962, USAEC Report ANL-6597, Aug. 15, 1962.
24. N. E. Daniel, E. L. Foster, J. A. DeMastry, A. A. Bauer, and R. F. Dickerson, Study of Aluminum Alloys Containing Up to 45 Wt.% Uranium, USAEC Report BMI-1183, Battelle Memorial Institute, Apr. 30, 1957.
25. Oak Ridge National Laboratory, Aug. 9, 1962. (Unpublished)
26. R. Burgett (Ed.), Summary Technical Report for the Period July 1–September 30, 1962, USAEC Report NLCO-860, National Lead Co. of Ohio, Oct. 31, 1962.
27. Argonne National Laboratory, Reactor Development Program Progress Report, September 1962, USAEC Report ANL-6619, Oct. 15, 1962.
28. M. J. F. Notley, E. N. Hodkin, and J. A. C. Davidson, The Oxidation of Plutonium and Certain Plutonium Alloys in Air and Carbon Dioxide, British Report AERE-R-4070, June 1962.
29. Hanford Atomic Products Operation, Plutonium Metallurgy Operation Quarterly Progress Report, April–June 1962, USAEC Report HW-74162, July 16, 1962. (Classified)
30. M. D. Freshly, Plutonium Spike Fuel Elements for the PRTR. Part I. The Mark I-G, USAEC Report HW-69200(Pt. I), Hanford Atomic Products Operation, March 1961.
31. T. I. Jones, The Irradiation of Aluminum-Plutonium Alloys in Zircaloy-2 Sheathing. Part III. Postirradiation Examination and Testing of Aluminum-Plutonium Alloys, Canadian Report CRRM-1097 (AECL-1589), July 1962.
32. J. E. Eichelberger, Mound Laboratory Monthly Progress Report for February 1962, USAEC Report MLM-1133, Mound Laboratory, Feb. 28, 1962.
33. H. Blank, G. Brossmann, and M. Kemmerich, Binary and Multicomponent Systems with Plutonium. Literature Search, Phase Diagrams, and Data. Part I. Pu-Ag to Pu-Sn, German Report KFK-105, June 1962.
34. G. R. Grove, L. V. Jones, and J. F. Eichelberger, Mound Laboratory Monthly Progress Report for June 1962, USAEC Report MLM-1138, Mound Laboratory, June 29, 1962.
35. J. F. Eichelberger, Mound Laboratory Monthly Progress Report for March 1962, USAEC Report MLM-1135, Mound Laboratory, Mar. 30, 1962.

36. J. F. Eichelberger, Mound Laboratory Monthly Progress Report for November 1961, USAEC Report MLM-1126, Mound Laboratory, Nov. 30, 1961.
37. Nuclear Materials & Equipment Corp., Development of Plutonium-Bearing Fuel Materials. Progress Report, July 1–September 30, 1962, USAEC Report NUMEC-P-102, October 1962.
38. T. D. Chikalla, C. E. McNeilly, and R. E. Skavdahl, The Plutonium-Oxygen System, USAEC Report HW-74802, Hanford Atomic Products Operation, September 1962.
39. Hanford Atomic Products Operation, August 1962. (Unpublished)
40. Hanford Atomic Products Operation, Plutonium Metallurgy Operation Quarterly Progress Report, July–September 1962, USAEC Report HW-74718, Oct. 15, 1962. (Classified)
41. Hanford Atomic Products Operation, Reactor and Fuels Research and Development Operation Monthly Report, September 1962, USAEC Report HW-75127A, Oct. 15, 1962. (Classified)
42. Hanford Atomic Products Operation, Reactor and Fuels Research and Development Operation Monthly Report, November 1962, USAEC Report HW-75625A, Dec. 15, 1962. (Classified)
43. S. Anselin and R. Pascard, Sur la Volatilite du Carbure et du Nitrure de Plutonium, *Compt. Rend.*, 255: 698-700 (1962).
    a. G. W. Wensch and B. E. Prince (Eds.), Report on Fast Reactor Activities of the United Kingdom AEA and the French Commissariat a l'Energie Atomique by the 1962 USA Fast Reactor Team, March 26–April 5, 1962, USAEC Report WASH-1036, May 1962. (Classified)
44. D. F. Carroll, Thermal Expansion of Plutonium Nitride, USAEC Report HW-75125, Hanford Atomic Products Operation, Oct. 2, 1962.
45. Hanford Atomic Products Operation, Research and Development Programs Executed for Division of Reactor Development, Quarterly Progress Report, January–March 1962, USAEC Report HW-73915, Aug. 1, 1962.
46. Hanford Atomic Products Operation, Reactor and Fuels Research and Development Operation Monthly Report, October 1962, USAEC Report HW-75376A, Nov. 15, 1962. (Classified)
47. Hanford Atomic Products Operation, Plutonium Metallurgy Operation Quarterly Progress Report, January–March 1962, USAEC Report HW-73318, Apr. 16, 1962.
48. J. M. Gerhart, The Postirradiation Examination of a PuO_2-UO_2 Fast Reactor Fuel, USAEC Report GEAP-3833, Vallecitos Atomic Laboratory, November 1961.
49. A. E. Ogard, C. C. Land, and J. A. Leary, The Thermal Expansion of PuC and PuC-UC Solid Solutions, USAEC Report LA-2768, Los Alamos Scientific Laboratory, Nov. 22, 1962.
50. C. E. Holley, Jr., The Thermodynamic Properties of the Uranium and Plutonium Carbides, USAEC Report LADC-5487, Los Alamos Scientific Laboratory, Oct. 10, 1962.
51. Hanford Atomic Products Operation, Research and Development Programs Executed for the Division of Reactor Development, Quarterly Progress Report, April–June 1962, USAEC Report HW-74761, Nov. 15, 1962.
52. B. Riley, The Hot Pressing of Uranium and Plutonium Carbides, British Report AERE-R-4154, September 1962; to appear in *J. Nucl. Mater.*
53. Los Alamos Scientific Laboratory, Quarterly Status Report on LAMPRE Program for Period Ending August 20, 1962, USAEC Report LAMS-2753, Sept. 28, 1962.
54. A. E. Ogard et al., The Preparation of Uranium Monocarbide–Plutonium Monocarbide Solid Solutions, Plutonium Sesquicarbide and Plutonium Monocarbide, *J. Inorg. Nucl. Chem.*, 24: 29-34 (January 1962).
55. Hanford Atomic Products Operation, Plutonium Metallurgy Operation Quarterly Progress Report, October–December 1961, USAEC Report HW-72161, Jan. 15, 1962. (Classified)
56. D. M. Provow and R. W. Fisher, The Electrical Resistivity of Molten and Solid Thorium-Magnesium Eutectic, USAEC Report IS-437, Ames Laboratory, May 1962.
57. Bureau of Mines, Metallurgical Progress Report No. 16 for the Period July 1–September 30, 1962, USAEC Report USBM-U-978.
58. Oak Ridge National Laboratory, Dec. 10, 1962. (Unpublished)
59. Oak Ridge National Laboratory, Nov. 7, 1962. (Unpublished)
60. G. W. Gibson and W. C. Francis, Annual Progress Report on Fuel Element Development for Fiscal Year 1962, USAEC Report IDO-16799, Phillips Petroleum Co., Aug. 15, 1962.
61. A Symposium on Ceramic-Matrix Fuels Containing Coated Particles, sponsored by the U. S. Atomic Energy Commission, Held at Battelle Memorial Institute, November 5–6, 1962 (proceedings to be published).
    a. P. G. Alfredson and R. C. Cairns, Coated Particle Studies for Beryllium Oxide Dispersion Type Fuels.
    b. T. Ishekawa and Nagaoki, Preparation of Granular Polymer Carbon-Coated Nuclear Fuel.
    c. Y. Akimoto, T. Suzuki, and C. Ito, Production of Spherical Uranium Dioxide Particles and Metallic Coating Thereon.
    d. L. Schäfer, Studies on Coated Particles at NUKEM.
    e. A. Auriol, C. David, G. Kurka, and E. Le Boulbin, Carbon Coated Particles for Dispersion Fuels.

f. P. Murray, Some Aspects of Harwell Research Relating to Dispersed Fuels.

g. G. B. Greenough, Dispersed Fuel Development Work at Reactor Fuel Development Laboratories, Springfields, England.

h. D. W. Savage, The Preparation of Graphite Matrix Fuel Compacts Containing Coated Carbide Particles.

i. R. A. U. Huddle, J. R. Gough, and H. Beutler, Coated Particle Fuel for the Dragon Reactor Experiment.

j. M. P. Lepie, Pyrographite Coating of Nuclear Fuel Particles.

k. N. E. Miller, R. L. Ritzman, R. J. Burian, and W. J. Zielenbach, Irradiation Studies.

m. R. J. Burian and J. E. Gates, Postirradiation Examinations.

n. L. R. Zumwalt, E. E. Anderson, and P. E. Gethord, Fission-Product Release from (Th:U)C_2-Particle Fuels.

62. C. C. Browne and R. E. Latta, General Electric Company, Flight Propulsion Laboratory Department, October 1962. (Unpublished)
63. European Nuclear Energy Agency, OECD High Temperature Reactor Project Dragon Third Annual Report, April 1, 1961–March 31, 1962, Report NP-12082.
64. F. Benesovsky and E. Rudy, Production of Graphite-Coated Particles for Nuclear Fuel by Fluidized Bed Process, *Metall.*, 16(10): 957-961 (October 1962).
65. W. V. Goeddel (Ed.), Pyrolytic-Carbon-Coated Carbide Fuel Particles and Their Use in Graphite-Matrix Fuel Compacts, USAEC Report GA-3588, General Atomic Division, General Dynamics Corp., Oct. 30, 1962.
66. R. W. Dayton and R. F. Dickerson, Progress Relating to Civilian Applications During September 1962, USAEC Report BMI-1596, Battelle Memorial Institute, Oct. 1, 1962. (Classified)
67. R. W. Dayton and R. F. Dickerson, Progress Relating to Civilian Applications During October 1962, USAEC Report BMI-1600, Battelle Memorial Institute, Nov. 1, 1962. (Classified)
68. R. W. Dayton and R. F. Dickerson, Progress Relating to Civilian Applications During November 1962, USAEC Report BMI-1603, Battelle Memorial Institute, Dec. 1, 1962. (Classified)
69. Oak Ridge National Laboratory, Oct. 25, 1962. (Unpublished)
70. Oak Ridge National Laboratory, Gas-Cooled Reactor Program Quarterly Progress Report for the Period Ending March 31, 1962, USAEC Report ORNL-3302, July 16, 1962.
71. R. W. Endebrock (Ed.), Properties of Fuels for High-Temperature Reactor Concepts, USAEC Report BMI-1598, Battelle Memorial Institute, Nov. 1, 1962.
72. R. C. Daniel, M. L. Bleiberg, H. B. Meieran, and W. Yeniscavich, Effects of High Burnup on Zircaloy-Clad, Bulk UO_2, Plate Fuel Element Samples, USAEC Report WAPD-263, Westinghouse Electric Corp., Bettis Atomic Power Laboratory, September 1962.
73. B. F. Rubin, R. M. Berman, and M. L. Bleiberg, The Irradiation Behavior of ZrO_2-UO_2 Fuels, USAEC Report WAPD-264, Westinghouse Electric Corp., Bettis Atomic Power Laboratory, October 1962.
74. N. M. Voronov and R. M. Sofronova, Reactions of Uranium Dioxide with Barium Oxide, in *Structures of Alloys of Certain Systems with Uranium and Thorium* (in Russian), Academy of Sciences of the USSR, Institute of Metallurgy, Gosatomizdat, Moscow, 1961.
75. H. S. Parker, S. Hasko, C. H. Schreyer, and H. J. Foster, A Fundamental Study of Ceramic Materials for Nuclear Reactor Applications, Summary Report, July 1, 1961–June 30, 1962, USAEC Report NBS-D-150, National Bureau of Standards. (Classified)
76. C. A. Alexander, Vapor-Solid Equilibrium in the Uranium Oxide-Oxygen System, Dissertation, Ohio State University, May 1962.
77. P. A. Lockwood, Investigations of Nuclear Fuel-Bearing Glasses, in Nuclear Reactor Chemistry, Second Conference, Gatlinburg, Tennessee, October 10–12, 1961, USAEC Report TID-7622, pp. 74-85.
78. W. M. Cashin and W. H. Howland, Silica-Uranium Fuel Systems, Part II, USAEC Report KAPL-1866, Knolls Atomic Power Laboratory, Sept. 9, 1957.
79. J. F. Carpenter, C. W. Kuhlman, and R. A. Nelson, Characterization of UO_2 Powders, Third Quarterly Report, April 10 to July 10, 1961, USAEC Report ORO-543, United Nuclear Corp.
80. J. D. Jackson and C. A. Alexander, Growth of UO_2 Single Crystals, Summary Report, USAEC Report BMI-X-210, Battelle Memorial Institute, Sept. 17, 1962.
81. Meeting on Characterization of Uranium Dioxide Held at Oak Ridge National Laboratory, Dec. 12–13, 1961, USAEC Report TID-7637, Oct. 1, 1962.
82. P. Baldock, J. R. McLaren, H. J. Hedger, and G. Briggs, A Ternary Compound in the U-Fe-C System, *J. Nucl. Mater.*, 5: 257-258 (February 1962).
83. A. F. Weinberg, R. G. Hudson, L. Yang, and F. D. Carpenter, Investigations of Carbides as Cathodes for Thermionic Space Reactors, Report GA-3245, General Atomic Division, General Dynamics Corp., June 1962.
84. S. Katz, High Temperature Reactions Between Refractory Uranium Compounds and Metals, *J. Nucl. Mater.*, 6: 172-181 (July 1962).
85. K. A. Peakall and J. E. Antill, Oxidation of Uranium Monocarbide, *J. Less-Common Metals*, 4: 426-435 (1962).

86. W. Chubb and R. F. Dickerson, Properties of Uranium Carbides, *Am. Ceram. Soc. Bull.*, 41: 564-569 (September 1962).

87. F. Benesovsky and E. Rudy, Studies of the Uranium-Thorium-Carbon System, USAEC Translation AEC-tr-5175 [translated from *Monatsh. Chem.*, 92: 1176-1183 (1961)].

88. M. Marchal and J. Trouve, Study of the System Carbon-Uranium-Thorium, Quarterly Progress Report No. 4, October 1–December 31, 1961, USAEC Translation AEC-tr-5174 (translated from French Report CEA-3677), Jan. 10, 1962.

89. D. L. Keller, Development of Uranium Mononitride, Quarterly Progress Report, April–June 1962, USAEC Report BMI-X-10006, Battelle Memorial Institute, July 1, 1962.

90. D. L. Keller, Development of Uranium Mononitride, Quarterly Progress Report, July–September 1962, USAEC Report BMI-X-10019, Battelle Memorial Institute, Oct. 1, 1962.

91. P. D. Shalek, G. D. White, and J. H. Handwerk, Preparation and Properties of Refractory Uranium Compounds, USAEC Report ANL-FGF-361, Argonne National Laboratory, June 25, 1962.

92. Argonne National Laboratory, Reactor Development Program Progress Report, August 1962, USAEC Report ANL-6610, Sept. 15, 1962.

93. General Electric Company, Flight Propulsion Laboratory Department, High Temperature Materials Program, Progress Report No. 17, Part A, USAEC Report GEMP-17A, Nov. 15, 1962.

94. W. J. Megaw and J. E. Bridges, Release of I-131 from Irradiated Uranium Oxidizing in Air and in CO_2, *Nature*, 195: 448-449 (Aug. 4, 1962).

95. P. Schmeling, Release of Fission Rare-Gas During PAD Heating as a Result of Chemical Interactions and Its False Interpretation as Being Diffusion, USAEC Report EURAEC-360, Hahn-Meitner-Institut für Kernforschung, Berlin, March 1962.

96. Y. M. Agranovich and E. Ya. Miklin, The Theory of Swelling of Porous Bodies (in Russian), *At. Energ. (USSR)*, 12: 385-391 (May 1962).

97. F. Hashimoto, Process of Formation of Bubbles in Irradiated Uranium, USAEC Translation AEC-tr-5074 [translated from *Nippon Genshiryoku Gakkaishi*, 2: 518-522 (1960)].

98. G. W. Greenwood, The Effects of Neutron Irradiation on γ-Uranium and Some Fissile Alloys of Cubic Crystal Structure, *J. Nucl. Mater.*, 6: 26-34 (May–June 1962).

99. W. S. Blackburn, The Irradiation Swelling of Uranium Under Mechanical Restraint, *J. Nucl. Energy, Pts. A & B*, 16: 387-390 (August 1962).

100. R. Lindner, H. Matzke, and F. Schmitz, Fission Product Diffusion and Self Diffusion in High Temperature Nuclear Fuels, USAEC Translation AEC-tr-5206 [translated from *Z. Elektrochem.*, 64: 1042-1045 (1960)].

101. A. Auskern and Y. Osawa, Xenon Diffusion in Uranium Carbide Powder, *J. Nucl. Mater.*, 6: 334-335 (August 1962).

102. A. R. Palmer, Emission of Fission-Product Rare Gases from UO_2-BeO and UO_2-ThO_2-BeO Specimens During Neutron Irradiation in BEPO, British Report AERE-R-4062, May 1962.

103. J. L. Bates, J. A. Christensen, and J. L. Daniel, Irradiation Effects in UO_2 Single Crystals, USAEC Report HW-SA-2500, Hanford Atomic Products Operation, June 14, 1962.

104. A. D. Whapham and M. J. Makin, The Nature of Fission Fragment Tracks in Uranium Dioxide, *Phil. Mag.*, 7(81): 1441-1455 (September 1962).

105. M. H. Rand, A. C. Fox, and R. S. Street, Radiation Self-Damage in Plutonium Compounds, *Nature*, 195: 567-568 (Aug. 11, 1962).

Section

II

Reactor Materials

Moderator Materials

Graphite

Sample descriptions, irradiation histories, and dimensional changes of vendor-supplied B_4C-graphite control-rod materials irradiated by General Atomic[1] are given in Table II-1. The postirradiation appearances of all specimens were good, with the exception of one that showed spalling of the surface. This defective surface, however, is believed to have been produced by a faulty capsule heater that short-circuited during the irradiation. The dimensional contractions observed were not more than would be expected for reactor-grade graphite in a similar test.

Dispersions of B_4C in graphite, prepared at General Atomic by a warm-press-and-sinter process, were irradiated to higher exposures. Such bodies containing 20, 30, and 40 wt.% boron were irradiated at 350 and 700°C to neutron exposures of 9.8×10^{20} or 2.4×10^{21} nvt (thermal). These exposures correspond to burnups equivalent to 33 and 100% of the expected burnups in the High-Temperature Gas-Cooled Reactor (HTGR). The overall appearances and microstructures of the compacts appeared unchanged after these tests. Small (0.1 to 0.2%) contractions in compact diameter and expansions in length ranging from 0.6 to 4.5% were observed. The tensile strengths of the 30 and 40 wt.% boron compacts showed no significant changes owing to irradiation, whereas a general increase was noted in the strength of the irradiated compacts containing 20 wt.% boron.

British researchers[2] have studied the process of impregnating a bed of porous nonconsolidated carbon, in which a large temperature gradient is maintained, with carbon formed by the pyrolysis of a hydrocarbon gas. Cotton wool,

Table II-1 IRRADIATION OF CONTROL-ROD MATERIALS[1] IN CAPSULE GA-310-1

Description of specimens	Vendor-supplied samples of B_4C in carbon and B_4C in graphite	
Size of samples for irradiation	0.8 in. in diameter by 2 in. long	
Irradiation history	Inserted 2/9/60; discharged 4/10/60; two cycles in GETR	
Temperature of sample	680 to 750°C (800°C on brief occasions)	
Exposure		
Thermal	8.7×10^{19} nvt	
Fast	2.5×10^{19} nvt	
Dimensional changes of samples		
		Diameter, % / Length, %
S-8736 [4.5% boron; graphitized (>2700°C)]		−0.25 / 0
S-8710 [0.3% boron; baked (850°C)]		−0.05 / 0
S-8734 [0.2% boron; graphitized (>2700°C)]		−0.1 / −0.05
S-8735 [13% boron; graphitized (>2700°C)]		−0.1 / +0.1
C-20 (20% boron; treatment not known)		−0.05 / 0
C-30 (30% boron; treatment not known)		0

wrapped on a carbon form and baked, provided a suitable base for impregnation, and impermeable tubes of wall thickness up to ¼ in. were produced.

Conclusions drawn from this study were as follows:

1. Tubes of carbon may be formed by deposition of pyrolytic carbon (PyC) onto a fiber matrix such that the final product may have a radial permeability as low as 10^{-10} cm^2/sec.

2. Benzene pyrolysis gives a material that graphitizes well at 2700°C, but other hydrocarbon gases tried generally give carbons that do not graphitize completely.

3. At the reported stage of development, it seems that only methane gas is a useful source of the pyrocarbon if very low permeabilities, e.g., 10^{-10} cm^2/sec, are required, but with the present base material, this gas does not give completely reproducible results. Other hydrocarbon gases at best give an increase of permeability to 10^{-8} cm^2/sec or higher on heat-treatment to graphitizing temperatures.

4. The microstructure of the material shows several variations of the usual optically active carbon deposited around the fibers, and optically inactive forms are also found in some regions.

5. Existing data on costs suggest that, if the process could be developed to give reproducible material, it may well be of commercial value for the production of very low-permeability carbon tubes.

The compatibility of type 304L stainless steel in intimate contact with graphite is being studied as a function of temperature and contact pressure at Oak Ridge.[3] Initial studies concerned surface reactions in the absence of gaseous contaminants under a vacuum of 10^{-6} mm Hg at temperatures from 540 to 705°C. Stainless-steel specimens were pretreated to provide three surface conditions: hydrogen fired, preoxidized, and copper plated. Surface-contact pressures ranged from 0 to 10,000 psi. Test results indicate that the lower temperature limit for significant diffusion between graphite and stainless steel is approximately 600°C. Above this temperature, diffusion between untreated or hydrogen-fired stainless-steel surfaces was found to effect complete bonding of the two materials at contact pressures as low as 500 psi. Bonding was effectively prevented by the presence of either an oxide film or a copper plate at temperatures up to 700°C. Where bonding occurred, diffusion rates measured for carbon in stainless steel were comparable with those previously reported for stainless steel in carbon-saturated sodium. However, phases produced in surface reactions between graphite and stainless steel were of higher order than those reported for the sodium carrier. Lack of carburization in control specimens not in contact with graphite indicates that the role of the gas phase is unimportant at the impurity pressures of 10^{-6} mm Hg.

Most irradiation-induced dimensional changes in graphite have been measured on small specimens (approximately 0.4 in. in diameter by 4 in. long); recently, data have become available[4] for measurements on large bars of graphite (4 by 4 by 24 in.) which differ from small-specimen data. Test temperatures were approximately 450 to 550°C; exposure was 18,600 Mwd/adjacent ton. The results for the three types of graphite tested are tabulated below:

Graphite type	Length change, %	
	Transverse	Parallel
CSO	−0.450	−0.690
CSF	−0.529	−0.758
CSGBF	−0.566	−0.785

The contraction rate of the large bars was more than twice that measured in comparable small-specimen tests. The reason for the size effect is not known. Perhaps greater stress relief in machining of small samples or absence of such stresses as may accumulate in large bars during irradiation accounts for the lower contraction in small specimens.

The effect of compressive stress on radiation-induced dimensional changes in graphite is being investigated at Hanford.[4] Preliminary results of tests (based on the length changes after about 1500 Mwd/adjacent ton) employing 150- and 300-psi compressive loads during irradiation at 650°C gave the following tentative conclusions:

1. Stress-induced deformation, defined as the change in length of the unstressed samples minus the change in length of the stressed samples, appears to be proportional to the applied stress.

2. The stress-induced deformation rates varied, depending upon graphite type, from 0.9×10^{-11} to 3.1×10^{-11} per dyne/cm^2 per 1000 Mwd/adjacent ton.

3. The stress-induced deformation rates due only to the effects of radiation (that is, the difference between the thermally annealed-sample and the irradiation-sample length changes) were 0.0 and 1.6×10^{-11} per dyne/cm^2 per 1000 Mwd/adjacent ton.

Data on the effects of high-energy neutron bombardment on carbon and graphite structure, dimensional stability, properties, and some gas reactions are presented in a review[5] prepared at General Atomic. The basic raw materials and general processes of fabricating nuclear graphite are reviewed, and emphasis is placed on correlation of irradiation effects with carbon structure. However, the preponderance of irradiation data have been obtained for highly graphitic materials, and the primary generalizations drawn from the review are for such material. In summary, this review states that carbon structures prepared with graphitizing raw materials and heating above 2500°C during manufacture appear to be the most stable during high-temperature irradiation. In this type of carbon structure, there are slight differences in crystallite perfection and pore structure, depending on the raw materials used and the manufacturing procedure. The differences in irradiation stability resulting from these differences in crystallinity are much less than those observed between graphitic and pseudographitic (low permeability) or nongraphitic structures.

The following general effects have been observed by analyzing the irradiation data on highly graphitic carbon structures:

1. Bulk expansion of graphite is observed in the direction perpendicular to the direction of extrusion, and bulk contraction is observed in the parallel direction, for samples irradiated near room temperature (30°C). The perpendicular expansion phenomenon decreases with increasing irradiation temperature, and contraction sets in at about 300 to 400°C and $\sim 6 \times 10^{20}$ nvt. The parallel contraction rate decreases with increasing irradiation temperature up to about 600°C, is essentially unchanged in the range 600 to 1000°C, and then increases in rate above 1000°C.

2. Unit cell parameters also change. The c_0 axis, or layer plane distance, increases rapidly during irradiation at room temperature. With increasing irradiation temperature, this expansion is minimized. The a_0 axis contracts at all irradiation temperatures, but the change is small. Crystallite sizes L_c and L_a decrease during irradiation and appear to be reduced sharply after a short exposure. This phenomenon is a degraphitization process, from a crystallographic view.

3. Most physical properties tend to be affected during irradiation at room temperature. The irradiated-graphite properties are driven in the direction of those generally ascribed to hard carbons; i.e., high electrical resistivity, low thermal conductivity, etc. This effect is minimized with increasing irradiation temperatures and is ascribed to irradiation annealing.

4. Mechanical properties, such as strength and modulus, are less affected, and in some cases the strength is increased.

5. Chemical reactions, such as oxidation, are accelerated by neutron irradiation. This may be a result of the influence of irradiation on the graphite, the oxygen, or both.

A technique of stereoscopic radiography[6] has provided a qualitative three-dimensional picture of the pore structure of graphite. Samples of virgin and oxidized nuclear graphite were impregnated with molten bismuth at various pressures. Subsequent cooling led to solidification of the bismuth in the pores of the graphite, and samples were sectioned for examination. These sample slices were radiographed in two positions, such that one radiograph viewed the sample at an angle of about 20° from the other. Appropriate viewing of these radiograph pairs then provided a three-dimensional picture of the bismuth contained within the graphite pore structure. (M. C. Brockway)

Beryllium Metal and Alloys

Mechanical Properties

In some space applications, where each additional pound of satellite costs about 10,000 lb at launching, beryllium is the cheapest construction material available. Hughel[7] points out that

beryllium not only has the highest modulus-to-density ratio (about 670 million in.) of any metal, but wrought beryllium at 100,000 psi ultimate strength has a strength-to-density ratio of about 1,500,000 in., which is higher than that of steel at 300,000 psi ultimate.

Work at General Motors, in conjunction with both major producers, resulted in an increase of the precision elastic limit of three forms of hot-pressed beryllium to over 13,000 psi. (The precision elastic limit is the load that will just produce a residual strain of the order of 10^{-6} in.) All three forms that contain higher than normal oxide content show very good dimensional stability at loads equalling 95% of the precision elastic limit.

Although beryllium has some outstanding properties and is admittedly a difficult material, Bunshah[8] insists that it is a normal metal whose nonsystematic behavior may be readily understood when it is realized that it is a complex, unstable, age-hardening type alloy, highly susceptible to precipitation-aging phenomena, which are dependent on impurity levels and prior mechanical thermal treatment. The microstructure is probably saturated with the principal impurities (oxygen, carbon, iron, etc.) and contains stable and unstable phases and precipitates. Thus the inherent room-temperature ductility of beryllium has never been measured.

Salmen and Gobble[9] made accurate measurements of the tensile properties of hot-pressed beryllium at room temperature and at each 200° interval from 400 to 600°F inclusive. It was found that the modulus of elasticity is definitely higher at 600 and 800°F than at room temperature. Maximum ductility as measured by reduction of area occurred at 800°F; however, on the basis of elongation, maximum ductility occurred at 1000°F.

Studies[10] of the corrosion-resistant beryllium-calcium alloys containing from 0.45 to 0.92 wt.% calcium indicated that the tensile strength, creep-rupture strength, and the creep-bending strength of tubes showed no major effects from the calcium additions. It is possible that about 0.2 wt.% calcium lowers the brittle-to-ductile transition temperature by about 50°C.

Two new bulletins issued by the Beryllium Corp.[11,12] hold answers to frequently asked questions about where beryllium is used and the physical, mechanical, and nuclear properties of the metal. One notes that sheet and plate are available in thicknesses from 0.020 to 0.500 in. in sizes up to 36 by 90 in., with minimum mechanical properties of 70,000 psi tensile and 50,000 psi yield strength and with 5% elongation. Thicknesses down to 1 mil may be obtained in strip or foil.

Table II-2 CREEP RATE OF BERYLLIUM[13]

	Stress, 1000 psi, required to produce a secondary creep rate of 10^{-5} in./(in.)(hr) at temperature indicated, °C						
	400	450	500*	500*	550	600	700
Beryllium, cast and extruded	114.3	57.2	33.0	17.2	9.54	4.98	2.85
Beryllium, 1% BeO, hot pressed	69.8	47.7	33.0	23.5	19.1	14.0	9.25
Carbon steel, 0.008 to 0.25% carbon, wrought, normalized	106.8	84.0	65.5	39.8	14.2		

*Possible misprint in original reference since no explanation was given for two sets of data at 500°C.

Finniston[13] included the creep data for beryllium (Table II-2) in a comprehensive review.

Beryllium Purification

Seagle et al.[14] reported that electron-beam melting of beryllium beads or vacuum-cast rounds does not improve the tensile properties of the extruded or annealed metal. However, it does reduce the oxygen, chromium, and possibly the manganese content, whereas the iron and nickel are concentrated owing to the rapid volatilization of beryllium.

Goosey et al.[15] studied the effects normally found in vacuum-cast induction-melted beryllium ingots. They concluded that a centerline defect present in certain grades of thermally

reduced metal may result from the segregation of titanium. The defect appears to be removed by alloying with aluminum.

Boisde et al.[16] used a variant of the electrorefining method for beryllium, developed by the U. S. Bureau of Mines at Boulder City, to obtain beryllium of the analysis shown below (the values given are in parts per million).

Al, < 25	Li, >30	Si, ≤15
Cu, ≤5	Mg, <10	Sn, < 15
Fe, ≤5	Mn, <3	O, 100 to 300
K, 100 to 250	Ni, ≤3	Cl, 300 to 1500

Concentration of impurities, especially iron, in the layer of salts closest to the deposited beryllium crystals makes the purity of the metal recovered strongly dependent on the efficiency of washing off attached salts. Potassium, lithium, and chlorine are each reduced to a few parts per million after the washed crystals are melted in a vacuum.

Fabrication of Beryllium

The effects of heat-treatment on the tensile properties and third-dimensional plastic strain of cross-rolled beryllium sheet were investigated at three temperature levels (1750, 1920, and 2020°F) and at three time periods (6, 60, and 600 min) by Grala et al.[17] In most cases the maximum response was obtained in 1 hr at the highest temperature. Grain size increased from 15 μ to 29 to 37 μ.

"The gross effects of these heat treatments on cross-rolled beryllium sheet were to reduce the strength properties back to the range of hot-pressed material. The tensile elongation remained several times higher than that of hot-pressed material. The third-dimension plastic strain increased, but still was considerably below that of hot-pressed material."

Syre and Logerot[18] studied special techniques to obtain high-density products with good mechanical properties. When presintered 10-in.-diameter blocks were canned in hard steel cans and then forged to disks of about 16 in. in diameter by $\frac{1}{4}$ in. thick, properties equivalent to those of hot-upset beryllium as produced in the United States, with higher density and better yields, were obtained without recanning. The forged disk could be machined into relatively complicated end products. Properties of this material are shown in Table II-3.

Murphy and Klein[19] reported the results of burst tests on finned tubes shown in Table II-4. Each value shown represents the average from five tests, one with the ends plugged and welded, and four with O-rings on both ends.

Brush Beryllium Co.[20] reported success in drawing fine wire from rod swaged from six-pass zone-refined crystal that had been made from "selected pebble." Previously, they had successfully swaged, but had been unable to draw, wire from single crystals supplied by the Franklin Institute. The principal difference in the Brush Beryllium and Franklin Institute crystals appeared to be the absence of BeO in the Brush Beryllium crystal. The total metallic-impurity content in the Brush Beryllium crystal was not less than that in the Franklin Institute crystals, but the distribution may have been different. The annealing time and the temperature schedule that had been used successfully in the earlier work now resulted in the growth of very large crystals. Strength of the annealed wires was influenced so much by the overly coarse crystal size as to be of little significance.

Table II-3 PROPERTIES OF SINTERED-FORGED BERYLLIUM[18]

Product	Reduction	Minimum density, g/cm³	Properties in plane of forged disk: Tensile strength, psi	Properties in plane of forged disk: Elongation, %
Disk, 15¾ in. in diameter	5:1	1.80	56,800	7
Disk, 11 13/16 in. in diameter	11:1	1.83	68,300	10

Table II-4 RESULTS OF BURST TESTS ON FINNED BERYLLIUM TUBES[19]

Tube dimensions, in.				Bursting pressure, 1000 psig	Hoop stress, 1000 psi
Diameter: Inside	Diameter: Outside	Wall thickness	Overall length		
0.4941	0.5695	0.0377	5	5.0	35.4
0.4963	0.5647	0.0342	5	6.1	47.5
0.4961	0.5645	0.0342	5	5.1	39.7
0.4975	0.5713	0.0369	5	4.2	30.6
0.5032	0.5882	0.0425	4⅞	6.8	43.9

However, the as-drawn wires had rather good strength properties, indicating that zone-refined beryllium can be strengthened sufficiently through metalworking to be structurally useful. The room-temperature ductility of the as-drawn wire was a little higher than would be expected in commercial wire.

Weismantel and Black[21] reported on a study of rolling parameters in the production of beryllium sheet metal. They found that the sheet with the most desirable properties was obtained by rolling with breakdown temperatures of 1500 to 1550°F and final rolling at as low as 1435°F for billets containing 1.9 wt.% BeO and 1350°F for those containing 1.25 wt.% BeO. The ductility of the lower oxide material was generally better, although the strength was somewhat lower than that of the higher-oxide-content sheets.

The desirable properties of beryllium as a structural material can often be enhanced, insofar as corrosion and wear are concerned, by the application of coatings. O'Boyle[22] reported the data on protective coatings shown in Table II-5. Metals that have been successfully plated on beryllium include aluminum, cadmium, copper, gold, indium, iron, silver, tin, and zinc. Surface finishes as fine as 1 μin., root mean square, have been produced on plating nickel over beryllium [Beach and Faust, *J. Electrochem. Soc.*, 100(6): 276-279 (1953)]. Thin deposits of silver or nickel are used to make the surface solderable for joining leads or making metal attachments. Oxide coatings are subject to damage from thermal shock, although they do not chip or peel when subjected to moderate shear forces. Electroless nickel is not subject to thermal-shock damage (because its coefficient of expansion closely matches that of beryllium), but it is limited to surface temperatures below 750°F because of softening (overaging) above this temperature.

Glorioso et al.[23] brazed 0.020-in. beryllium sheet to steel and titanium honeycomb core to form a sandwich panel. The breakage associated with handling or sawing thin-gauge beryllium is greatly reduced when the sheet is brazed into a sandwich. However, an undesirable amount of diffusion or dissolution of the base metals was experienced with the commercial silver-base brazing alloy used. The full potential of brazed construction will not be realized, they believe, until a braze alloy with properties compatible with beryllium has been developed. However, Westlund[24] reported that satisfactory joints were made between beryllium and B120VCA titanium, and between beryllium and stainless steel, by brazing with pure silver at 900°C. Although this is well below the melting point of silver, the braze metal became fluid as beryllium and other components diffused into and dissolved in the silver. Good joints were not obtained at temperatures above 960°C. When beryllium is being joined to beryllium with pure silver, the braze metal is sluggish and does not wet the beryllium uniformly. Wetting was improved by painting the beryllium with a suspension of titanium hydride in isobutyl methacrylate and by using a preplaced silver foil. It appeared that a quantity of titanium hydride equal to 2% of the weight of the 0.003-in.-thick silver foil was the smallest amount that could be applied uniformly and that this was the optimum amount to use. The best results were obtained in the temperature range 960 to 1060°C. Brazes made at 1060°C with a holding time of 30 min showed no corrosion of the base metal. All the brazing described by Westlund was carried out in a dynamic vacuum at a pressure of 10^{-5} mm Hg.

Table II-5 PROTECTIVE COATINGS FOR BERYLLIUM[22]

Coating method	Thickness range, in.	Wear resistance	Density, g/cm^3	Composition of coating
Oxide film (natural and high temperature)	30–2000*	Fair	3.0	BeO
Anodized oxide	10^{-6}–0.002	Good	2.2	BeO
Electroless nickel	0.0002–0.008	Excellent	7.9	92 Ni–8 P
Electroplating	0.0001–0.010	Depends on metal plated	Variable	Metals
Flame spraying	0.005–0.100	Excellent	3–17	Oxides and refractory metals

*Angstroms.

Cline[25] brazed beryllium to titanium–6 wt.% aluminum–4 wt.% vanadium alloy and type 303 stainless steel using filler alloys of silver, lithium, copper, aluminum, manganese, zinc, cadmium, and nickel. Tensile testing from room temperature to 1060°F indicated that the highest ultimate tensile strength is achieved when utilizing a silver-copper-lithium filler.

Physical Metallurgy of Beryllium

Martin[26] et al. determined the electrical resistivity and the temperature coefficient of electrical resistivity for zone-refined beryllium crystals. A crystal identified as 8C contained a total of 808 ppm of metallic impurities at the pure end and 1835 ppm at the impure end. Similar data for crystal 15B were 973 and 15,820 ppm, respectively, with 15,558 ppm of impurities in the central region. The resistivity of crystal 8C, 2 cm from the pure end, was 3.60 μohm-cm; 2 cm from the impure end, it was 4.25 μohm-cm. The corresponding values for crystal 15B were 4.38 and 7.05 μohm-cm, respectively. The temperature coefficient of electrical resistivity for crystal 15B is shown in Table II-6. Nakatani[27] reported that the temperature coefficient of the electrical resistivity of sintered beryllium from 0 to 100°C is 6.3×10^{-3}/°C.

Table II-6 VARIATION OF TEMPERATURE COEFFICIENT OF ELECTRICAL RESISTIVITY OF ZONE-REFINED BERYLLIUM CRYSTAL[26]

	Coefficient of electrical resistivity, 10^{-4}/°C, at indicated temperature			
Location	20°C	400°C	700°C	900°C
Pure end	628	220	6.7	20.8
Central portion	219	100	44	11.4
Impure end	7.5	24.5	78.7	95

The behavior of inclusions in cast beryllium subjected to deformation shows the following properties:[28]

1. Coherent deformation of an aluminum-rich phase
2. Separation of inclusions from the matrix
3. Cleavage of inclusions
4. Initiation of new slip and twinning in the matrix at the boundary between the inclusions and the matrix
5. Occurrence of cracks from the boundary into the matrix
6. "When a crack approaches inclusions including a cluster of oxide, the crack is developed with further deformation accompanying the separation of the inclusions from the matrix and/or the cleavage of the inclusion."

Jacobson et al.[29,30] attribute the poor ductility of machined beryllium to highly twinned areas acting as favored loci for crack formation. The presence of cracks is less detrimental since cracks apparently do not grow unless they are suitably oriented. When many twins are present, the possibility of nucleating favorably oriented cracks is greater. Hence care must be taken to ensure that all surface damage is removed. Annealing the beryllium at a suitable time and temperature removes the great majority of twins and eliminates the residual stresses that result from machining. Etching after annealing to remove machining cracks and the balance of the twins further improves the properties of the beryllium.

Gasc and Badeau[31] observed four modes of recrystallization of cast extruded beryllium with the optical microscope. Beryllium bars press forged at 400°C showed practically no nucleation after only 4% reduction. On reheating, rapid growth of some grains, induced by the forging process, started at 770°C. Above 850°C this was replaced by classic continuous grain growth. After 8 to 16% forging reduction, induced grain growth and nucleation starting from twins were observed simultaneously. At temperatures near 700°C certain grains showed an appearance like polygonization, and continuous growth started at about 820°C. After reductions of 22 to 35%, polygonization became general even before thermal treatment. When the material is reheated to above 700°C, nucleation becomes very important, and continuous growth starts at 800°C. The authors think that the gross polygonization, if it can be called that, and the nucleation from twinning are phenomena observed only in beryllium.

Spangler et al.[32] reported the resolved shear-stress shear-strain tensile curve shown in Fig. II-1 for a single beryllium crystal that had had 12 zone-refining passes. The crystal reached the point of duplex glide and then continued for an additional 24% glide strain before necking down to a knife-edged fracture.

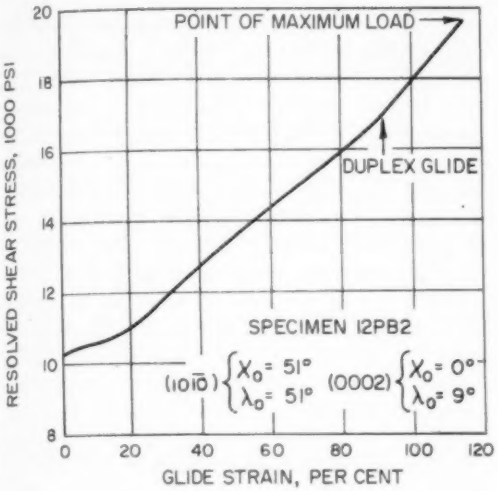
POINT OF MAXIMUM LOAD
DUPLEX GLIDE
SPECIMEN 12PB2
(10$\bar{1}$0) χ_0 = 51° λ_0 = 51°
(0002) χ_0 = 0° λ_0 = 9°
RESOLVED SHEAR STRESS, 1000 PSI
GLIDE STRAIN, PER CENT

Fig. II-1 Resolved shear-stress shear-strain tensile curve for zone-refined beryllium in prism-plane glide.[32]

It was concluded that there is an increase in prism-plane ductility with increased purity, even though there is essentially no reduction in the critical resolved shear stress for prism glide. The effect of purification on the critical resolved shear stress of zone-refined beryllium was studied also by Nuclear Metals.[33] Crystals of different purity levels, oriented favorably for either basal or prismatic slip, were stressed in tension at room temperature. The inverse resistance ratio (ratio of electrical resistance at 4.2°K to that at room temperature) was used as a measure of impurity content. This inverse ratio decreases with increasing purity of the material. Critical resolved shear-stress data for both basal and prismatic slip are shown in Fig. II-2, and the temperature dependence of the latter is shown in Fig. II-3, compared with earlier data by Tuer and Kaufmann.

Glide dislocations in deformed specimens of vacuum-melted Pechiney flake, and in commercial beryllium, were studied by transmission electron micrographs.[32] From this work at the Franklin Institute, it was deduced that the frictional force of dislocations is very high in both types of beryllium.

Adda et al.[34,35] found that aluminum which is but slightly soluble in beryllium of commercial purity is dispersed as a liquid phase at 650°C and above. It plays an important role in the segregation of other impurities. These are eliminated from the beryllium matrix through selective solution in the liquid phase during heat-treatments carried out between 650 and 800°C. Iron and silicon particularly are gathered in the liquid aluminum phase in this temperature range. If the beryllium is heat-treated at 1000°C and quenched, the iron leaves the aluminum and redistributes itself in the beryllium matrix. These effects, shown by studies with a microprobe, appear to explain the changes in ductility noted in beryllium after heat-treatment by Sawkill and others.

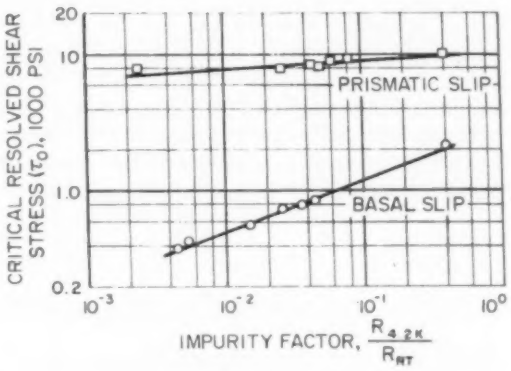

Fig. II-2 Purity dependence of critical resolved shear stresses for basal and prismatic slip in zone-refined beryllium.[33]

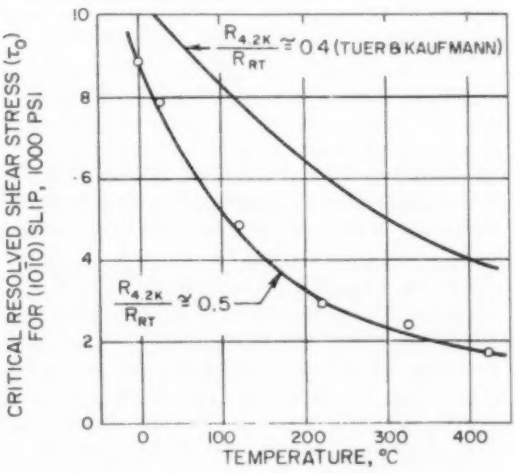
$\frac{R_{4.2K}}{R_{RT}} \cong 0.4$ (TUER & KAUFMANN)
$\frac{R_{4.2K}}{R_{RT}} \cong 0.5$
CRITICAL RESOLVED SHEAR STRESS (τ_0) FOR (10$\bar{1}$0) SLIP, 1000 PSI
TEMPERATURE, °C

Fig. II-3 Effect of purification on temperature dependence of critical resolved shear stress for prismatic slip in beryllium.[33]

An investigation[36] by optical microscope of the aging characteristics of beryllium-iron alloys containing 0.03 to 0.18 wt.% iron showed striking differences between the behavior of alloys containing 0.03 and those containing 0.04 wt.% iron, although in no case was a single-phase solid solution retained on quenching to 20°C. In alloys of low iron content, the principal aging reaction occurs at less than 575°C. However, when such alloys were aged at temperatures in the neighborhood of 750°C, a subsidiary precipitation aging effect was observed. Over-aging after solutionizing could not always be induced in alloys containing 0.04 wt.% iron. Attempts to re-solutionize the precipitate after aging suggested that the reaction was subject to approximately 100°C hysteresis for material containing less than 0.04 wt.% iron but not for samples containing 0.04 wt.% iron or more.

Donze et al.[37] redetermined the limits of solubility of iron in beryllium by means of diffusion couples that were examined with the

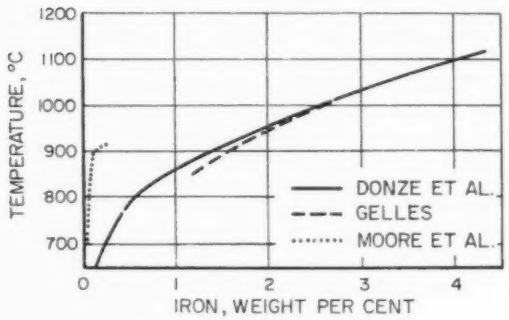

Fig. II-4 Solubility limit, iron in beryllium.[37]

microprobe. This made it possible to complete the equilibrium diagrams at lower temperatures and with greater precision than had been done previously. Results of this work are shown in Fig. II-4, along with results by other authors for comparison. The relatively high solubility limit (2600 ppm) found at 700°C would indicate that it is impossible to precipitate iron from commercial beryllium containing about 400 ppm iron by thermal treatments. The authors suggest that this confirms the theory, advanced by Adda et al.,[34] that the mechanism of purification of beryllium during heat-treatments which reportedly increase the ductility is in reality the solution of iron in

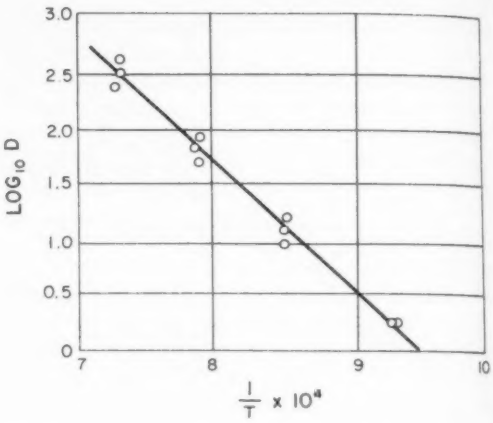

Fig. II-5 Variation of the coefficients of diffusion of iron in beryllium.[37]

aluminum and that this iron-aluminum phase is insoluble in beryllium. The authors also report that the coefficient of diffusion of iron in beryllium varies with the temperature according to the equation $D = 1.0 \exp(-53{,}000/RT)$. The activation energy for the diffusion of iron in beryllium is 53 kcal/mole (Fig. II-5).

Corrosion and Nuclear Properties of Beryllium

A study of oxidation in beryllium[29] suggested two processes: (1) penetration of the oxides along crystallographic planes of the base metal and (2) a subsequent detachment of some oxide and/or beryllium from the surface.

Jepson[38] concluded an extensive survey of studies on the oxidation of beryllium in oxygen, carbon dioxide, and carbon monoxide, with and without the presence of water vapor. The corrosion of beryllium can be influenced by its mode of fabrication, which in turn can affect the distribution of impurities in the metal. No conclusion can be made yet as to why, at temperatures of 650°C and above, water vapor is able to promote film cracking and subsequent grain-boundary attack.

Trowse[39] compared the oxidation of tubes of pure beryllium in moist atmospheres with those of beryllium-calcium alloy tubes. In general, the pure beryllium tubes exposed in moist gas (100 ppm H_2O) showed breakaway oxidation in from 1500 to 4500 hr at 650°C. Tubes containing between 0.1 and 0.7 wt.% calcium were tested for times up to 7000 hr. Some of the

0.1 wt.% calcium tubes showed no breakaway in moist gas, but others failed. All the 0.2 wt.% alloy tubes with a machine finish were satisfactory, but those with an as-extruded finish were not. The 0.6 and 0.7 wt.% calcium tubes were all satisfactory.

Pemsler et al.[40] found that beryllium samples exposed to high-temperature water exhibited extreme variations in corrosion behavior. The mode of attack varied with the metallurgical history of the sample, but only samples fabricated directly from powder showed appreciable corrosion resistance. It was demonstrated that resistance to corrosion decreases with increasing purity of the beryllium and that specimens subjected to a prior heat-treatment and aging are more corrosion resistant than unaged materials. Coarse-grained distilled and single-crystal zone-refined specimens underwent rapid catastrophic corrosion in water at 650°C.

Preliminary studies indicate that a satisfactory means of preventing reaction between beryllium metal and uranium dioxide may be anodizing of the beryllium. At the same time the rapid oxidation of beryllium in moist CO_2 is prevented or delayed. The best anodizing films for the purpose were produced in a bath of pure chromic acid.[41]

Adams et al.[42] reported that breakaway corrosion of beryllium in moist CO_2 can be avoided if the beryllium is fabricated from preoxidized powder. The beryllium powder was preoxidized at 700°C, and the pressed-and-sintered component was exposed to moist CO_2 at 700°C. Since the grain boundaries were already covered with an adherent layer of oxide, penetration of oxidation arising from the decomposition of water vapor in contact with beryllium was avoided. The tests appeared to be limited to 200-hr exposures, however.

The formation of dislocation loops and possibly small clusters of defects causes beryllium irradiated at fairly low temperatures to start to embrittle after a neutron dose of more than 3×10^{18} nvt. Some of this embrittlement can be removed by annealing beryllium above 500°C; at higher annealing temperatures small helium bubbles form, but these have no effect on the properties as they grow.[43]

Miscellaneous Beryllium Literature

The applicability of beryllium in nuclear uses is reviewed in a French journal,[44] which presents an outline of specific current applications of beryllium and beryllium oxide. Data on production, consumption, reserves, and stockpiling of beryllium and the location of plants for processing beryllium minerals are given for the United States, France, and Britain. World prices of beryl concentrates and beryllium metal are tabulated.

Lowenstein[45] presented a concise summary of the properties of beryllium that make it attractive as a construction material in nuclear reactors and of the difficulties that tend to keep it from being used. The author discusses irradiation behavior, compatibility with reactor coolants, fuel and structural materials, and mechanical properties and toxicity as well as the problem of brittleness.

The National Research Corporation of Cambridge, Mass., is attempting to develop submicron beryllium powder with a lower oxygen content than coarse powder. This may lead to a more ductile form of beryllium.[46]

(W. Hodge)

Beryllium Oxide

Measurements of microhardness of BeO single crystals at Atomics International[47] showed no significant differences between the various faces of a crystal; single-crystal microhardnesses were about the same as those measured on polycrystalline bodies. Chemical differences between the faces were detected, the different faces showing characteristic etch patterns when treated with hot H_3PO_4. Piezoelectric and pyroelectric characteristics were detected in the crystals, indicating that the structure along the c axis is polar. Modulus of elasticity measured normal to the c axis by piezoelectric coupling agreed fairly well with the modulus of polycrystalline bodies.

General Electric workers[48] found a strong effect of crystallographic orientation on the coefficient of thermal expansion of BeO extrusions. The axial expansion of an extrusion up to 1200°C was found to be a linear function of the degree of orientation in the extrusion. The differences in the thermal expansion of random and oriented bodies, and the known degree of orientation in the oriented body, have enabled estimates of the expansion coefficients of the a axis and c axis of single-crystal BeO. Comparisons of coefficients, α, derived in this

manner showed that $\alpha_{a\ axis}$ exceeds $\alpha_{c\ axis}$ by about 13%, and the degree of anisotropy is independent of temperature between 300 and 1200°C. General Electric scientists have confirmed this expected anisotropic thermal expansion of BeO by high-temperature X-ray diffraction techniques. They have reported the following coefficients for the temperature range 25 to 1200°C:

$$\alpha_{a\ axis} = 9.91 \times 10^{-6}/°C$$

$$\alpha_{c\ axis} = 8.73 \times 10^{-6}/°C$$

Varying degrees of orientation have been observed at General Electric[48] by X-ray diffraction peak-intensity ratio in sintered UOX–0.5 wt.% MgO extruded bodies. Also observed microscopically were large, needlelike oriented crystals in low-fired extrusions. It was hypothesized that orientation originates with these crystals, and the degree of orientation is increased on sintering by preferred growth of initially oriented crystals. General Electric workers have shown a direct grain-size dependency on degree of orientation. Also, they have devised a method for assigning a "percent orientation" to an extruded body.

In other work at General Electric, the effect of compressive stress on the thermal annealing behavior of irradiated BeO is being investigated. Two types of BeO specimens that were irradiated to exposures of about 2×10^{20} nvt showed linear expansions ranging from 3.7 to 5.7 mils/in. These specimens were annealed at 900 and 1000°C for up to 500 hr. Some specimens were loaded compressively with 3000 psi during annealing, and others were left to anneal freely.

The annealing curves, i.e., plots of expansion recovery vs. time, were similar in shape and magnitude for both loaded and unloaded specimens of each type of BeO. It was concluded that compressive stress does not influence the annealing process; conversely, radiation damage of the type investigated here does not lead to abnormal deformation under compressive stress. (A. K. Smalley)

Beryllides

The effects of particle size, stoichiometry, temperature, and time upon sintered density, grain size, and strength of $NbBe_{12}$, Nb_2Be_{19}, Nb_2Be_{17}, $TaBe_{12}$, and Ta_2Be_{17} were studied by the Brush Beryllium Co.[49] The feasibility of scaling-up to large and complicated shapes by isostatic pressing, slip casting, extrusion, hot pressing, and flame spraying was demonstrated in these studies. General Electric has also studied the fabrication of niobium and zirconium beryllides.[50] Small cast shapes were produced by arc-melting and casting techniques, and the feasibility of extruding $ZrBe_{13}$ by coextrusion techniques was established.

Aitken and Smith[51] report that zirconium and niobium beryllides, like beryllium, are attacked by moisture, which causes them to oxidize and break into powder. Hot-pressed $ZrBe_{13}$ showed these effects on exposure to temperatures in the range 1100 to 1700°F, but apparently not at 1000 or 1800°F higher, at least in tests up to 100 hr long.

The intermediate-temperature oxidation of the zirconium beryllides was studied in detail by Denver Research[52] and Brush Beryllium.[53] In $ZrBe_{13}$, fracture was transgranular during oxidation testing, even though some intergranular precipitate was observed in the grain boundaries. Denver Research indicated that stresses induced by oxide formation may have caused the observed severe disintegration of the beryllide.

Brush has added 0.35 to 0.45 wt.% aluminum to $ZrBe_{13}$ and has achieved excellent oxidation resistance at intermediate temperatures in both ambient air and moist air (57°F dewpoint). This addition impairs the high-temperature strength of this material but appears to give it unusually high room-temperature strength. The mechanism by which these effects are achieved is not known.

Brush workers have determined that aluminum has a low solubility in $ZrBe_{13}$ and a much higher solubility in Zr_2Be_{17}, as indicated by lattice expansion. They point out[53,54] that Zr_2Be_{17} plays an important role in the oxidation behavior at intermediate temperatures. They report an increase in the amount of Zr_2Be_{17} in a $ZrBe_{13}$ + Zr_2Be_{17} specimen as a function of temperature, with a pronounced increase in Zr_2Be_{17} in the interval between 1810 and 2000°F. Along with the solubility data, a marked difference in the thermal-expansion coefficient for temperatures up to 2000°F is reported—$8.90 \times 10^{-6}/°F$ for $ZrBe_{13}$ and $7.76 \times 10^{-6}/°F$ for Zr_2Be_{17}. Apparently stresses, differences in coefficients

of expansion, and changes in solubility as a function of temperature are all influential in the catastrophic intermediate-temperature oxidation of the zirconium beryllides.

Not all beryllides show this intermediate-temperature oxidation behavior. The niobium beryllides show it to a slight extent, but $TaBe_{12}$, Ta_2Be_{17}, $MoBe_{12}$, $TiBe_{12}$, and WBe_{12} have excellent oxidation resistance[54] in the temperature interval from room temperature to 2000°F.

In their annual report,[54] Brush presented a summary of typical properties of selected beryllides. These are reproduced in Table II-7.

The British have studied the crystal structure of $CaBe_{13}$ and $MgBe_{13}$ and reported[55] measurements of atomic spacing. Livermore[56] reports that the crystal structure of $ReBe_{22}$ is face-centered cubic (fcc) with $a = 11.561$ A. The Russian literature[57] gives the basic trigonal lattice constants of Ti_2Be_{17} as $a = 7.40$ A, $c = 10.84$ A, and $c/a = 1.465$. In another article[58] the Russians report that there is a continuous series of solid solutions between $ThBe_{13}$ and UBe_{13} as determined by metallographic examination, X-ray diffraction, and hardness tests of a series of annealed specimens.

Oak Ridge[59] has reported that $ThBe_{13}$-UBe_{13} alloys are amenable to reprocessing in boiling $4\,M$ HNO_3 containing $\frac{1}{20}M$ HF. Workers there also state that $ThBe_{13}$ has good oxidation resistance in flowing dry air. They are planning irradiation of UBe_{13} to 12,000 Mwd/metric ton of UO_2.

(R. W. Getz)

Table II-7 TYPICAL PROPERTIES OF SELECTED BERYLLIDES[54]

	Test temp., °F	$NbBe_{12}$	Nb_2Be_{17}	Nb_2Be_{19}	$TaBe_{12}$	Ta_2Be_{17}	$ZrBe_{13}$	Zr_2Be_{17}	(U, Zr) Be_{13}–10 wt.% U
Structure		Tetragonal	Hexagonal	Hexagonal?	Tetragonal	Hexagonal	Cubic	Hexagonal	Cubic
Melting point, °F		3070	3100	~3100	3360	3610	3500	3600	~3500
Density, g/cm³		2.91	3.28	3.15	4.18	5.05	2.72	3.08	2.91
Vickers Hardness No. (2.5-kg load)	Room	500	1000	1050	720	1120	1000	1130	
Modulus of rupture, 10^3 psi	Room	22	31	30	31	30	25	25	
Modulus of rupture, 10^3 psi	1600	15	35	30		40	18	23	
Modulus of rupture, 10^3 psi	2300	45	70	70	53	78	40	40	50
Modulus of rupture, 10^3 psi	2500	45	63	65	43	56	37	40	45
Modulus of rupture, 10^3 psi	2750	22	36	27	26	35	25	35	25
Young's modulus, 10^6 psi	Room	47	43		27	50	47	45	45
Young's modulus, 10^6 psi	1600	40*	40*		33	40*	40*	40*	40*
Young's modulus, 10^6 psi	2500	25*	25*		34	20*	20*	20*	20*
Elongation at rupture, %	Room	0.1	0.1	0.1	0.1	0.1	0.05	0.1	0.05
Elongation at rupture, %	1600	0.1	0.15	0.15	0.1	0.2	0.07	0.1	0.05
Elongation at rupture, %	2500	1.0	2.0	2.0	1.1	2.6	0.25	0.3	0.7
Elongation at rupture, %	2750	2.4	~7	3.0	2.6	~5	0.6	1.1	0.7
Compressive strength, 10^3 psi	Room	200			150*		190		180
Compressive strength, 10^3 psi	1600	130			190		150		150*
Compressive strength, 10^3 psi	2500	80					70		90
Oxidation, mils penetration in 100 hr	2500	0.9	0.6		0.5	0.3	0.5	0.5	0.5
Oxidation, mils penetration in 100 hr	2700	2.0	1.9		0.9	0.9	1.3	1.2	~1.0
Specific heat, Btu/(lb)(°F)	1000	0.39			0.27	0.22	0.38		0.39
Specific heat, Btu/(lb)(°F)	2700	0.44			0.30	0.26	0.47		0.40
Thermal expansion, 10^{-6} in./(in.)(°F)	80–2750	9.36	8.83		8.42	8.72	9.86	8.39	9.13
Thermal conductivity, Btu/(hr)(sq ft)(°F/ft)	1400	17.5	18.8		17.7	17.3	21		17
Thermal conductivity, Btu/(hr)(sq ft)(°F/ft)	2700	19	19.8		21.7	18.9	21		15
Electrical conductivity, 10^3 mhos/cm	80	18			23		62		33
Electrical conductivity, 10^3 mhos/cm	1200	6			9		13		12
Electrical conductivity, 10^3 mhos/cm	2300	~5			7.5		10		10

*Preliminary values.

Solid Hydrides

Zirconium Hydride

The results of extensive work on the zirconium-hydrogen system have been reported by Beck of Denver Research Institute.[60,61] It was shown that only the fcc delta-hydride phase can exist in true equilibrium with the alpha or beta phases at ordinary pressures. The body-centered tetragonal (bct) gamma hydride, for which much conflicting information has been presented in the past, was identified conclusively by X-ray diffraction and metallography. It was shown to be a metastable decomposition product of the delta hydride. The gamma hydride is precipitated on cooling of the delta phase below the eutectoid temperature, apparently by a diffusion-controlled mechanism. The structure of the gamma hydride appears to be the same as the epsilon hydride, except that only half of the tetrahedral sites are occupied by hydrogen atoms.

The bct epsilon-hydride phase approaches the stoichiometric ZrH_2 composition, but it exists over a fairly broad range of composition down to 62.5 at.% hydrogen. The epsilon phase is a low-temperature allotrope of the delta phase and is formed directly by a diffusionless transformation. The broad delta-plus-epsilon two-phase region observed by some investigators was shown to have resulted from oxygen contamination.

Although the composition of the eutectoid is still somewhat questionable, the evidence favors a composition about 40 at.% hydrogen. All reactions in this system were shown to have moderately high rates, except for the eutectoid reaction on heating.

The lattice parameters for the delta- and epsilon-hydride phases as a function of hydrogen content are shown in Fig. II-6. The change in hardness as hydrogen content increases is presented in Fig. II-7. The abrupt drop in hardness at 62.5 at.% hydrogen indicates the phase change from delta to epsilon hydride.

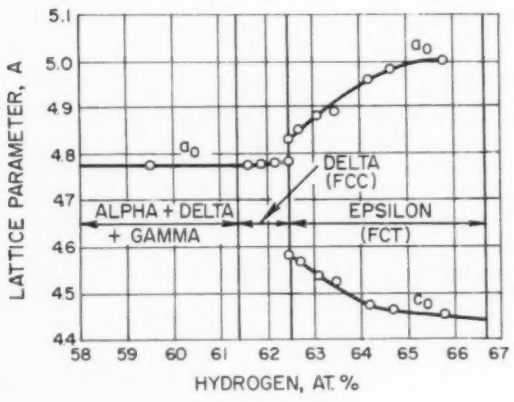

Fig. II-6 Lattice parameters for pure zirconium hydride.[60]

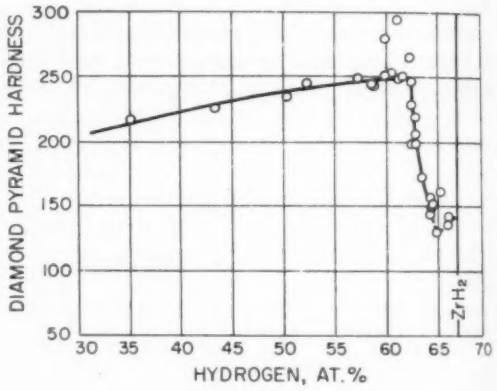

Fig. II-7 Hardness of zirconium-hydrogen alloys.[60]

The thermal conductivity of three hydride compositions is given as a function of temperature in Fig. II-8. The sample containing 60 at.% hydrogen was in the delta region at all temperatures and shows a negative temperature coefficient. Above 600°C the sample with 45.3 at.% hydrogen is in the all-beta region, where a positive coefficient is noted. The conductivity at 550°C is the same on all three plots, as this is the eutectoid temperature, where the alpha, beta, and delta phases are in equilibrium.

Changes in thermal expansion with temperature are shown in Fig. II-9. Above the eutectoid temperature the different compositions are in different phases; hence the lack of uniformity of the values.

Both heat-capacity and specific-heat values for the delta and epsilon phases are given in Fig. II-10, where the latter is seen to have the higher values because of its higher hydrogen content.

Lithium Hydride

Studies of lithium hydride by X-ray and neutron diffraction were conducted by Calder and associates.[62] They found that the lithium ion is largely unaffected by the crystalline field, whereas the hydrogen ion undergoes pronounced contraction. The degree of electron transfer in lithium hydride was found to be in the range $0.8 \rightarrow 1$.

The transition pressure at which lithium hydride may be expected to go from a sodium chloride to a cesium chloride structure was calculated by Schumacher.[63] He obtained values of 3050 and 3800 kg/cm^2, using two different potential functions.

Ternary Hydrides

The thorium-hydrogen-carbon system was studied by Peterson and Rexer[64] at Iowa State University. By measurement of hydrogen equilibrium pressures at various compositions and temperatures, they distinguished two compounds: (1) $ThH_2 \cdot ThC$, having a hexagonal close-packed lattice with $a_0 = 3.816$ and $c_0 = 6.302$; and (2) $2ThH_2 \cdot ThC$, having a monoclinic structure with $a_0 = 6.50$, $b_0 = 3.80$, $c_0 = 10.91$, and $\beta = 119°$. A patent,[65] assigned to AEC, has been issued on the preparation of these compositions by reaction of ThC and thorium at 500 to 950°C in an atmosphere of hydrogen.

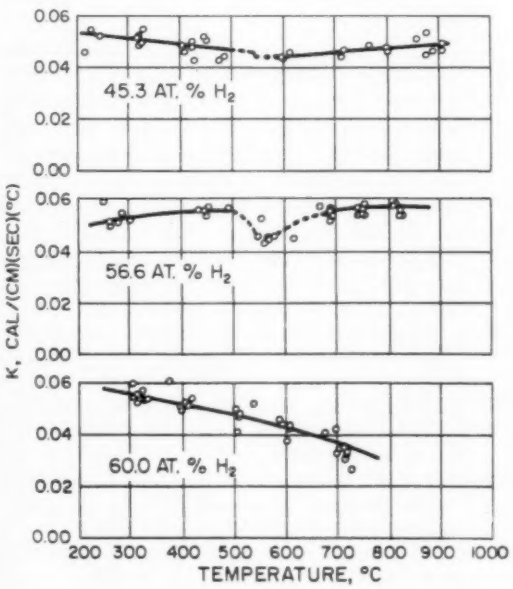

Fig. II-8 Thermal conductivity for zirconium hydride at various levels of hydrogen.[61]

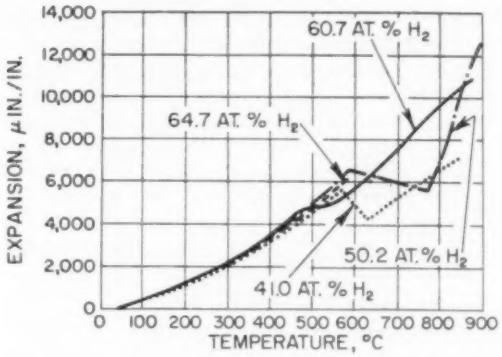

Fig. II-9 Dilatometric linear expansion of zirconium-hydrogen alloys.[65]

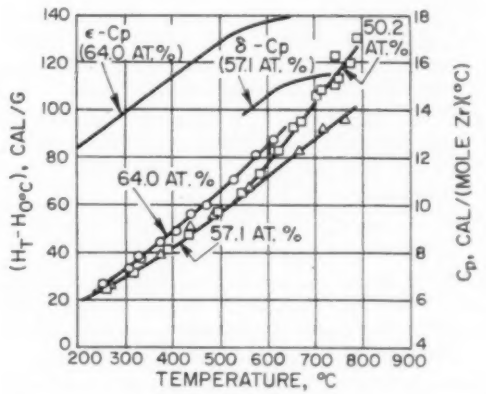

Fig. II-10 Heat capacity of zirconium-hydrogen alloys.[65]

A theoretical study of the zirconium-hydrogen-uranium system has been reported by Nathan[66] of Atomics International. He presented a solution of the diffusion equation for isothermal single-phase hydriding of cylinders of the 90 wt.% zirconium–10 wt.% uranium alloy. The kinetics of hydriding and the stresses resulting from hydriding are considered for zirconium hydride compositions from $ZrH_{1.60}$ to $ZrH_{1.80}$. (H. H. Krause)

References

1. W. V. Goeddel, Development and Evaluation of B_4C–Graphite Control-Rod Materials for the

HTGR, USAEC Report GA-2827, General Atomic Division, General Dynamics Corp., Apr. 4, 1962.

2. K. W. arley-Macauly and M. Mackenzie, Special Ceramics Symposium, 1962 — Pyrolytics Session. The Development of New Types of Pyrolytic Carbon (to be published in *Proceedings of a Symposium on Special Ceramics, July 1962*, sponsored by British Ceramics Research Association).
3. B. Fleischer, J. H. DeVan, and J. H. Coobs, Graphite–Stainless Steel Compatibility Studies, USAEC Report ORNL-TM-338, Oak Ridge National Laboratory, Sept. 25, 1962.
4. S. Goldsmith and P. F. Ashbrook (Eds.), Research and Development Programs Executed for the Division of Reactor Development, Quarterly Progress Report, January–March 1962, USAEC Report HW-73915, Hanford Atomic Products Operation, Aug. 1, 1962.
5. G. B. Engle, High-Energy Neutron-Induced Changes in Carbon and Graphite. A Review, USAEC Report GA-2802, General Atomic Division, General Dynamics Corp., Sept. 20, 1962.
6. G. E. Hewitt and E. W. Sharratt, Bismuth Impregnation Studies of Virgin and Oxidized Nuclear Grade Graphite, British Report AERE-R-3993, June 1962.
7. T. J. Hughel, Beryllium — A Space Age Metal, *ASM Metals Eng. Quart.*, 2(2): 42-51 (1962).
8. R. F. Bunshah, A Fresh Look at the Problems in Beryllium Metallurgy, USAEC Report UCRL-6410, University of California Lawrence Radiation Laboratory, Mar. 31, 1961.
9. W. J. Salmen and L. P. Gobble, Tensile Properties of Beryllium from Room Temperature to 1600°F (to appear in *Am. Soc. Testing Mater. Proc.*, 1962).
10. E. G. Wilson, P. Wells, and G. Sumner, The Mechanical Properties of Corrosion-Resistant Beryllium-Calcium Alloys at Elevated Temperature, British Report TRG-Report-311, June 7, 1962.
11. The Beryllium Corp., Products and Applications of Beryllium, Bulletin 2120, 1962.
12. The Beryllium Corp., Properties of Beryllium, Bulletin 2125, 1962.
13. H. M. Finniston, Beryllium: A Problem Metal, *Research (London)*, 15: 109-118 (March 1962).
14. S. R. Seagle, R. L. Martin, and O. Bertea, Electron Beam Melting, *J. Metals*, 14(11): 812-820 (November 1962).
15. R. Goosey, R. A. Knight, and A. J. Martin, The Induction Melting and Casting of Beryllium, *J. Less-Common Metals*, 4(2): 199-212 (1962).
16. G. Boisde, M. Broc, G. Chavin, H. Coriou, J. Hure, and P. Jarny, Contribution to the Study of the Production of High-Purity Beryllium by Electrorefining in Molten Salts (in French), *J. Nucl. Mater.*, 6(3): 256-264 (1962).
17. E. M. Grala, R. G. O'Rourke, H. F. Larson, and J. N. Hurd, Rolling Improved Beryllium Sheet, Phase II Report, Isotropic Ductility, Report NP-12152, Brush Beryllium Co., August 1962.
18. R. Syre and J. M. Logerot, Application of Some Powder-Metallurgy Techniques to the Transformation of Beryllium, in *Powder Metallurgy in the Nuclear Age*, edited by F. Benesovsky, Metallwerk Plansee A.G., Reutte/Tyrol, Austria, 1962 (in French).
19. E. A. Murphy and J. G. Klein, Helical Finned Tube Development, Progress Report, April 16–May 15, 1962, USAEC Report ORO-557, Brush Beryllium Co.
20. A. G. Gross, Jr., and R. G. O'Rourke, Development of Fine Diameter High-Purity Wire from Zone-Refined Beryllium, Progress Report No. 3, August 1–September 30, 1962, Report NP-12253, Brush Beryllium Co.
21. E. E. Weismantel and E. E. Black, The Effect of Rolling Parameters on the Properties of Beryllium Sheet Metal, *Trans. Am. Soc. Metals*, 55(3): 685-696 (September 1962).
22. D. O'Boyle, Surface Coatings for Beryllium Parts, *Machine Design*, 33: 147-150 (Dec. 21, 1961).
23. S. V. Glorioso, D. P. O'Keefe, and C. W. Rogers, Development of Brazed Beryllium Sandwich Construction, Report ERR-FW-043, Convair Division, General Dynamics Corp., December 1960.
24. E. F. Westlund, Vacuum Furnace Brazing of Beryllium, USAEC Report UCRL-6391, University of California Lawrence Radiation Laboratory, March 1961.
25. C. L. Cline, Brazing Beryllium for Aerospace Applications, paper presented at the American Welding Society 43rd Annual Meeting, April 1962.
26. A. J. Martin, J. E. J. Bunce, and P. D. Tilbury, A Study of the Electrical Conductivity of Beryllium and the Effect of Purity, *J. Less-Common Metals*, 4(2): 191-198 (1962).
27. H. Nakatani, The Effect of the Particle Size of Sintered Beryllium Powder on Its Apparent Density and Electrical Resistivity (in Japanese), *Denki Shikensho Iho*, 26: 278-284 (April 1962).
28. S. Koda and S. Morozumi, Behavior of Inclusions Under Compression (in English), *J. Nucl. Mater.*, 6(1): 5-12 (1962).
29. Nuclear Metals, Inc., Beryllium Research and Development Program, Report ASD-TDR-62-509, Vol. I, October 1962.
30. M. I. Jacobson, F. M. Almeter, and E. C. Burke, Surface Damage in Beryllium, *Trans. Am. Soc. Metals*, 55(3): 492-504 (September 1962).
31. C. Gasc and M. Badeau, Various Modes of Recrystallization of Beryllium (in French), *J. Nucl. Mater.*, 6(1): 120-122 (1962).
32. G. E. Spangler, M. Herman, E. J. Arndt, D. B. Hoover, V. V. Damiano, and G. S. Tint, Prepara-

tion and Evaluation of High Purity Beryllium, Quarterly Progress Report, Apr. 2–July 1, 1962, Report NP-12162, Franklin Institute.

33. Nuclear Metals, Inc., Fundamental and Applied Research and Development in Metallurgy, USAEC Report NMI-2107, July 31, 1962.
34. Y. Adda, Noël Azam, G. Donze, J. Mallen, F. Maurice, and M. Weisz, Contribution to the Study of the Segregation of Impurities in Beryllium of Commercial Purity (in French), *Compt. Rend.*, 254: 1052-1054 (Feb. 5, 1962).
35. G. Donze, D. Dutilloy, R. LeHazif, and Y. Adda, Morphology of a Liquid Phase Based on Aluminium in the Grain Boundaries of Beryllium (in French), *J. Nucl. Mater.*, 6(1): 137-138 (1962).
36. H. M. Lindsay and A. Moore, A Metallographic Study of the Aging Characteristics of Beryllium-Iron Alloys, Between 400°C and 1050°C, British Report AWRE-O-48/62, August 1962.
37. G. Donze, R. LeHazif, F. Maurice, D. Dutilloy, and Y. Adda, Diffusion and Solubility of Iron in Beryllium (in French), *Compt. Rend.*, 254: 2328-2330 (Mar. 26, 1962).
38. W. B. Jepson, The Oxidation of Beryllium, *Research (London)*, 15: 288-294 (July 1962).
39. F. W. Trowse, The Corrosion Testing of Beryllium for Use in a Carbon Dioxide Cooled Reactor, British Report GCM/UK/47, March 1962.
40. J. P. Pemsler, D. S. Kneppel, and R. G. Jenkins, Beryllium Corrosion, USAEC Report NMI-1903, Nuclear Metals, Inc., Aug. 31, 1962.
41. L. J. Vachon, Protection of Beryllium Metal by Anodic Films (in English), *J. Nucl. Mater.*, 6(1): 139-141 (1962).
42. R. B. Adams, G. H. Price, and W. I. Stuart, Reactions of Preoxidized Powder in Moist Carbon Dioxide, Australian Report AAEC/E-88, June 1962.
43. J. B. Rich and G. P. Walters, Some Effects of Irradiation on Beryllium, in *Powder Metallurgy in The Nuclear Age*, edited by F. Benesovsky, Metallwerk Plansee A.G., Reutte/Tyrol, Austria, 1962.
44. Beryllium—Some Figures Concerning Its Economic Aspects (in French), *Energie Nucl.*, 4: 129-135 (March–April 1962).
45. P. Lowenstein, The Status of Beryllium Metal in Nuclear Reactors (in English), *Atompraxis*, 8: 122-128 (April 1962).
46. Fine, Low-Oxygen Powders May Be Key to Ductile Beryllium, *Metal Progr.*, 82(5): 8 (November 1962).
47. Atomics International, Annual Technical Progress Report, AEC Unclassified Programs, Fiscal Year 1962, USAEC Report NAA-SR-7400, Nov. 15, 1962.
48. General Electric Company, Flight Propulsion Laboratory Department, High-Temperature Materials Program Progress Report No. 16, Part A, USAEC Report GEMP-16A, Oct. 15, 1962.
49. R. S. Truesdale, B. B. Lympany, C. A. Bielawski, E. M. Grala, and W. W. Beaver, Investigation of the Effects of Processing Variables and Fabrication Techniques upon the Properties of Intermetallic Compounds, Report ASD-TDR-62-476, Brush Beryllium Co., February 1962.
50. D. A. Mannas and J. P. Smith, Beryllium Intermetallic Compounds—Their Preparation and Fabrication, *J. Metals*, 14: 575-578 (August 1962).
51. E. A. Aitken and J. P. Smith, Oxidation of Beryllium Intermetallic Compounds (in English), *J. Nucl. Mater.*, 6(1): 119 (1962).
52. F. C. Perkins, Intermediate Temperature Oxidation of Beryllides, Monthly Letter Report No. 11, July 1–August 1, 1962, USAEC Report TID-16479, Denver Research Institute, Aug. 9, 1962.
53. R. M. Paine, A. J. Stonehouse, and W. W. Beaver, Development of Intermetallic Compounds for Very High Temperature Applications, Quarterly Progress Report, January 1–March 31, 1962, USAEC Report BBC-113, Brush Beryllium Co., May 31, 1962.
54. R. M. Paine, A. J. Stonehouse, and W. W. Beaver, Development of Intermetallic Compounds for Very High Temperature Applications, Annual Report, January 1–December 31, 1961, USAEC Report BBC-115, Brush Beryllium Co., September 1962.
55. T. W. Baker, Interatomic Distances in the Intermetallic Compounds $MgBe_{13}$ and $CaBe_{13}$, *Acta Cryst.*, 15: 175-179 (Mar. 10, 1962).
56. D. E. Sands, Q. C. Johnson, A. Zalkin, O. H. Krikorian, and K. L. Kromholtz, The Crystal Structure of $ReBe_{22}$, *Acta Cryst.*, 15: 823-844 (Sept. 10, 1962).
57. E. E. Vainshtein, S. M. Blakin, and P. I. Kripyakevich, An X-Ray Spectroscopic Study of the Titanium Beryllides Having a High Content of Beryllium, *Doklady Akad. Nauk SSSR*, 142: 85-87 (Jan. 1, 1962).
58. Academy of Sciences of the USSR, Institute of Metallurgy, *Structures of Certain Systems with Thorium and Uranium* (in Russian), Gosatomizdat, Moscow, 1961; T. A. Badayeva and R. I. Kuznetsova, Structure of $ThBe_{13}$-UBe_{13} Alloys, Abstract No. 8I152 in *Ref. Zh. Met.*, (8): 23-24 (1962).
59. Oak Ridge National Laboratory, Metals and Ceramics Division Annual Progress Report for Period Ending May 31, 1962, USAEC Report ORNL-3313, Aug. 16, 1962.
60. R. L. Beck, Zirconium-Hydrogen Phase System, *Trans. Am. Soc. Metals*, 55(3): 542-555 (September 1962).
61. R. L. Beck, Thermophysical Properties of Zirconium Hydride, *Trans. Am. Soc. Metals*, 55(3): 556-564 (September 1962).
62. R. S. Calder, W. Cochran, D. Griffiths, and R. D. Lowde, An X-Ray and Neutron Diffraction Analysis of Lithium Hydride, *Phys. Chem. Solids*, 23: 621-632 (July 1962).

63. D. P. Schumacher, Polymorphic Transition in Lithium Hydride, *Phys. Rev.*, 126: 1679 (1962).

64. D. P. Peterson and J. Rexer, Ternary Compounds Between Thorium Monocarbide and Thorium Dihydride, USAEC Report IS-247, Ames Laboratory, Jan. 5, 1961.

65. D. P. Peterson and J. Rexer, Self-Moderating Fertile Compounds, U. S. Patent 3,044,847 (to USAEC), July 17, 1962.

66. M. E. Nathan, Theoretical Kinetics and Stresses for Delta-Phase Isothermal Hydriding of Uranium-Zirconium, USAEC Report NAA-SR-6264, Atomics International, July 15, 1962.

Section

III

Reactor Materials

Nuclear Poisons

Metallic Poison Materials

After two seed lives in the Shippingport Pressurized-Water Reactor, a hafnium control rod was destructively tested to determine the effects of irradiation on its mechanical properties.[1] The hardness was increased from $R_A = 53.1$ to $R_A = 62.6$ after a neutron dose of 1×10^{22} nvt (>0.625 ev). The changes in other mechanical properties are given in Table III-1. The decrease in ductility was not serious enough to limit the use of hafnium after an exposure of 1×10^{22} nvt. The corrosion at the Zircaloy-2-to-hafnium weld joint was found to be more than expected and may be the result of contamination during welding.

Effects of heat-treatment on the hardness and tensile properties of cold-rolled hafnium were investigated by Bettis.[2] Specimens were heat-treated at 700, 800, 900, 1000, and 1100°C. The data revealed a decrease in room-temperature ductility, as measured by elongation and reduction of area, when heat-treatments greater than 900°C were employed. No corresponding changes in yield or ultimate tensile strength were noted. Additions of up to 40 wt.% zirconium to hafnium were found to increase its strength and decrease its ductility.[3]

A review of phase analysis and structure studies on the hafnium-aluminum system has been published.[4] The structures and properties of the various phases are discussed and compared with those of some transition-metal borides.

It was found at Knolls[5] that 700 ppm hydrogen dissolved in hafnium does not affect its corrosion resistance in 680°F water and 750°F steam.

Oxidation studies at 1000°C showed that hafnium boride is more oxidation resistant than pure hafnium.[6] Hafnium-rhenium and hafnium-dysprosium alloys were found to have poorer oxidation resistance than hafnium. Improved oxidation resistance was obtained for all the hafnium alloys and for unalloyed hafnium by coating with phosphorus. A patent[7] has been obtained on a method of depositing a uniform, adherent, corrosion-resistant boride coating on a metal. The metals that may be borided in this way are those having atomic numbers 23 to 29, 41 to 47, and 73 to 79, as well as alloys containing these metals as major constituents.

Phase-diagram data on the silver-cadmium-zinc system were extended, with special emphasis on the melting equilibrium and the four-phase transformation.[8] Three four-phase equilibria, at 440, 285, and 270°C, were determined. Data are also given on deformability, straining, hardness, and tensile strength of the alloy after butt welding. Graves et al. describe[9] a nickel coating, 5 to 50 mils thick, on silver-indium-cadmium control-rod alloys. This coating was found to resist undercutting. These same authors review the results of using silver-indium-cadmium control rods in the Yankee power reactor.

Chemical and physical properties of metallic erbium of 99.35% purity are reported.[10] Five percent erbium is found to be miscible with aluminum, magnesium, iron, and titanium. Erbium has no apparent solubility in tantalum.

(M. Kangilaski)

Dispersion Control Materials

In the past few years, Russian workers have conducted a great deal of research in the area of boron and boron-containing materials. Recently the AEC has made available translations of two compilations which include recent Rus-

Table III-1 TENSILE PROPERTIES* OF PWR HAFNIUM[1]

Specimen	Total exposure (>0.625 ev), nvt	Test temp., °F	Yield strength (0.2% offset), psi	Ultimate tensile strength, psi	Reduction of area, %	Total elongation, %	Unit elongation, %	Difference in yield strength		Difference in ultimate tensile strength		$\%\ R_A/(\%\ R_A)_0$	$\%$ elongation/$(\%$ elongation$)_0$	True necking strain	n†	K‡
								Psi	%	Psi	%					
	0	RT	27,450	58,600	32.5	34.2	28.1							0.140	0.208	100,150
N1C	5.33×10^{21}	RT	72,600	78,100	25.1	18.5	4.2	45,150	164.5	19,500	33.3	0.77	0.54	0.247	0.039	92,140
N1A	5.64×10^{21}	RT	72,800	80,400	29.6	18.0	4.7	45,350	165.2	21,800	37.2	0.91	0.53	0.306	0.046	96,780
G3A	9.05×10^{21}	RT	83,700	92,600	24.6	13.0	4.4	56,250	204.9	34,000	58.0	0.76	0.38	0.240	0.046	111,730
G3C	9.12×10^{21}	RT	82,400	90,800	20.8	13.0	3.2	54,950	200.2	32,200	54.9	0.64	0.38	0.202	0.048	110,400
F1C	9.74×10^{21}	RT	83,900	94,500	20.2	16.5	6.4	56,450	205.6	35,900	61.3	0.62	0.48	0.165	0.052	116,200
F1A	10.3×10^{21}	RT	89,300	100,800	18.0	16.0	5.9	61,850	225.3	42,200	72.0	0.55	0.47	0.142	0.053	124,160
	0	300	32,650	49,500	40.8	43.7	29.1							0.273	0.138	77,200
N2C	5.33×10^{21}	300	61,900	64,700	28.6	16.5	2.7	29,250	89.6	15,200	36.7	0.70	0.38	0.310	0.028	73,460
N2A	5.64×10^{21}	300	60,400	63,000	29.5	21.6	3.7	27,750	85.0	13,500	27.3	0.72	0.48	0.313	0.027	71,490
F1D	9.74×10^{21}	300	75,600	81,800	17.9	17.0	4.4	42,950	131.5	32,300	65.25	0.44	0.39	0.155	0.039	26,600
F1B	10.3×10^{21}	300	79,400	86,700	24.6	11.1	3.0	46,750	143.2	37,200	75.2	0.60	0.25	0.252	0.044	104,280
	0	600	22,350	34,700	48.9	50.7	36.7							0.360	0.149	56,300
N3A	5.03×10^{21}	600	46,500	46,900	39.9	20.0	1.4	24,100	108.1	12,200	35.2	0.82	0.39	0.495	0.011	49,880
N3X	5.07×10^{21}	600	45,700	45,700	39.3	20.0	0.4	23,350	104.5	11,000	31.7	0.80	0.39	0.497		
F2C	9.74×10^{21}	600	61,800	63,100	30.8	19.0	2.7	39,450	176.5	28,400	81.8	0.63	0.37	0.343	0.019	69,560
F2A	10.3×10^{21}	600	66,100	68,100	26.9	14.0	2.1	43,750	195.7	33,400	96.3	0.55	0.28	0.291	0.020	74,920

*Testing speed was 0.02 in./(in.)(min) for unnotched specimens.

†n = work-hardening exponent.

‡K = strength coefficient.

sian work, as well as references to western work. A two-volume book on boron and boron compounds, edited by G. V. Samsanov,[11] discusses the processing of boron raw materials and the production, properties, and use of elementary boron, boranes, and borides in Volume 1. The second volume discusses alloys of boron and their application and the analytical chemistry of boron and boron compounds. All the boron systems known at the time of publication (1960) are covered. In general, the book is well referenced and serves as a good source book. In addition, it offers considerable insight into the Russian work on boron and boron compounds. A similar book covering only borides of rare-earth metals and written by Samsanov and Paderno[12] has also been published in English by the AEC.

Workers at Oak Ridge[13] are developing fabrication techniques for four-section aluminum-clad control-rod plates for the High-Flux Isotope Reactor. The four sections are: (1) a 26-in.-long type 6061 aluminum "white" region, (2) a 7-in.-long "gray" region of 40 vol.% tantalum dispersed in aluminum, (3) a 20-in.-long "black" region of 40 vol.% Eu_2O_3 dispersed in aluminum, and (4) a 12-in.-long "white" section of type 6061 aluminum. Roll-cladding techniques are being utilized to produce $\frac{1}{4}$-in.-thick plates with 0.031-in.-thick cladding. Also, Gd_2O_3-Al_2O_3 materials are being fabricated[14] in an effort to produce a control-rod material for the Molten-Salt Reactor. Such materials are designed to withstand air- and moisture-contaminated nitrogen atmospheres at temperatures to 1400°F.

Atomics International[15] workers have studied the compatibility of AISI 4130 steel, types 304 and 430 stainless steel, and copper with B_4C. They concluded (1) that 4130 steel is not compatible at a temperature of 900°F or higher, (2) that type 304 stainless steel is compatible at 1100°F, and (3) that both type 430 stainless steel and commercial copper are compatible at 1300°F. They also concluded that boron carbide with a 5 wt.% excess of carbon or of boron did not significantly affect the compatibility results.

Dispersions of 30 wt.% Dy_2O_3 in cobalt are being studied at Argonne.[16] The dispersion has a compression strength of about 112,000 psi, compared to 210,000 psi for cobalt. In thermal-shock tests no cracking was observed after cycling 125 times through the cobalt alpha-beta transition temperature, but cracks were observed after quenching from 800°C. After testing was conducted for 1012 hr in boiling water, the only noticeable corrosion was a slight attack on Dy_2O_3 particles located at the pellet surface.

Atomics International[17] has also studied Gd_2O_3 and Gd_2O_3-Sm_2O_3 materials for use as neutron-absorber materials. Tests have been conducted to establish the radiation stability of these materials with regard to their dimensional, chemical, and thermal characteristics. The materials were exposed to approximately 5×10^{20} ($\pm$ 10%) nvt at the surface of the cylindrical containers. The reported results indicate that:

1. No appreciable changes in oxide-container dimensions occurred.

2. The apparent thermal conductivity of the mixed oxides (45 wt.% Gd_2O_3–45 wt.% Sm_2O_3, balance low-cross-section materials), irradiated at 950 and 1200°F, remained constant, at 1.25 ± 0.05 and 1.05 ± 0.05 Btu/(hr)(ft)(°F), respectively; and the apparent thermal conductivity of the 90 wt.% Gd_2O_3 (balance low-cross-section materials), irradiated at 1200°F, remained essentially constant at 1.30 ± 0.10 Btu/(hr)(ft)(°F).

3. Power generation in the poison materials also remained constant, at about 1.30 ± 0.1 kw/(ft)(10^{13} nv) in the mixed oxides and about 1.40 ± 0.1 kw/(ft)(10^{13} nv) in the 90 wt.% Gd_2O_3.

4. Helium gas, with which the oxide containers had been pressurized, was either lost through leaks in the containers or absorbed by the oxides.

5. No appreciable change in oxide particle sizes occurred.

6. The generation of heat in the poison material was apparently uniform, since calculated temperature profiles, based on the assumption of uniform heat generation, agreed closely with measured temperature profiles.

(G. W. Cunningham)

References

1. G. J. Salvaggio, F. A. Nichols, and J. P. Bacca, Jr., Properties of Hafnium Control Rod After Exposure During Two Seed Lives in PWR Core 1, USAEC Report WAPD-TM-337, Westinghouse Electric Corp., Bettis Atomic Power Laboratory, November 1962.
2. J. G. Goodwin, The Effects of Heat Treatments on the Hardness and Tensile Properties of Cold

Rolled Iodide Hafnium, USAEC Report WAPD-248, Westinghouse Electric Corp., Bettis Atomic Power Laboratory, June 1962.

3. A. G. Imgram, D. N. Williams, and H. R. Ogden, Tensile Properties of Binary Titanium-Zirconium and Titanium-Hafnium Alloys, *J. Less-Common Metals*, 4(3): 217-225 (June 1962).
4. L. E. Edshaminar, Crystal Structure Investigations on the Zirconium-Aluminum and Hafnium-Aluminum Systems, *Acta Chem. Scand.*, 16: 20-30 (1962).
5. Knolls Atomic Power Laboratory, Reactor Technology Report No. 22—Chemistry, USAEC Report KAPL-2000-19, September 1962.
6. Nuclear Corp. of America, Research Chemicals Division, Refractory Intermetallic Compounds, Final Report, Report NP-12174, February 1962.
7. N. C. Cook, Corrosion-Resistant Coating, U. S. Patent 3,024,176 (to General Electric Company), Mar. 6, 1962.
8. G. Petzow and E. Wagner, Structure and Properties of Silver-Cadmium-Zinc Alloys, *Z. Metallk.*, 53: 189-195 (March 1962).
9. H. W. Graves, Jr., J. J. Lombardo, and J. S. Theilacker, Silver-Indium-Cadmium, A Control Rod Material for Pressurized Water Reactors, *Nucl. Sci. Eng.*, 13: 299-300 (July 1962).
10. E. M. Savitskii, V. F. Terekhova, and O. P. Naumkin, Erbium and Its Alloys, *Tsvetn. Metal.*, 33(1): 43 (1960).
11. G. V. Samsanov (Ed.), Boron, Its Compounds and Alloys, USAEC Translation AEC-tr-5032 (Book I and Book II) (translated from Russian), July 1962.
12. G. V. Samsanov and Yu. B. Paderno, Borides of Rare Earth Metals, USAEC Translation AEC-tr-5264 (translated from Russian), October 1962.
13. Oak Ridge National Laboratory, Dec. 10, 1962. (Unpublished)
14. Oak Ridge National Laboratory, Molten-Salt Reactor Program, Semiannual Progress Report for Period Ending August 31, 1962, USAEC Report ORNL-3369, Dec. 12, 1962.
15. Atomics International, Annual Technical Progress Report, AEC Unclassified Programs, Fiscal Year 1962, USAEC Report NAA-SR-7400, Nov. 15, 1962.
16. Argonne National Laboratory, Reactor Development Program Progress Report, September 1962, USAEC Report ANL-6619, Oct. 15, 1962.
17. T. E. Redding, Irradiation Test of Gadolinium and Samarium Oxides for the HNPF Control Rod Program, USAEC Report NAA-SR-6514, Atomics International, Nov. 30, 1962.

LEGAL NOTICE

This document was prepared under the sponsorship of the U. S. Atomic Energy Commission. Neither the United States, nor the Commission, nor any person acting on behalf of the Commission:

A. Makes any warranty or representation, expressed or implied, with respect to the accuracy, completeness, or usefulness of the information contained in this report, or that the use of any information, apparatus, method, or process disclosed in this report may not infringe privately owned rights; or

B. Assumes any liabilities with respect to the use of, or for damages resulting from the use of any information, apparatus, method, or process disclosed in this report.

As used in the above, "person acting on behalf of the Commission" includes any employee or contractor of the Commission, or employee of such contractor, to the extent that such employee or contractor of the Commission, or employee of such contractor prepares, disseminates, or provides access to, any information pursuant to his employment or contract with the Commission, or his employment with such contractor.

☆ U. S. GOVERNMENT PRINTING OFFICE : 1963 O - 652342 (4)